Aus dem Adolf-Butenandt-Institut
Lehrstuhl: Molekularbiologie
(im BioMedizinischen Centrum München, BMC)
der Ludwig-Maximilians-Universität München
Vorstand: Prof. Dr. rer. nat. Peter B. Becker

Characterisation of *Xenopus laevis* Transcription Factor *mespa* in Mesodermal and Cardiovascular Development

Dissertation zum Erwerb des Doktorgrades der Medizin
an der Medizinischen Fakultät der
Ludwig-Maximilians-Universität zu München

vorgelegt von
Stephanie Caroline Frenz
aus Düsseldorf

2018

Mit Genehmigung der Medizinischen Fakultät
der Universität München

Berichterstatter:	Prof. Dr. Ralph A. W. Rupp
Mitberichterstatter:	Prof. Dr. Angelika Böttger
	Prof. Dr. André Werner Brändli
	Prof. Dr. Olivier Gires
Dekan:	Prof. Dr. med. dent. Reinhard Hickel
Tag der mündlichen Prüfung:	05.07.2018

Eidesstattliche Versicherung

Frenz, Stephanie
(Name, Vorname)

Ich erkläre hiermit an Eides statt,
dass ich die vorliegende Dissertation mit dem Thema

Characterisation of *Xenopus laevis* Transcription Factor *mespa* in Mesodermal and Cardiovascular Development

selbstständig verfasst, mich außer der angegebenen keiner weiteren Hilfsmittel bedient und alle Erkenntnisse, die aus dem Schrifttum ganz oder annähernd übernommen sind, als solche kenntlich gemacht und nach ihrer Herkunft unter Bezeichnung der Fundstelle einzeln nachgewiesen habe.

Ich erkläre des Weiteren, dass die hier vorgelegte Dissertation nicht in gleicher oder in ähnlicher Form bei einer anderen Stelle zur Erlangung eines akademischen Grades eingereicht wurde.

München, 01.09.2017 — Stephanie Frenz
(Ort, Datum) — (Unterschrift Doktorandin)

This work gave rise to the following publication:

“Maximilian C.M. Kriegmair, Stephanie Frenz, Marina Dusl, Wolfgang-M. Franz, Robert David, Ralph A.W. Rupp; Cardiac differentiation in *Xenopus* is initiated by *mespa*, Cardiovascular Research, Volume 97, Issue 3, 1 March 2013, Pages 454–463.“

Table of contents

Zusammenfassung

Die kardiovaskuläre Entwicklung während der Embryogenese ist ein hoch konservierter Prozess in Wirbeltieren, der von einem komplexen Netzwerk aus verschiedenen Transkriptionsfaktoren orchestriert wird. Um neue, Stammzell-basierte Therapien für die Behandlung von ischämischen Herzerkrankungen zu generieren, ist es unabdingbar, die zugrunde liegenden Prozesse der kardiovaskulären Differenzierung zu erforschen. Darüberhinaus ist dies notwendig, um die embryologischen Ursachen von angeborenen Herzfehlern zu verstehen. Dem Transkriptionsfaktor MesP1 wurde eine wichtige Rolle in der kardiovaskulären Differenzierung während der Gastrulation von Säugetieren und in embryonalen Stammzellen zugesprochen.

Der afrikanische Krallenfrosch *Xenopus laevis* ist aufgrund seiner zahlreichen methodischen Vorteile ein sehr geeigneter Modellorganismus um die Embryogenese *in vivo* zu studieren. Der Transkriptionsfaktor *mespa* wurde als das funktionelle Homolog von MesP1 in *Xenopus laevis* identifiziert. Jedoch wurde *mespa* bislang noch nicht umfassend bezüglich seiner Funktionen in der Entwicklung von *Xenopus laevis* untersucht. Daher war das Ziel dieser Doktorarbeit, *mespa* in kardiovaskulärer und mesodermaler Entwicklung von *Xenopus laevis* zu charakterisieren.

Basierend auf *loss*- und *gain-of-function*-Experimenten konnte gezeigt werden, dass *mespa* für die Expression der kardiogenen Transkriptionsfaktoren *nkx2.5* und *isl.1*, sowie des *wnt*-Antagonisten *dkk1* benötigt wird. Außerdem wurde zum ersten Mal *in vivo* demonstriert, dass *mespa* über die Induktion des vaskulogenen *apelin receptor* in der vaskulären Entwicklung involviert ist. Des Weiteren agiert *mespa* mit Hilfe des Membranproteins *paraxial protocadherin*, um morphogenetische Bewegungen während der Gastrulation zu generieren. Schließlich konnte demonstriert werden, dass *mespa* zusätzlich auch für die Expression von skeletomyogenen Faktoren wie *myoD* und *myf5*, sowie für den wichtigen mesodermalen Regulationsfaktor *xbra* notwendig ist.

Zusammenfassend konnte gezeigt werden, dass *mespa* während der Entwicklung von *Xenopus laevis* umfassende Funktionen hat, die über kardiovaskuläre Entwicklung hinausgehen und Vaskulogenese, Morphogenese, skelettale Myogenese und Mesodermformation beinhalten.

Summary

Cardiovascular development during embryogenesis is a highly conserved process in vertebrates, which is orchestrated by a complex network of different transcription factors. Uncovering the processes underlying cardiovascular differentiation is essentially in order to engineer new stem cell based therapies to treat ischaemic heart disease. Moreover, it will help to understand developmental origins of congenital heart defects.

The transcription factor MesP1 was found out to play an important role in cardiovascular differentiation during gastrulation in mammals and ES cells.

The African clawed frog *Xenopus laevis* is a versatile model organism for studying embryogenesis *in vivo* due to its numerous methodical advantages. The transcription factor *mespa* has been identified as the functional homologue of MesP1 in *Xenopus laevis*. However, *mespa* has not been investigated thoroughly regarding its functions in development of *Xenopus laevis* so far. Therefore, the aim of this study was to characterize *mespa* in cardiovascular and mesodermal development of *Xenopus laevis*.

Based on loss- and gain-of-function experiments it was shown that *mespa* is required for expression of the cardiogenic transcription factors *nkx2.5* and *isl.1*, as well as the *wnt* antagonist *dkk1*. Moreover, it was demonstrated for the first time *in vivo* that *mespa* is involved in vascular development by inducing the vasculogenic *apelin receptor.* Furthermore, *mespa* acts via the membrane protein *paraxial protocadherin* to generate morphogenic movements during gastrulation. Finally, it was demonstrated that *mespa* is required additionally for expression of skeletomyogenic factors like *myoD* and *myf5*, as well as for expression of the important mesodermal regulator *xbra*.

Taken together, *mespa* has been shown to have broad functions in development of *Xenopus laevis*, which exceed cardiovascular development and include vasculogenesis, morphogenesis, skeletal myogenesis and mesoderm formation.

1. Introduction

1.1 Clinical background

Ischaemic heart disease continues to be the leading cause of death and morbidity in the world (Bui, Horwich et al. 2011; Lozano, Naghavi et al. 2012; Finegold, Asaria et al. 2013). In the year 2012, over seven million people in the world died because of ischaemic heart disease (WHO 2012). Therefore, heart disease has become a global burden for public health systems. The main causes of heart failure are due to a deficiency of functioning cardiac muscle cells, termed cardiomyocytes, as the human heart loses up to a billion cardiomyocytes after a severe myocardial infarction (Murry, Reinecke et al. 2006). Heart disease cannot be treated causally due to the extremely limited regenerative potential of cardiomyocytes, with a turnover rate of approximately 0.45 % per year at the age of 75 (Bergmann, Bhardwaj et al. 2009). Until now only the progression of the disease can be slowed (Murry, Reinecke et al. 2006; Laflamme and Murry 2011; Konstantinidis, Whelan et al. 2012). The only available cure is allogeneic heart transplantation, which is, because of an absence of donor hearts, not a promising strategy (Stehlik 2011). Thus, to devise new therapies for the treatment of ischaemic heart disease, it is mandatory to understand, how mature cardiomyocytes develop from stem cells to multipotent cardiovascular progenitor cells (Ptaszek, Mansour et al. 2012). A compelling approach might consist of remuscularization of the infarcted myocardium via engraftment of *in vitro*-generated cardiomyoctyes (Sahara, Santoro et al. 2015), because it has been shown that cardiomyocytes derived from human embryonic stem cells (hESCs) could repair to some extent an injured primate heart after myocardial infarction (Chong, Yang et al. 2014). In fact, the first case report of a human treated with hESC-derived cardiovascular progenitor cells has recently been published (Menasché, Vanneaux et al. 2015).

Elucidating the processes of cardiac specification in embryogenesis will also lead to a better understanding of the pathologic mechanisms that cause congenital heart defects, with an incidence of almost 1% in all newborns the most common type of birth defect (Hoffman and Kaplan 2002; van der Linde, Konings et al. 2011). Additionally, severe congenital heart defects are estimated to account for 10% of cases of stillbirths (Hoffman 1995). Improvement of diagnostics and treatment of

congenital heart disease has led to an increase in survival rate of the affected infants. Hence, the prevalence of adult patients with congenital heart defects is approximately 21 million worldwide (van der Bom, Zomer et al. 2011). Since changes in expression of regulatory proteins during cardiogenesis have been shown to be an essential genetic mechanism underlying congenital heart disease, deciphering these networks might enable molecular tools to further enhance prenatal diagnostic and following treatment of congenital heart defects (Fahed, Gelb et al. 2013).

Due to its importance in both pathogenesis and embryogenesis cardiovascular development deserves to be studied intensively.

1.2 The cardiogenic transcription factor MesP1

There is a highly conserved transcriptional regulatory network, which orchestrates the determination and specification of mesodermal pluripotent cells to cardiovascular progenitor cells (Olson 2006). These progenitors differentiate into different types of cells: cardiomyocytes, endothelial cells and vascular smooth muscle cells (Wu, Chien et al. 2008). Much effort has been attributed to the question of which factors determine cell fate decision during early cardiovascular development (Schultheiss and Lassar 1999).

A basic helix-loop-helix (bHLH) transcription factor now thought to reside on top of the cardiovascular developmental hierarchy was identified and named Mesoderm posterior 1 (MesP1), according to its expression in the posterior part of the mesoderm in mice embryos (Saga, Hata et al. 1996).

The members of the bHLH transcription factor family are composed of two α-helices linked by a loop. Basic amino acids of the larger helix allow binding to a conserved consensus sequence, termed E-box motif, which contains the core sequence CANNTG (Murre, McCaw et al. 1989). The smaller helix region heterodimerizes with different partner proteins.

MesP1 was shown to be an essential primary factor for cardiovascular development (Saga, Miyagawa-Tomita et al. 1999; Saga, Kitajima et al. 2000). MesP1 double knockout mice exhibited aberrant cardiac morphogenesis, resulting in cardia bifida (Saga 1998). David, Brenner et al. (2008) discovered that this

factor is not only required for the formation of a proper heart tube, but is also sufficient to induce cardiogenesis.

MesP1 was subsequently reported to be highly effective in cellular reprogramming for potential cardiac stem cell therapies. Transient MesP1 expression stimulated cardiovascular differentiation of murine ES cells and human iPS cells (Bondue, Lapouge et al. 2008; David, Brenner et al. 2008; Lindsley, Gill et al. 2008; Hartung, Schwanke et al. 2012). In combination with other factors, MesP1 could even transdifferentiate murine and human fibroblasts to cardiac cells (Islas, Liu et al. 2012; Christoforou, Chellappan et al. 2013; Fu, Stone et al. 2013).

Recently, mutations in the MesP1 gene were found in patients with congenital heart defects, such as ventricular septal defect and tetralogy of Fallot (Werner, Latney et al. 2016), which underlines MesP1's importance in human cardiac development.

As MesP1 double knockout mice showed severe cardiac malformations ranging from randomized looping to two separated heart tubes, these mice died before day 10.5 post coitum, that is, at a very early stage in embryogenesis (Saga 1998). Inactivation of MesP1 together with the closely related Mesp2 led to complete loss of the heart anlage and the embryos died even earlier (Kitajima, Takagi et al. 2000). Thus, mutation studies in mice could only investigate the very early developmental processes, when MesP1 is required during embryogenesis, but could not analyse late gene functions in organogenesis or impact of MesP1 on further developmental processes. Although stem cell models are suitable to recapitulate cardiovascular specification *in vitro* (Musunuru, Domian et al. 2010), they lack the ability to simulate signalling environment, morphogenetic patterning and cell-cell interactions occurring *in vivo* (Chan, Shi et al. 2013).

Therefore an alternative model organism was needed to study the role of MesP1 in vertebrate cardiovascular development further in detail.

1.3 The African clawed frog *Xenopus laevis*

1.3.1 *Xenopus laevis* as model organism

Since its initial use in pregnancy tests back in the 1930s (Elkan 1938), the South African clawed frog, *Xenopus laevis,* has been one of the most popular amphibian

model organisms for the investigation of vertebrate embryonic development, basic cell and molecular biology (Harland and Grainger 2011), neurobiology, toxicology and to model human diseases (Wallingford, Liu et al. 2010; Hardwick and Philpott 2015; LaBonne and Zorn 2015). In comparison to other model systems, *Xenopus* offers several advantages to study embryological processes. Among these features are an abundant amount of eggs, the external fertilization and development in simple saline solution, a relatively large size of the embryo, amenability and robustness to microinjections and microdissections. A range of established molecular techniques that allow protein knockdown or overexpression of specific genes and their detailed analysis, complement the main features of the *Xenopus* organism. Moreover the *Xenopus* frog has a closer evolutionary relationship to humans than other model organisms, like e.g. the zebrafish (Wheeler and Brändli 2009). However, being allotetraploid may cause difficulties for genetic studies in *Xenopus laevis*. Therefore its relative species *Xenopus* tropicalis should be used for genetic screens, as its diploid genome is fully sequenced (Hellsten, Harland et al. 2010). Finally, this genus of frog is fully aquatic and therefore easy to maintain in captivity.

Different studies have shown that it is feasible to use *Xenopus* to study vertebrate cardiovascular development (Warkman and Krieg 2007; Kinoshita, Ariizumi et al. 2010; Kaltenbrun, Tandon et al. 2011). It is only at the tadpole stage, when the heart begins to beat and the cardiac function becomes indispensable for the supply of nutrients to the cells (Jorgensen, Steen et al. 2009). Furthermore, *Xenopus* heart development approximates cardiogenesis in higher vertebrates, as the frog heart consists of an outflow tract, two asymmetric atria, atrio-ventricular valves and one ventricle with trabeculae (Warkman and Krieg 2007). Finally, *Xenopus* has been proven to be an eligible model organism to analyse congenital heart defects (Kaltenbrun, Tandon et al. 2011). Therefore, the process of cardiogenesis can be studied from very early until late stages of development under experimental conditions, which would be lethal in mammalian embryos.

1.3.2 Life cycle of *Xenopus laevis*

Xenopus development can be mainly divided into germ layer induction, embryonic patterning, organogenesis and metamorphosis (Fig. 1). Nieuwkoop and Faber

(1967) established a table of development according to time after fertilization at normalized environmental temperature, which constitutes a simple tool to gauge the embryo's phase of development.

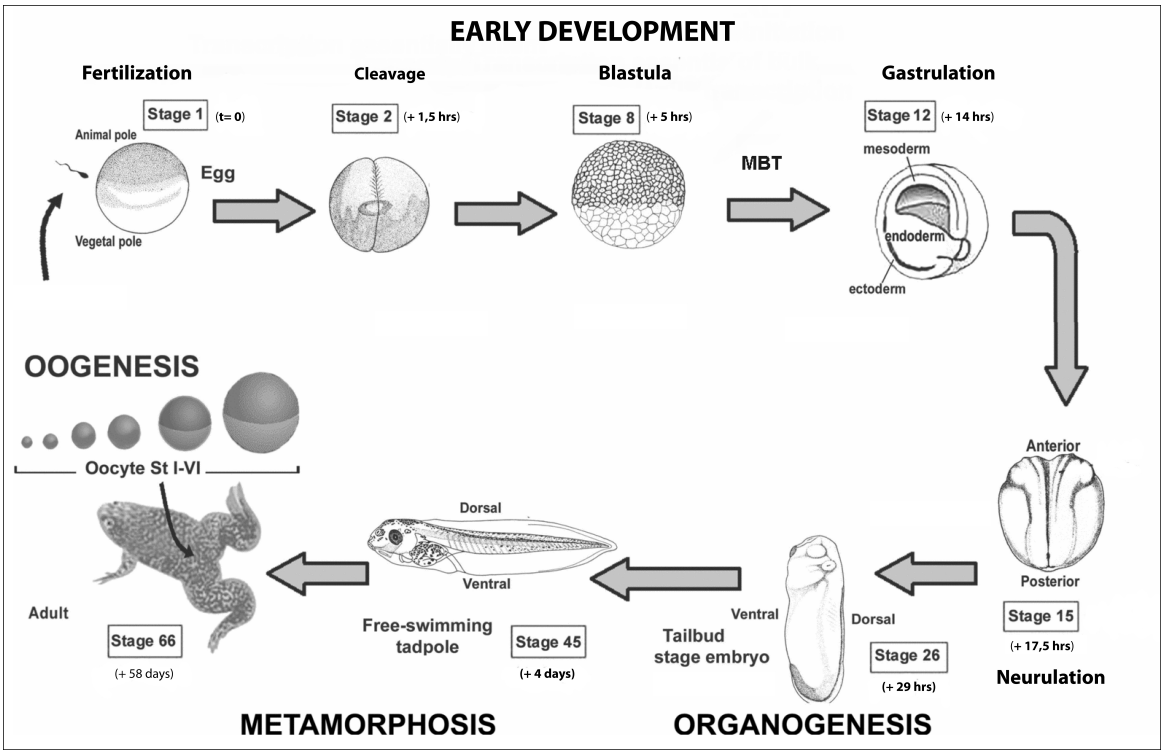

Figure 1. Life cycle of *Xenopus laevis*. Main phases of development are depicted. Stages after Nieuwkoop and Faber (1967) and developmental time (t) post fertilization are shown. After fertilization of the eggs (stage 1), the blastomeres divide until blastula stage (stage 8). Mid-blastula transition (MBT) leads to gastrulation (stage 12). During gastrulation the three germ layers are formed and the body plan is established. Neurulation begins with the formation of the neural plate (stage 15), which folds up to form the neural tube. Organogenesis follows to create a free-swimming tadpole (stage 26), which then undergoes metamorphosis (stage 45). Adapted from Méreau, Le Sommer et al. (2007).

Xenopus eggs present a dark pigmented animal pole and a bright non-pigmented vegetal pole, containing yolk cells. *In vitro* fertilization initiates a sequence of twelve mitotic divisions, which starts one and a half hour post fertilization and ends at mid-blastula stage. At blastula stage, five hours post fertilization, the embryo has been transformed from a single-cell egg to a spherical shaped embryo of 4000 cells (Kirschner, Newport et al. 1985). Activation of zygotic transcription presents the next step in development, called mid-blastula transition (Newport and Kirschner 1982). At mid-blastula stage the embryonic cells are still pluripotent but already biased by inductive events and cell interactions relying on maternal protein molecules (Heasman, Wylie et al. 1984).

Subsequently gastrulation begins, establishing the vertebrate basic body plan with its three embryonic germ layers - ectoderm, mesoderm and endoderm - and laying down the primary body axes. Fourteen hours post fertilization gastrulation is

completed. The processes of gastrulation will be described thoroughly in the next paragraph.

Subsequently the neural tube is formed, which will give rise to the brain and the spinal cord. This process is called neurulation. As a next step in development organogenesis occurs, concomitant to the elongation of the main body axis and formation of the postanal tadpole tail. Within four days the *Xenopus* embryo becomes a free-swimming tadpole, which demarcates the end of embryogenesis.

Finally, metamorphosis commences and transforms the tadpole into an adult froglet, which becomes sexually mature within 12 months (Nieuwkoop and Faber 1967).

1.4 Gastrulation

Specification of the heart and blood vessels occurs at the onset of gastrulation in the mesoderm (Sater and Jacobson 1989; Sater and Jacobson 1990) at the same time and location, where MesP1 is expressed (Saga, Hata et al. 1996). Therefore, the processes of gastrulation, specifically the movement of the mesoderm will be described in detail.

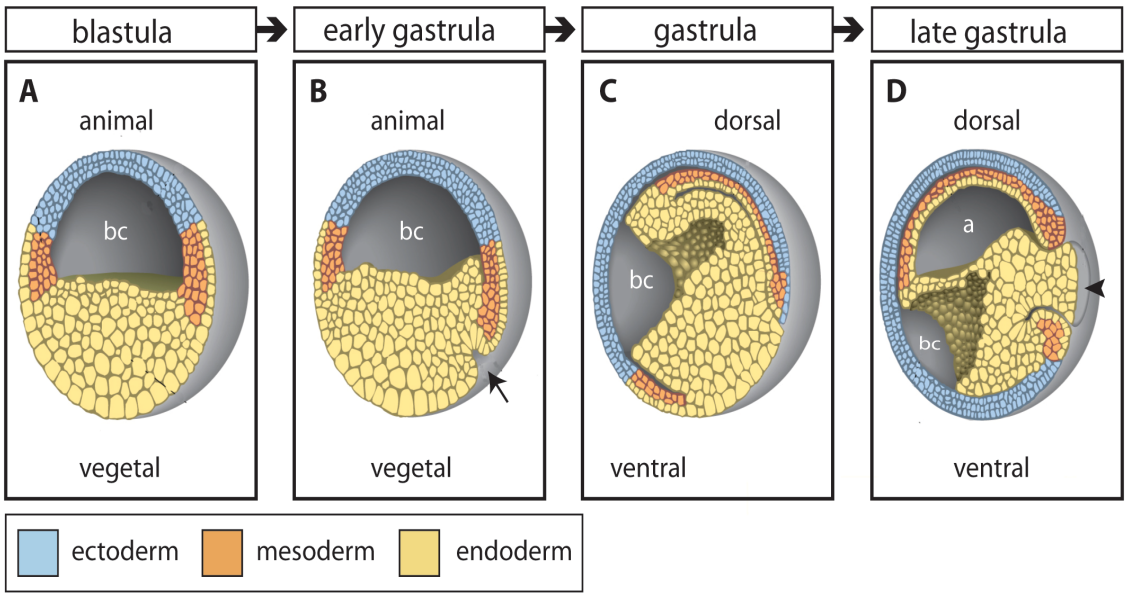

Figure 2. Gastrulation. Gastrulation movements inside the embryo from blastula to late gastrula stages are shown. Anterior to the left, posterior to the right. Gastrulation starts at the vegetal pole by involution of the mesoderm between ectoderm and endoderm (black arrow). The blastopore (black arrowhead) marks the zone of involution. The fluid filled blastocoel (bc) diminishes and the archenteron (a) is formed. Adapted from Wolpert (2011).

As mentioned above, gastrulation transforms the embryo into a multi-layered organism (ectoderm, mesoderm, endoderm) and determines the embryo's main body axes (dorsal-ventral, posterior-anterior). The combined movements and rearrangements of the germ layers during gastrulation place the cells in a specific position to regulate cell fate (Gerhart and Keller 1986) and precede the formation of tissues and organs in the following stages.

The different cell movements inside the embryo from blastula to late gastrula stage are depicted in Figure 2. The blastula embryo (Fig. 2 A) can be divided into three different regions, which encompass the blastocoel, a fluid filled cavity. The animal pole forms the blastocoel roof and will develop into the ectoderm. The vegetal pole represents the bottom of the blastocoel, contains the yolk cells and will give rise to the endoderm. The equatorial region in between is called the marginal zone, which will mainly form the mesodermal layer later on (Heasman 2006).

In early gastrula a so-called blastopore lip appears at the prospective dorsal side of the vegetal zone (Fig. 2 B). The Spemann-Mangold organizer, a crucial signaling center for patterning and regulation of gastrulation (Spemann and Mangold 1924), is formed above the blastopore lip. Bottle cells trigger the initial process of involution of the prospective dorsal mesodermal mantle between ectoderm and endoderm. Through apical constriction, the bottle cells invaginate and ingress into the inner part of the embryo, dragging the cells of the involuting marginal zone with them (Hardin and Keller 1988). The zone of involution begins at the prospective dorsal midline, progresses on both sides and reaches the ventral side two hours later (Fig. 2C, D). The fluid filled blastocoel shrinks, which is due to the involution movements and aquaporin proteins, which pump water out of the cavity. Subsequently, the archenteron, which will give rise to the gut lumen, is formed (Fig. 2D). The mesoderm will be described thoroughly in the following paragraph.

1.4.1 Mesoderm gastrulation

Figure 3 illustrates specifically various properties and movements of the mesodermal layer during gastrulation. As mentioned above, the region at the beginning of gastrulation, which will give rise to mesoderm, is called marginal zone. On the one hand, the marginal zone can be divided into the involuting

marginal zone (IMZ), the non-involuting marginal zone (NIMZ) and the deep zone (DZ). The NIMZ is not shown in Figure 3. The deep zone is situated inside and opposite to the IMZ and forms the front of involution. It will give rise to anterior mesoderm. The IMZ turns inside out: the superficial layer (not shown in Fig. 3) forms the roof of the archenteron. The deeper layer of the IMZ (Fig. 3, red and orange) will become the posterior mesoderm (Gerhart and Keller 1986).

On the other hand, according to its morphogenetic processes during gastrulation, the mesodermal mantle can be separated into two different regions: one is termed "migrating" mesoderm and the other one "extending" mesoderm (Keller and Tibbetts 1989). The "migrating" mesoderm corresponds to the deep zone of the marginal zone (Fig. 3, green) and the "extending" mesoderm to the involuting marginal zone (Fig. 3, red and orange).

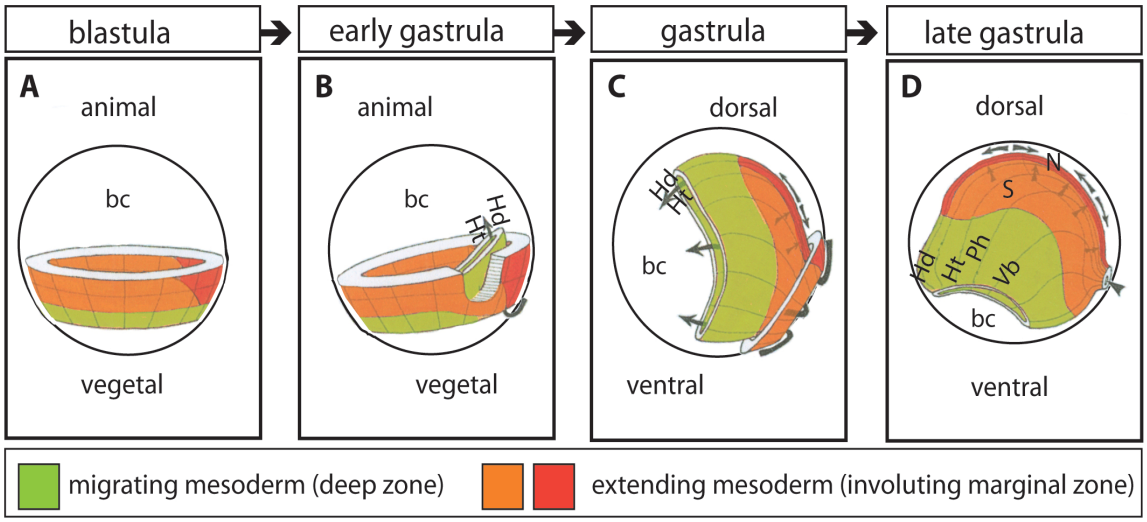

Figure 3. Mesoderm gastrulation. Detailed view of the mesodermal mantle from blastula to late gastrula stage. Anterior to the left, posterior to the right. By migration of the deep zone and convergence extension movements of the marginal zone the different parts of mesoderm are established. At the end of gastrulation head mesoderm (Hd), heart mesoderm (Ht), pharyngeal arch mesoderm (Ph) ventral blood island mesoderm (Vb), somite mesoderm (S) and notochord mesoderm (N) is formed. Blastocoel, bc; Archenteron, a. Adapted from (Keller 1991).

The migrating mesoderm represents the primarily involuting leading edge mesoderm, which migrates anteriorly and spreads on the blastocoel roof. This anterior leading edge mesoderm gives rise to different structures in the anterior end of the embryo: the head mesoderm originates from a middorsal position. On each side laterally of the head mesoderm are the areas of lateral plate mesoderm: Lateral plate mesoderm consists of heart mesoderm dorsally, pharyngeal arch mesoderm and prospective blood islands mesoderm, which continue ventrally (Keller 1976).

The extending mesoderm represents the late involuting mesoderm, which undergoes convergence and extension movements through mediolateral cell intercalation. The extending mesoderm lies in a posterior, dorsal and ventral position at the end of gastrulation and will become somites and notochord mesoderm (Keller and Tibbetts 1989). The somitogenic extending mesoderm involutes ventrally at the end of gastrulation, as gastrulation movements reach the ventral side about two hours later (Hausen 1991). Due to dorsal convergence and extension of the marginal zone, the embryo elongates, the blastopore narrows and consecutively closes at the ventral edge at the end of gastrulation (Gerhart and Keller 1986).

In summary, the question how mesodermal cells become determined to adopt different cell fates is yet not completely understood. One manner to approach this question is identifying the mesodermal regions, which will give rise to the different tissues. Hence, the detailed description of the mesodermal layer during gastrulation was mandatory for an understanding of the results presented in the following chapters.

1.5 Cardiovascular development in *Xenopus*

1.5.1 Cardiogenesis

The heart is the first organ to form during embryogenesis and heart development is highly conserved in all vertebrate organisms. Although anatomical differences exist between vertebrate hearts and the *Xenopus* heart starts to beat late in embryogenesis, the development from early to late stages, up to chamber formation is remarkably similar (Warkman and Krieg 2007).

Figure 4 illustrates cardiac development in the frog embryo. The heart originates from two bilateral patches of dorsal leading edge mesoderm at the onset of gastrulation (Sater and Jacobson 1989; Sater and Jacobson 1990). In the course of gastrulation the cardiac precursor cells migrate anteriorly with the progression of the leading edge mesoderm. During neurulation the two precardiac areas of progenitors proceed ventrally and finally, in the tailbud embryo (NF 22), fuse on the ventral midline, posterior to the cement gland (Keller 1976). In this ventral and anterior position the cells form a continuous sheet of mesodermal tissue, termed

cardiac crescent. The cardiac crescent is folded up in later stages to a linear heart tube.

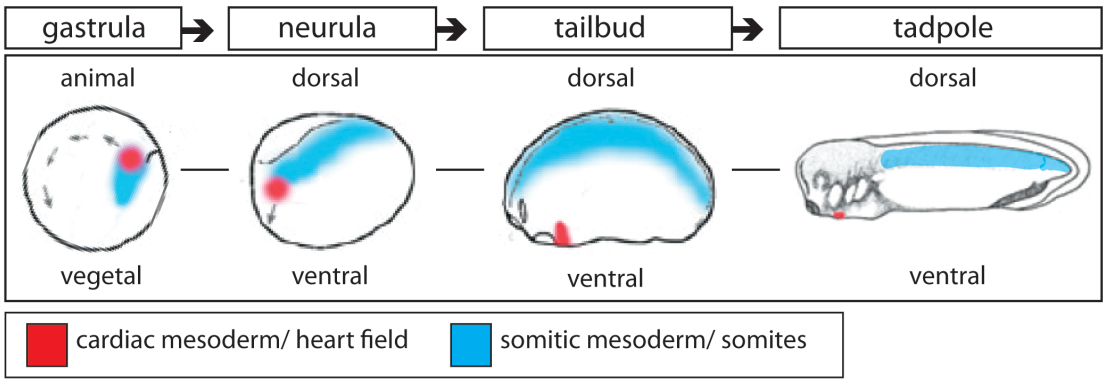

Figure 4: Cardiogenesis. Cardiac mesoderm (red) arises in an animal posterior position at the forming blastopore flanked by the somitic mesoderm (blue). During gastrulation and neurulation the cardiac precursor cells migrate anteriorly and ventrally. At tailbud stage the bilateral cardiac patches fuse on the ventral midline forming the cardiac crescent. Adapted from Mohun (2003).

In mammals the linear heart tube gives rise to the left ventricle and parts of the left and right atria. In the last decade an additional reservoir of multipotent progenitor cells in the adjacent pharyngeal mesoderm has been identified in mammals and termed second heart field (Kelly, Brown et al. 2001; Waldo, Kumiski et al. 2001). This progenitor population progressively adds to the poles of the early heart tube, when the tube undergoes looping. Thereby the heart tube elongates and grows. The anterior part of the second heart field adds to the arterial pole and gives rise to the right ventricle and outflow tract. The posterior part contributes to the venous pole and forms parts of the atria and the atrial septum (reviewed in (Kelly 2012)). In contrast to the mammalian four-chambered heart the three-chambered amphibian heart consists of a single ventricle, two atria, a spirally septated outflow tract and a sinus venosus, with the pulmonary vein (Mohun, Leong et al. 2000). In *Xenopus* a second heart field has been identified (Brade, Gessert et al. 2007), which contributes cells to the outflow tract, but not the ventricle (Lee and Saint-Jeannet 2011). This may imply that the left ventricle in mammals corresponds to the single ventricle in amphibians and that the right ventricle developed during evolution (Kelly 2012). Nevertheless, it is still under debate, whether in *Xenopus* there is a truly regionally different location of progenitor cells outside the cardiac crescent or just different lineages of cells originating from the same region (Gessert and Kuhl 2009).

1.5.2 Vasculogenesis

For proper blood circulation, development of the heart is closely linked to development of blood vessels. Endothelial precursors, which are termed angioblasts, are specified throughout gastrulation from mesodermal cells. These angioblasts differentiate, proliferate and coalesce to build a primary tubular network of blood vessels. The process is termed vasculogenesis. Subsequent to vasculogenesis follows angiogenesis, which describes the process of sprouting and branching of pre-existing vessels in the mature organism (Risau and Flamme 1995). Cardiac and vascular progenitor cells are often termed cardiovascular progenitor cells, which emphasizes their close developmental relationship.

As the progeny of MesP1 expressing mesodermal cells was found to contribute a large part to the vasculature of the mouse embryo (Saga, Kitajima et al. 2000), vasculogenesis in *Xenopus* was examined.

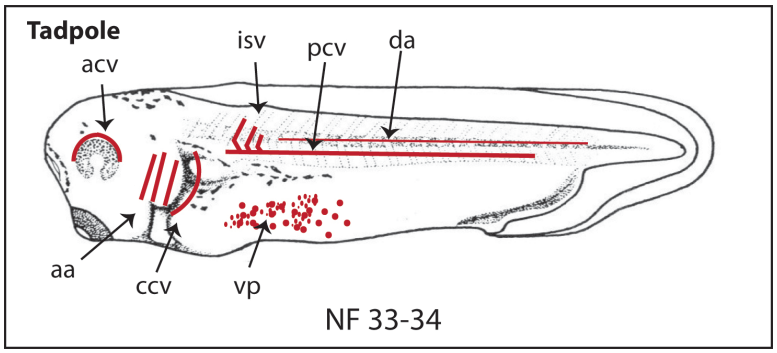

Figure 5: Vasculogenesis. Vascular structures of a tadpole stage embryo are shown. Acv, anterior cardinal vein; aa, aortic arches; ccv, common cardinal vein; isv, intersomitic veins; pcv, posterior cardinal vein; da, dorsal aorta; vp, vascular plexus. Adapted from Mills, Kruep et al. (1999)

Figure 5 depicts the main vascular structures of the *Xenopus* tailbud stage embryo, which consist of two cardinal veins and the aortic arches on each side of the embryo. The anterior cardinal veins are situated in the head, proceed below the brain and join the common cardinal veins in the heart region. The posterior cardinal veins extend horizontally lengthwise on both sides along the notochord and run from the tailbud to the common cardinal veins. The bilateral common cardival veins drain the blood into the heart's sinus venosus. The aortic arches are located ventrolaterally to the anterior notochord region. On each side five arterial arches diverge from the ventral aorta and fuse to create the dorsal aorta (Mills, Kruep et al. 1999; Levine, Munoz-Sanjuan et al. 2003).

Vasculogenesis in the *Xenopus* embryo will be discussed further in chapter 3.3.

1.5.3 Induction of cardiac tissue

The answer to the question why cells adopt different cell fates is most likely to be found on the molecular level of each cell. Due to the rapid progress and extent of research, a complete summary of the genes involved in cardiac development is certainly beyond the capacity of this thesis. The following brief review presents the main principles of induction of cardiac tissue in embryogenesis.

Processes directing cell fate determination can be divided into cell-autonomous signals, which are intrinsic to a cell, and non-cell-autonomous signals, which drive cell fate decision by concentration gradients of morphogenic molecules extrinsic to a cell. Thus, mesodermal movements and cell interactions during gastrulation create a specific signalling environment for each mesodermal region.

In cardiovascular lineage specification different families of proteins create non-cell-autonomous signals. The endoderm underlying the mesoderm and the dorsal midline organizer region secrete proteins, which contain Fibroblast growth factors (FGFs), members of the Transforming growth factor β (TGFβ) superfamily and canonical and non-canonical Wnt signaling.

FGF is essential for early cardiac induction and maintenance (Harvey 2002; Samuel and Latinkic 2009; Deimling and Drysdale 2011), but becomes downregulated later in the myocardium (Watanabe, Zaffran et al. 2012).

Bone morphogenetic proteins (BMPs) and Nodal related proteins belong to the TGFβ superfamily. Gradients of BMPs (Harvey 2002; Klaus, Saga et al. 2007; Prall, Menon et al. 2007) and Nodal proteins (Foley, Korol et al. 2007; Samuel and Latinkic 2009) were shown to play an important role in differentiation of cardiac progenitors.

The wingless-type MMTV integration site (Wnt) family initially establishes a morphogen gradient along the dorso-ventral axis in the embryo. The so-called canonical Wnt-pathway denotes β-catenin mediated intracellular signalling upon binding of different Wnt-ligands to the receptor. Wnt-antagonists like Crescent and Dickkopf1 (Dkk1) have been shown to induce heart formation in tissue explants in *Xenopus* and ES cells (David, Brenner et al. 2008), whereas overexpression of canonical Wnt blocks cardiac differentiation. Thus, a region of low canonical Wnt signalling is required for cardiac formation (Schneider and Mercola 2001; Klaus, Saga et al. 2007). Contrary to the canonical Wnt, the non-canonical Wnt-pathway, which acts through other downstream effectors than β-catenin, appears to have an

enhancing impact on cardiogenesis (Garriock, D'Agostino et al. 2005; Cohen, Miller et al. 2012). The initial broad domain of cells capable of cardiac differentiation is gradually restricted as development progresses via non-cell-autonomous cues. Most of the intrinsic cell-autonomous molecules directing cell fate are transcription factors. Among those involved in cardiovascular development are the GATA-family (Latinkic 2003; Peterkin, Gibson et al. 2005; Zhao, Watt et al. 2008; Laforest and Nemer 2011) and T-box transcription factors (Brown, Martz et al. 2005). Two transcription factors provide a link between the early specification of cardiac fate during gastrulation and the later onset of cardiac differentiation in tailbud stage. These are, the homeobox transcription factor Nkx2.5 and the LIM homeodomain transcription factor Islet1 (Isl.1), which will be described later.

In summary, a fine-tuned balance between FGF and Nodal/BMP signalling adjusted by inputs from Wnt/β-catenin and FGF signalling, form the extrinsic setting for cardiovascular differentiation (Noseda, Peterkin et al. 2011), which induces MesP1 expressing progenitor cells. Moreover it was reported that MesP1 was induced by the T-box transcription factors Eomesodermin (Costello, Pimeisl et al. 2011; van den Ameele, Tiberi et al. 2012) and Brachyury(T) (David, Jarsch et al. 2011). MesP1 then activates the main cell-autonomous and non-cell-autonomous pathways.

In ES-cells MesP1 activates many key genes (e.g. Nkx2.5, Isl.1 and GATA4) of the cardiac transcriptional network by direct binding to promoter sites (Bondue, Lapouge et al. 2008), and initiates activation of structural cardiac genes (Lindsley, Gill et al. 2008).

1.5.4 Molecular basis of mesodermal movements

The molecular basis underlying the complex morphogenetic movements during gastrulation is not well characterized (compare (Wang and Steinbeisser 2009).

The transmembrane protein paraxial protocadherin (*PAPC*) has been assumed to play an important role in gastrulation movements in *Xenopus laevis*.

Protocadherins comprise a large subfamily of cadherins. In contrast to classical cadherins, protocadherins consist of up to seven cadherin-like repeats in their extracellular domain, a single transmembrane domain and a cytoplasmatic signalling domain (Chen and Maniatis 2013). The extracellular domain of *PAPC*

was shown to mediate cell sorting (Chen and Gumbiner 2006), while the intracellular domain promotes convergence extension and tissue separation during gastrulation (Kim, Yamamoto et al. 1998; Medina, Swain et al. 2004; Unterseher, Hefele et al. 2004). These features are prerequisites for the coordinated movement of the mesoderm as a cohesive layer during gastrulation. Furthermore, the gastrulation movements set up concentration gradients of signalling molecules and cell-cell interactions, which are essential for subsequent tissue formation.

1.6 MesP1 homologue in *Xenopus laevis*

The genome of the *Xenopus* embryo contains three genes, which were classified to as potential homologues of mammalian MesP1 due to their sequence similarity. These genes were termed *mespa*, *mespb* and *mespo*. The *mesp*-family members *mespb* and *mespo* have been characterized in the context of somitogenesis in Zebrafish (Sawada, Fritz et al. 2000; Terasaki, Murakami et al. 2006) and *Xenopus* (Wang, Li et al. 2007). *Mespa* was found out to play a role in somitogenesis as well (Moreno, Jappelli et al. 2008; Hitachi, Kondow et al. 2009). However, it was not mentioned in the context of cardiogenesis in *Xenopus*.

1.7 Objectives

Based on our finding that *mespa* is the functional homologue of mammalian MesP1 in *Xenopus laevis*, the work described in the following chapters attempts to characterize downstream target genes and transcriptional pathways of *mespa* in cardiovascular development.

In order to examine *mespa's* different properties, loss and gain of function experiments were performed, which rely on microinjection of Morpholino oligonucleotides for gene knockdown and microinjection of mRNA for transient gene upregulation, respectively. RNA *in situ* hybridization provides a versatile means to examine the different phenotypes and to analyze gene expression pattern.

Since cardiovascular development is a highly complex process, specific aspects of *mespa* function were investigated. The following aspects will be addressed in this study:

First, *mespa*'s known role in cardiogenesis was analysed into further detail. The *wnt*-antagonist *dkk1* was investigated to establish a signalling pathway, which has been described *in vitro* in ES cells (David, Brenner et al. 2008), in embryonic development *in vivo*. Essential cardiac transcription factors as *isl.1* and *nkx2.5* were analysed as novel potential target genes during gastrulation.

Second, *mespa*'s function in early and late vasculogenesis was examined, since a large amount of MesP1 positive cells were found in the vasculature of the mouse embryo (Saga, Kitajima et al. 2000). Hence, a possible interaction between *mespa* and the *apelin receptor*, a core molecule in vasculogenesis, was analysed.

Third, MesP1 was described to have an effect on cell migration (Saga, Miyagawa-Tomita et al. 1999), which plays a pivotal role especially in gastrulation and the formation of the heart. However, no downstream target of MesP1 that could mediate cell movement behaviour has been found to date. Therefore the *paraxial protocadherin* (*PAPC*) was investigated as potential target gene for *mespa* mediated cell movement.

Finally, as my results indicated that MesP1 has a broader function in development than promoting only cardiovascular differentiation a novel function of *mespa* in mesoderm induction and skeletomyogenesis was analysed.

2. Materials and Methods

2.1 Laboratory Equipment

The following laboratory equipment was used for molecular biological assays and embryological techniques. Manufacturer's name is indicated in brackets.

Laboratory Equipment	
Camera	Leica DFC 310FX (Leica).
Centrifuges	Eppendorf centrifuge 5417C (Eppendorf); Micro 22R (Hettich Zentrifugen); Sigma 3-18 (Sigma Laborzentrifugen); PicoFuge (Stratagene)
Developer	Curix-60 (Agfa)
Gel documentation System	G:BOX (Syngene)
Glass needles	Glass 1BBL W/FIL 1.0 mm (World Precision Instrument)
Incubators	Heraeus (GS); Standard-430 (GS)
Microneedle Puller	P-87 (Sutter Instrument)
Micromanipulator	Mm-33 (Science Products); Oxford micromanipulator (Micro Instruments, Oxford, UK)
Microscopes	Stereomicroscope Stemi SV11 (Zeiss); Stereo-fluorescence System M205FA (Leica)
Pneumatic Micro-Injector	Pli-100 (Digitimer Ltd.).
Software	Illustrator CS5 (Adobe); Photoshop CS5 (Adobe); Office 2008 for Mac (Microsoft); Endnote X4 (Thomson); Leica Application Suite V3 3.0 (Leica)
Spectrophotometer	Nanodrop ND-1000 (PeqLab)
Thermo shakers	Multitron (Infors HT); Thermo Shaker TS-100 (PeqLab)
Vibratome	Vibratome 1000 (Technical Products International, INC.)
Water bath	Minitherm 2 (Dinkelberg)

2.2 Reagents

2.2.1 Chemicals

The subsequent chemicals were ordered from Fluka, Merck, Sigma or USB.

Chemical	**Company**
Agar	Difco
Agarose	Gibco/BRL
Ampicillin, Streptomycin	Difco
Chicken serum, Lamb serum	Gibco/BRL
Glycogen	Fermentas
Chorionic Gonadotropin (Ovogest)	MSD Animal Health
Levamisol	Vectro Laboratories
Triazol Reagent	Invitrogen
Tricaine methanesulfonate	PharmaQ LTD

2.2.2 Enzymes and Proteins

Enzyme/Protein	**Company**
Albumin fraction V	Roth
Alexa Fluor 488, Alexa Fluor 594	Invitrogen
Leupeptin, Pepstatin	Sigma
Phusion High-Fidelity DNA Polymerase	Finnzymes
Proteinkinase K	Sigma
rAPid Alkaline phosphatase	Roche
Restriction endonucleases with 10x restriction buffer system	NEB, Roche, Ferments
RNaseA	Sigma
RNasin	Promega
RNase free DNase Set	Qiagen
T3, T7, SP6 RNA Polymerase	Promega
T4 DNA Ligase	Roche

2.2.3 Kits

Kit	Company
DyNAmo cDNA Synthesis Kit	NEB
DNA extraction from agarose gel	NEB
DNA plasmid miniprep	NEB
QIAquick Gel extraction kit	Qiagen
QIAprep Spin miniprep Kit	Qiagen
RNeasy mini kit	Qiagen

2.2.4 Bacteria

For transformation the following E. coli strain was used:

Strain: XL1Blue

Genotype: endA1 gyrA96(nalR) thi-1 recA1 relA1 lac glnV44 F'[::Tn10proAB+ lacIq " (*LacZ*)M15 Amy CmR] hsdR17(rK- mK+)

Provider: Stratagene

2.3 DNA templates

2.3.1 Plasmids for *in vitro* transcription

Plasmid Name	Cloning Sites	Restriction Enzyme	Polymerase
pCS2-**FL-*PAPC***	EcoRI/XhoI	Not1	SP6
pCS2-***MyoD***	EcoRI/XbaI	xbaI	SP6
pCS2-**n-ßGal**		Not1	SP6
pSP6-Globin-**XL*Mespa*** IRES-EGFP	Sac1/Sal1	Afl2	SP6
pSP6-Globin-Δ5'UTR-**x*Mespa***-IRES-EGFP	Sac1/Sal1	Afl2	SP6
pSP6-Globin-**XL*Mespb***-IRES-EGFP	Sac1/Sal1	Afl2	SP6
pSP6-Globin-**XL*Mespo***-IRES-EGFP	Bgl2/Sal1	Afl2	SP6

2.3.2 Plasmids for *in situ* hybridization probes

Plasmid Name	Cloning Sites	Restriction Enzyme	Polymerase
pBS-**FL-*PAPC***	EcoRI/XhoI	Not1	T7
pBSK2-**xIsl1**	EcoRI/XhoI	EcoRI	T7
pBSK-**XL*Mespa***	EcoRI/XhoI	EcoRI	T7
pBSK-**XL*Mespo***	EcoRI/XhoI	EcoRI	T7
pCS2-**X*MyoD***b	EcoRI/XbaI	EcoRI	T7
pGEM3z-**x*Nkx2.5***	EcoRI	HindIII	T7
pIBI31wt-**XMsr**		BglII	T7
pRN-**Xdkk1**		BglII	T7
pSP73-**X*Myf5***-2	EcoRI/BamHI	EcoRI	SP6
pSP72-***Xbra***	EcoRI	HindIII	T7

2.4 Morpholino oligonucleotides

Morpholino oligonucleotides were ordered from Gene Tools (http://www.genetools.com/). "X" refers to *Xenopus laevis*. Morpholino oligonucleotides were dissolved in milliQ water to a final concentration of 3mM, aliquoted in 5µl aliquots and stored at -20°C. *Xmespa*, x*mespo*, x*mespb* and control morpholinos were injected from 10 to 20ng/embryo. Their translation-blocking function was demonstrated by coupled *in vitro* transcription/translation assays (Promega). Lineage tracing for unilaterally injected embryos was achieved by coinjection of Alexa Flour® 488 Dextrane (Invitrogen) or *LacZ* mRNA (100-150pg/blastomere), followed by β–Galactosidase staining.

Morpholino	Sequence	Target genes
Control MO	5'-CCTCTTACCTCAGTTACAATTTATA-3'	-
x*mespa* MO	5'-AACTAGGAATAAACAAGACATGGAT-3'	x*mespa*, x*mespa*'
x*mespb* MO	5'-GACAACATGGATTTCTCTCCAACAA-3'	x*mespb*, x*mespb*'
x*mespo* MO	5'-TACTACTGATGGAGACTCTGCACCA-3'	x*mespo*, x*mespo*'

2.5 Antibody

Whole-mount RNA *in situ* hybridizations were performed as described. The following antibody was used: Sheep anti-digoxigenin Fab fragment, conjugated with alkaline phosphatase (1:2000, Roche).

2.6 Molecular biological methods

2.6.1 Solutions

Alkaline Phosphatase (AP) buffer	100mM Trichlorethane Tris/HCl, pH 9.5 100mM NaCl 50mM $MgCl_2$ 0,1% Tween 20
Embryo bleaching solution	1% H_2O_2 5% Formamide 0,5x SSC
DEPC-H_2O	MilliQ water with 0.1% Diethylpyrocarbonate (DEPC), stirred at Room Temperature (RT) overnight and autoclaved afterwards.
DIG NTP mixture (10mM)	10mM ATP, CTP, GTP 6,5mM UTP 3,5mM Dig-11-UTP
Hybridization solution	5x SSC 50% Formamide 1% Boehringer-Mannheim Block 0,1% Torula yeast RNA 0,01% Heparin 0,1% Tween-20 0,1% CHAPS 5mM EDTA
Loading dye for gel electrophoresis	50% Glycerine 10mM EDTA 0.05% Orange G

Maleic Acid Buffer (MAB)	500mM Maleic acid 750mM NaCl, pH 7,6 at 23°C
MEMFA	100mM 3-(N-Morpholino)-propanesulfonic acid (MOPS) 2mM EGTA 1mM $MgSO_4$ 3,7% Formaldehyd pH 7,4
MOPS buffer	200mM MOPS 50mM Natriumacetat 10mM EDTA
Paraformaldehyde	4% Paraformaldehyde in PBSw
Posphate buffered saline (PBS)	137mM NaCl 2,7mM KCl 8mM Na_2HPO_4 1,7mM KH_2PO_4; pH 7,2
PBSw	1x PBS 0,1% Tween-20
Proteinkinase K	10µg/ml Proteinkinase K in PBSw
SSC (20x)	3M NaCl 0,3M Sodium Citrate pH 7,0
Staining solution	1ml AP Buffer 3,5µl 5-Bromo-4-Chloro-Indolylphosphate (BCIP) 50mg/ml in 100% Dimethylformamide stored at -20°C (Biomol) 4,5µl Nitroblue Trazoliumchloride (NBT) 75mg/ml in 70% Dimethylformamide stored at -20°C (Biomol).
TE buffer	1mM EDTA 10mM Trichlorethen Tris/HCl pH 9,5 pH 8,0 at RT
TBE buffer	83mM Borate 100mM Trichlorethen Tris/HCl pH 9,5

	0,1mM EDTA pH 8,6 at RT

2.6.2 DNA techniques

2.6.2.1 Agarose gel electrophoresis

DNA fragments were electrophoresed in horizontal 1% TBE agarose gel (Biozym) depending on the size of the respective fragment. The Ethidium bromide concentration in the gel was 0.25µg/µl. The samples were mixed with 1x loading dye and 1Kb or 1000bp DNA ladder (Fermentas) were used as size standard.
Afterwards, DNA fragments were visualized by UV light and the gels were photographed using the Geldocumentation System G-BOX (Syngene).

2.6.2.2 Isolation of DNA fragments from agarose gels

The appropriate bands of the DNA fragments were cut out from the agarose gel under UV light. The DNA was extracted using QIAquick Gel extraction kit (Qiagen), according to the manufacturer's protocol.

2.6.2.3 DNA restriction digest

For plasmid linearization or cloning restriction digest was carried out in the following reaction set-up for 1 hour at 37°C:

Component	**40µl reaction**
Plasmid template	10µg
Buffer 10x	4µl
Restriction enzyme 20U/µl	3µl
H_2O	Ad to 40µl

By loading an aliquot of the digested template side by side with the same amount of unlinearized plasmid from a mock reaction (no restriction enzyme) on 1% agarose gel complete linearization was controlled. Linearized plasmids were stored at -20°C.

2.6.2.4 Isolation of plasmid DNA from E.coli

Plasmid DNA preparation from E.coli was carried out using the DNA QIAprep Spin minipreparation Kit (Qiagen) according to the manufacturer's protocol.

2.6.3 RNA techniques

2.6.3.1 *In vitro* transcription of sense RNA

In order to synthesize capped sense-strand run-off transcripts for microinjection, the following setup was used:

Component	**50µl reaction**
Linearized DNA plasmid	2µg
Transcription buffer 5x	10µl
NTPs-Mix 100mM	10µl
DTT 100mM	5µl
G(5')pppGcap analog 25mM	5µl
RNasin 40U/µl	0.5µl
RNA-Polymerase 10-20U/µl	2µl
DEPC-H_2O	Ad to 50µl

The setup was incubated for 2 hours at 37°C. After two hours, an additional 1µl of RNA polymerase was added. The reactions were incubated overnight at 37°C. An on-column DNA digestion step was carried out. Afterwards, the transcribed mRNA was purified using RNeasy mini kit (Qiagen) according to the manufacturer's protocol. The concentration of the mRNA was measured using Nanodrop ND-1000 Spectrophotometer. The samples were stored at -80°C.

2.6.3.2 *In vitro* transcription of digoxygenin-labelled RNA

Plasmids were linearized as described and antisense RNA containing digoxgenin-labelled uridin was synthesized for RNA *in situ* hybridization. The reaction setup was as following:

Component	50µl reaction
Linearized DNA plasmid	2µg
Transcription buffer 5x	10µl
Dig-NTPs mix 10mM	5µl
DTT 100mM	5µl
RNasin 40U/µl	0.5µl
RNA-Polymerase 10-20U/µl	2µl
DEPC-H_2O	Ad to 50µl

The reactions were incubated for 2h at 37°C. After two hours, an additional 1µl of RNA polymerase was added. The reactions were incubated overnight at 37°C. An on-column DNA digestion step was carried out.

The transcribed mRNA was purified using RNeasy mini kit (Qiagen) according to the manufacturer's protocol. An 1µg aliquot of the transcription product was used for quality control by electrophoretic gel analysis. The synthesized dig-RNA was mixed 1:1 with formamide and stored at -20°C.

2.6.3.3 RNA *in situ* hybridization

Embryos were fixed in freshly made MEMFA for 1.5 hours at room temperature in 5ml storage vials (Roland Vetter Laborbedarf) on a rotating wheel. Tissue explants were fixed in MEMFA for 30 minutes and then processed like embryos. After fixation embryos were washed in 1x PBS for 3x 5minutes with rocking. PBS was replaced by absolute ethanol for dehydration. The samples were stored at -20°C at least overnight to dissolve the lipid membranes. Rehydration was achieved by serial washes in decreasing ethanol concentrations (75%, 50%, 25%) in 1x PBSw. After 3 washes in PBSw, the solution was exchanged with PBSw + 10µg/ml Proteinase K and incubated for 20 min at room temperature (5 min incubation for explants). Embryos were then washed twice in PBSw and refixated with 4% paraformaldehyde in PBSw for 20 min. Samples were washed five times in PBSw, 5 min for each step. PBSw was replaced by hybridization solution, first a 50% concentration, then 100% hybridization solution, each wash for 3 min.

The solution was discarded and 0.5ml of fresh hybridization solution added to each vial. Embryos were incubated at 65°C for one hour in a water-bath to inacti-

vate endogenous phosphatases. Subsequently, they were prehybridized at 60°C for 2-6 hours in a water-bath. To 100µl of hybridization solution, 30-50ng of digoxigenin-labelled RNA probe was added, heated to 95°C for 3 min, cooled down and then added to the embryos in the hybridization solution. The embryos were incubated at 60°C with the digoxigenin-labelled RNA probe in the water-bath overnight.

Afterwards, the hybridization solution containing the dig-probe was transferred into a new 1.5ml eppendorf tube, stored at -20°C and reused 3-4 times.

Samples were rinsed for 10 min at 60°C in fresh hybridization solutions and washed three times in 2x SSC solution for 20 min at 60°C. Afterwards they were washed twice for 30 min at 60°C in 0.2x SSC and then in MAB solution for 10 min. MAB solution was replaced with 1ml of 2% BMB blocking solution (Böhringer Mannheim) containing MAB. The embryos were agitated for 1 h at room temperature on a rocking table. Solution was replaced by fresh MAB containing 2% BMB blocking solution and the affinity-purified anti-digoxigenin antibody coupled to alkaline phosphatase in a 1:2000 dilution. For antibody binding of the hybridized probe the embryos were incubated for four hours with rocking.

By washing 6-7 times for one hour in MAB excess of antibody was removed. Then the embryos were washed twice for 5 min in alkaline phosphatase buffer (AP buffer) and equilibrated for 15 min in AP buffer. For the chromogenic reaction the solution was replaced by 0.5ml AP buffer containing 4.5µl/ml NBT and 3.5µl/ml BCIP and embryos incubated in the dark. Colour reactions were stopped at near-saturation by washing the embryos three times for 10 min in 1x PBS. Embryos were subsequently fixed in MEMFA for at least 90 min on a rotator.

In order to remove embryonic pigment, the embryos were washed twice in 1x PBS containing 75% ethanol for 30 min and incubated in bleaching solution on a light box for at least 3 hours. Finally, samples were washed three times in 1x PBS and photographed under a Fluorescence Stereomicroscope (Leica M205FA).

2.7 Histological techniques

2.7.1 Solutions

Albumin	Albumin Fraktion V (Roth)

β-Galactosidase staining solution	5mM $KuFe(CN)_6$ 5mM $K_3Fe(CN)_6$ 2mM $MgCl_2$ 0.25mM X-Gal Add 1x PBS
Glutaraldehyde	Glutaraldehyde 25% (Sigma-Aldrich)
MEMFA	100mM 3-(N-Morpholino)-propanesulfonic acid (MOPS) 2mM EGTA 1mM $MgSO_4$ 3,7% Formaldehyd pH 7,4 Freshly prepared
PBS	137mM NaCl 2,7mM KCl 8mM Na_2HPO_4 1,7mM KH_2PO_4, pH 7,2
PBSw	1x PBS 0,1% Tween-20
Paraformaldehyde (PFA)	4% Paraformaldehyde in PBSw
X-Gal (5-Bromo-4-chloro-3-indolyl-DGalactosidase)	40mg/ml X-Gal in 25ml Dimethylsulfonoxid

2.7.2 β-Galactosidase staining

For lineage tracing of the injected region the embryos were co-injected with nuclear RNA of the β-Galactosidase gene (*LacZ* gene). The embryos were fixed for 30 min in MEMFA at room temperature and subsequently washed three times in 1x PBS for 30 min. For the colour reaction 1ml of β-Galactosidase staining solution was added to each sample and incubated in the dark. The vials were periodically checked for the appearance of the staining, which usually occurred after 30-40 min. Then the reaction was stopped by washing three times in PBS. The embryos were fixed for 30 min in MEMFA. Before transferring the embryos into ethanol they were washed three times in PBS, and stored in 100% ethanol at -20°C.

2.7.3 Vibratome sections of embryos

After whole mount RNA *in situ* hybridization for *mespa* as described above, embryos were rinsed in a gelatine/albumin mixture (2.2g of gelatine dissolved in 500ml 1x PBS subsequently supplemented with 135g of albumin (Roth) and 90g of Sucrose). To 2ml of albumin/gelatine mixture 100-200µl of 25% glutaraldehyde (Sigma-Aldrich) was added. Then the solution was quickly vortexed and poured into a small plastic tray in order to create a bottom layer. Embryos were placed on top and positioned within the solidifying layer to the desired orientation. Another aliquot of albumin/gelatine mixture containing 25% glutaraldehyde was prepared and poured onto the embryos forming a second layer. The plastic tray containing the embedded embryo was allowed to stand for at least 30 min. The gelatinized block was cut out under a dissecting microscope and glued onto a metal support. Sections of 30-50µm were created using a Vibratome 1000 (Technical Products International, INC.). The slices were transferred onto glass slides, dried, covered with X-TRA Kit mounting medium (Medite) and images taken with a Leica M205FA Fluorescence Stereomicroscope.

2.7.4. Fluorescent labelled embryos

Embryos injected with a fluorescent dye, which were not subjected to *in situ* hybridization, were fixed for two hours in PFA. Subsequently they were photographed with a Fluorescence Stereomicroscope (Leica M205FA) using either the green filter (Alexa Fluor 488 dye) or the red filter (Alexa Fluor 594 dye).

2.8 Embryological methods

2.8.1 Solutions

Cysteine solution	0.1x MBS 2% L-Cysteine (Sigma) pH 7.8 at RT
Chorionic Gonadotropin (Ovogest)	1000 IU/ml in ddH_2O
Modified Barth's Saline (MBS, 1x)	88mM NaCl 1mM KCl

	2.5mM $NaHCO_3$ 1mM $MgSO_4$ 0.7mM $CaCl_2$ 5mM HEPES pH 7.6 at RT
Modified Barth's Saline (MBS) high salt (1x)	1x MBS 50mM NaCl
Tricaine methanesulfonate	3-aminobenzoic acid ethyl ester methanesulfonate

2.8.2 Experimental animals

Adult wild type *Xenopus laevis* frogs were obtained from commercial breeding farms (Nasco, *Xenopus* Express). Animal work has been conducted in accordance with Deutsches Tierschutzgesetz and the Regierung von Oberbayern has licensed experimental use of *Xenopus* embryos. Animals were kept at a water temperature of 17-19°C in a population density of 5l water per frog. Three times per week the frogs were fed with Pondsticks Premium Brittle (Interquell GmbH, Wehringen).

2.8.3 Superovulation of female frogs

Xenopus laevis females were stimulated to ovulate by injection of 500-800 units of Chorionic gonadotropin into the dorsal lymph sac. After incubation overnight at 18-20°C water temperature, egg laying started about 12-16 h later.

2.8.4 Excision of testis

A male frog was anaesthetized in 0.5% Tricaine methanesulfonate for 30 min. The animal was killed by neck fracture. Through an incision of the abdomen the two testes were taken from the retroperitoneal fat body, to which they are connected. The testes from X. *laevis* were stored in MBS/CS at 4°C for a maximum of 5 days.

2.8.5 *In vitro* fertilization of eggs

Freshly laid eggs from a superovulated female were mixed with a small piece of testis minced in 1x MBS. After 5 min the eggs were coated with 0.1x MBS and incubated at 16-23°C in cultivation petri dishes.

2.8.6 Removal of the egg jelly coat

The jelly coat is a multi-layered protein network with elastic properties, which encapsulates the eggs. It needs to be removed prior to microinjection. One hour past fertilization the jelly coat was dissolved by gently swaying the embryos in Cysteine solution for about 5 min. Embryos were washed three times in 0.1x MBS before further use.

2.8.7 Microinjection of embryos

2.8.7.1 Injection needles

An injection needle was made from a glass capillary (World Precision Instrument, Inc.; glass thin wall W/Fil 1.0mm, 4IN) using the Microneedle Puller (settings: heat: 800; pull: 35; vel: 140; time: 139; Sutter Instrument, model P-87). The needle was placed in a fixed holder (Medical System, model Pi-100) or put into a free-hand needle holder next to the microscope. The tip of the needle was broken back carefully with Dumont-tweezer forceps until the needle produced a 5nl drop with one injection pulse (30psi/30ms).

2.8.7.2 Microinjection technique

Injection needles were filled from the front using the “fill”-function of the Pi-100 injector. Morpholino containing probes were held at 37°C until injection to prevent precipitation. RNA probes were kept on ice. Embryos were injected at two to sixteen cell stage into specific blastomeres with injection volumes ranging from 5nl to 2.5nl. For lineage tracing either 0.5% Alexa (green Alexa Fluor A488) or 150pg of *LacZ* mRNA was added to the injection solution. For rescue experiments 250pg of MO-insensitive *mespa* mRNA was added to the injection solution.

After injection, around 50 embryos were cultivated in 0.1xMBS in a 60mm petri

dish at 16-23°C. The petri dish floor was covered with 1% agarose in 0.1x MBS. The saline was exchanged every day. Uninjected and injected embryos from the same batch were cultured in parallel.
At the desired stage, injected embryos were sorted into right- or left-injected cohorts based on Alexa-Fluor488 fluorescence or alternatively β-Galactosidase staining was performed.

2.8.8 Animal cap explants

For induction studies embryos were injected into the animal pole four times with 2.5nl *mespa* mRNA, *mespo* mRNA, *mespb* mRNA, *myoD* mRNA or *GFP* mRNA, according to the experimental setup (1ng of each mRNA per embryo) at two- to four-cell stage. When the embryos reached the blastula stage (NF 8.5) the vitelline membrane was removed manually in 60mm petri dishes covered with 1% agarose in 0.5x MBS. By two to three cuts with Dumont tweezers the animal cap was separated from the embryo and singly transferred into 1% agarose grids in petri dishes containing 0.5x MBS. The tissue explants were cultivated in 0.5x MBS until control siblings reached the required stage.

3. Results

MesP1 is a key transcription factor in cardiogenesis (Saga, Miyagawa-Tomita et al. 1999; Saga, Kitajima et al. 2000) and potent enough to stimulate the expression of cardiac and vascular markers in murine ES cells (Bondue, Lapouge et al. 2008; David, Brenner et al. 2008; Lindsley, Gill et al. 2008) and human iPS cells (Hartung, Schwanke et al. 2012). Moreover, MesP1 was shown to be have broader roles in mesodermal development (Lindsley, Gill et al. 2008; Chan, Shi et al. 2013).

The goal of this project was to characterize the transcription factor *mespa*, the functional homologue of MesP1 in *Xenopus laevis.*

A special focus was placed on *mespa*'s role in cardiogenesis in *Xenopus* and on providing new insights into *mespa*'s functions in vasculogenesis, morphogenesis, as well as mesoderm induction and skeletomyogenesis *in vivo*. Therefore, each of these developmental roles was analysed by spatial and temporal gene expression under normal and *mespa* loss and gain of function conditions.

3.1 Gene expression analysis of *mespa*

Mespa gene expression in *Xenopus* has been described in relation to somitogenesis Gene expression pattern of *mespa* during development was examined in detail, in order to correlate the spatial and temporal areas of transcription with the transcription factor's putative functions in early embryonic development.

3.1.1 RNA *in situ* hybridization of *mespa*

RNA *in situ* hybridization was used to detect *mespa* gene transcription. Figure 6 shows different views of consecutive developmental stages of gastrulation. At the beginning of gastrulation, *mespa* is expressed in the preinvoluted and involuted mesoderm in an open annular shape surrounding the blastopore leaving out the dorsal organizer region (Fig. 6 A-E). This pattern resembled those of other mesodermal genes, like *myoD*, which is a bHLH-family core transcription factor in skeletomyogenesis (Weintraub, Davis et al. 1991). A link between mespa and *myoD* will be adressed later on (see chapter 3.5).

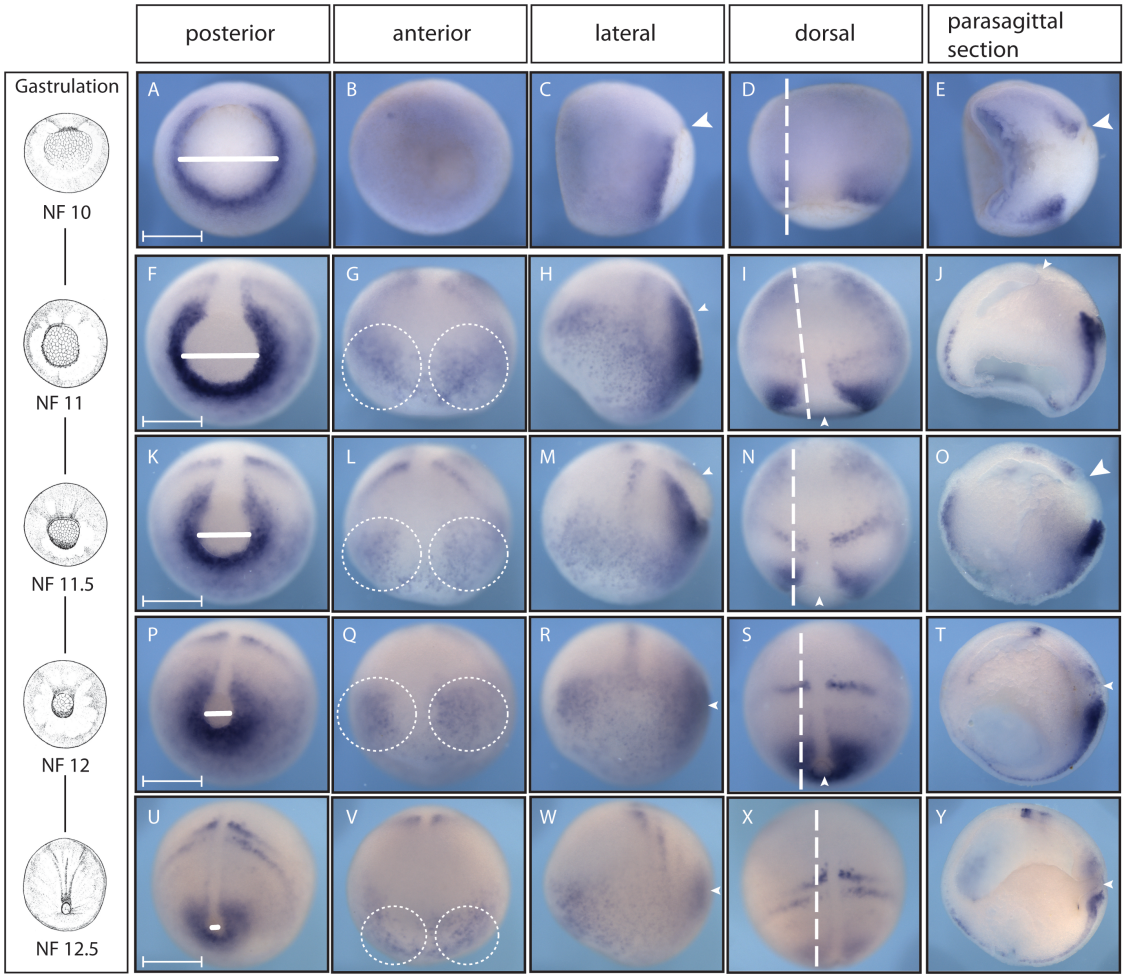

Figure 6. *Xenopus laevis mespa* gene expression during gastrulation. *Mespa* mRNA expression was detected by RNA *in situ* hybridization at the indicated developmental stages **(A-Y)**. Panels show different views according to the denotation at the top. *Mespa* mRNA was expressed from early gastrula stage on (NF 10) **(A-E)** and primarily expressed in an annular region surrounding the blastopore **(A)** excluding the dorsal notochordal zone. Parasagittal sections **(E, J, O, T)** show that this expression was restricted to the mesodermal layer. *Mespa* was both present in the involuting, as well as in the involuted dorsal and ventral mesoderm **(J)**. Lateral examinations **(C, H, M, R, W)** revealed *mespa* gene expression in the lateral mesoderm. Within the course of gastrulation *mespa* positive cells were visible in the anterior part of the embryo **(G, L, Q, V)**, corresponding to leading edge mesoderm. As gastrulation proceeded, the blastopore was narrowing. At NF 11 **(H, I)** *mespa* mRNA was detected in the presumptive paraxial mesoderm. Towards the end of gastrulation *mespa* expression was diminished and present in two bands in the somitic mesoderm, in a collar circulating the blastopore, in ventral mesoderm and anterior leading edge mesoderm **(U-Y)**. Arrowheads indicate blastopore. Dashed circles mark anterior expression in leading edge mesoderm. Dotted lines indicate plane of section. Scale bars: 500 µm.

At midgastrula *mespa* mRNA was additionally detected in the presumptive paraxial mesoderm (Fig. 6 H, I). As gastrulation proceeded, *mespa*-expressing tissue continued to involute on the dorsal and ventral side and migrated anteriorly. This was confirmed by parasagittal sections, which revealed *mespa* positive cells in the anterior leading edge mesoderm (Fig. 6 J, O). These positive cells corresponded to expression in the anterior region of the embryo, which could be seen from outside in a punctate pattern (Fig. 6 G, L). The sections confirmed that gene transcription was only present in the mesodermal layer. Later on, expression was also observed

in lateral parts of mesoderm, which will become lateral plate mesoderm (Fig. 6 H, M, R, W).

Towards the end of gastrulation *mespa* expression was detected in a mesodermal collar circulating the blastopore, which expanded dorsally along the midline to two bands in the somite mesoderm (Fig. 6 U). Moreover, gene expression could still be distinguished in the anterior leading edge mesoderm, as well as in the ventral mesoderm (Fig. 6 V, W, Y).

The broad domain of *mespa* expression at the beginning of gastrulation indicates that *mespa* probably has a wider ranging function than only induction of cardiogenesis, as it is transcribed in diverse regions of the gastrula mesoderm, which will later give rise to heart, vasculature, muscle and other mesodermal tissue (comp. Fig. 3).

As Mesp1 is only transiently expressed in the murine gastrula mesoderm (Saga, Hata et al. 1996), it was of special interest to determine, for how long *mespa* transcription remains detectable in the heart forming mesoderm in *Xenopus*.

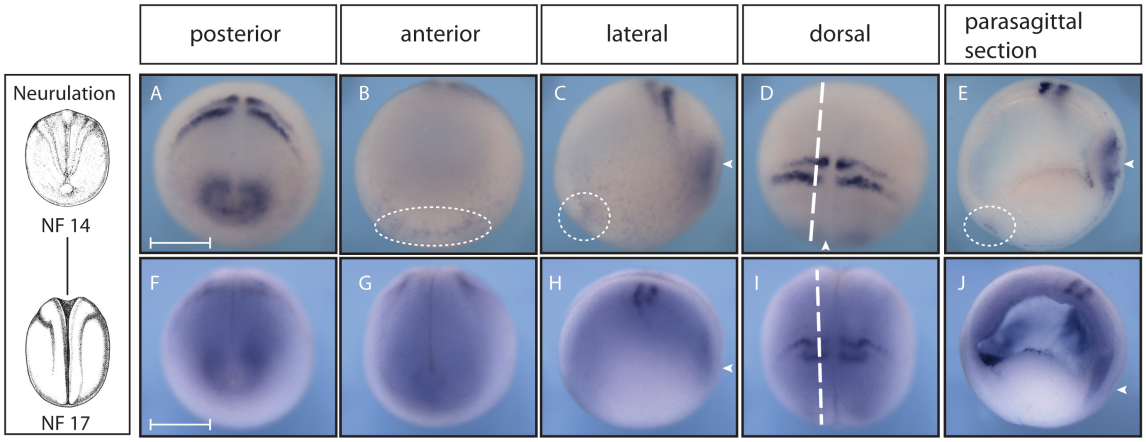

Figure 7. *Xenopus laevis mespa* gene expression during neurulation. *Mespa* mRNA expression was detected by RNA *in situ* hybridization at the indicated developmental stages **(A-J)**. Panels show different views according to the denotation at the top. During neurulation gene expression was located in enlarged bands of forming somites and around the blastoporal region. Until NF 14 there was still a faint expression in the anterior heart forming mesoderm **(B, C, E)**, marked by dotted circles. Arrowheads indicate posterior region.. Dotted lines indicate plane of section. Scale bars: 500 µm.

During neurulation *mespa* expression was located in dorsally expanding bands of forming somites and in the posterior part of the embryo (Fig. 7). Strikingly, at NF 14 there was still a faint expression in the anterior heart forming mesoderm, which could be seen in the sectioned embryo (Fig. 7 B, E).

At the end of neurulation *mespa* gene expression was restricted to the forming somites (Fig. 7 F-J).

At tailbud stage *mespa* gene expression was limited to two stripes of somitomeres and to the most posterior part of the tailbud region (Fig. 8). By late tailbud stage, this expression was vanished and *mespa* was not expressed anywhere (Fig. 8 C). This analysis of its gene expression pattern supported a role for *mespa* in the early development of different mesodermal tissues, as heart, vasculature and skeletal muscle.

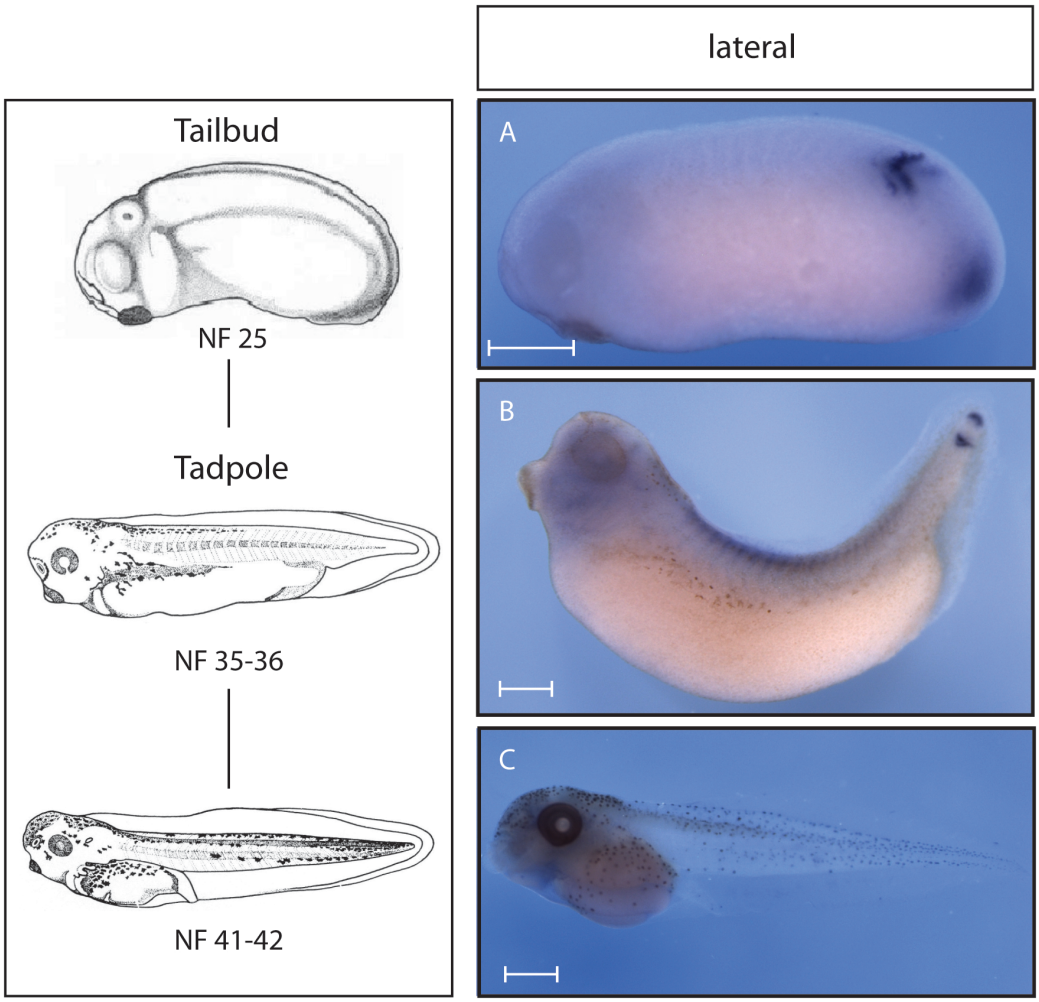

Figure 8. *Xenopus laevis mespa* gene expression during tailbud stage. *Mespa* mRNA expression was detected by RNA *in situ* hybridization at the indicated developmental stages **(A-C)**. Lateral view, anterior is to the left, dorsal to the top. During tailbud stage *mespa* mRNA was visible in the somitomeres and at the tailbud **(A, B)**. Expression disappeared until late tailbud stage completely **(C)**. Scale bars: 500 µm.

3.1.2 Composite map of gastrula mesoderm in comparison with *mespa* expression pattern

Keller (1976) used vital dye staining of the deep marginal zone to map prospective mesodermal areas and their fate during gastrulation and neurulation. He summarized different dye marks of many individual embryos and created fate maps for different stages. For a correct assignment of the mesodermal expression domains the composite fate map of the gastrula mesoderm was compared to the expression pattern of *mespa* (Figure 9).

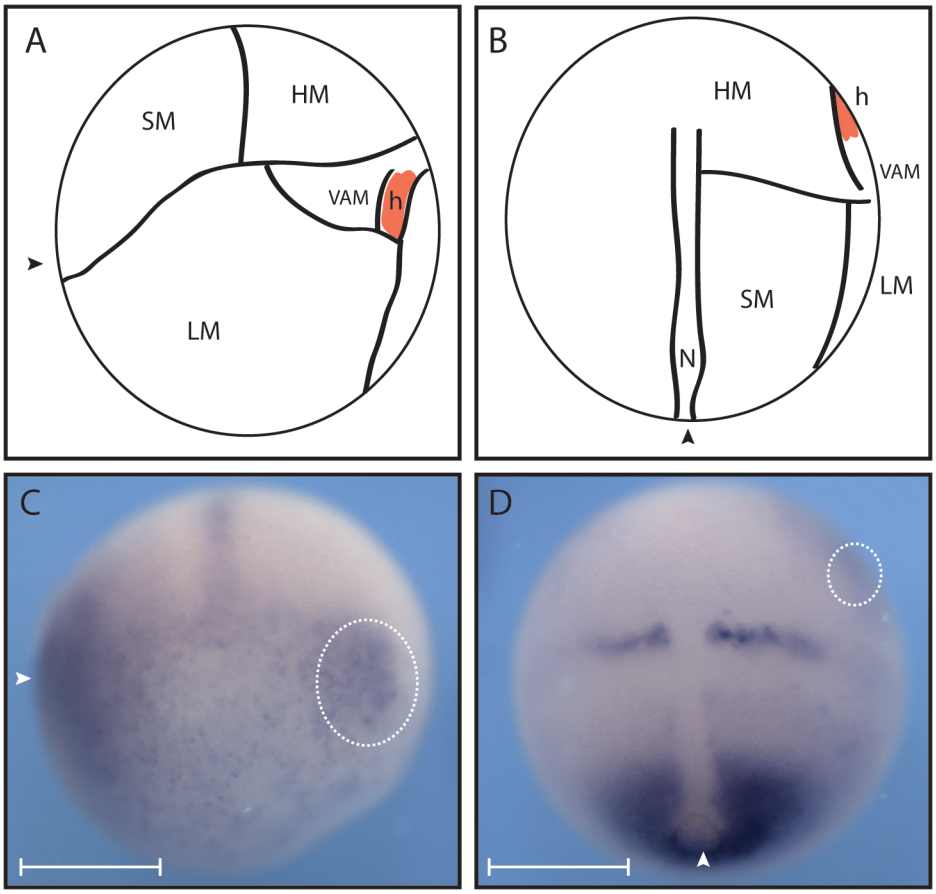

Figure 9. Composite map of the gastrula mesoderm in comparison with *mespa* expression pattern. (A, C) Lateral view. **(B, D)** Dorsal view. Prospective mesodermal parts at Stage NF 12.5 are marked as follows: SM, somite mesoderm; HM, head mesoderm; LM, lateral mesoderm; VAM, visceral arch mesoderm; h, prospective heart mesoderm. Arrowheads indicate blastopore. Fate mapping studies (modified from (Keller 1976)) defined different mesodermal regions of the gastrulating embryo adding to distinct tissues **(A, B)**. In comparison to the fate map *mespa* gene expression detected by RNA *in situ* hybridization was present at the border of somite and head mesoderm, in the lateral mesoderm and in the prospective heart forming mesoderm (dashed circles). Scale bars: 500 µm.

Keller described that at late gastrula stage the future dorsal part of visceral arch mesoderm is positioned close to the first head somite mesoderm. The future ventral part of visceral arch mesoderm is continuously linked to heart mesoderm

(Keller 1976). Accordingly, *mespa* was expressed in the somitic mesoderm around the blastopore and a stripe at the border of somite to head mesoderm, but absent from head mesoderm (Fig. 9 D). Most notably, it was expressed in the visceral arch mesoderm, probably most pronounced in heart mesoderm (Fig. 9 C). Moreover, transcription was detected in some not clearly demarcated cells in lateral mesoderm (Fig. 9 C, D; see also Fig. 6).

3.1.3 Vibratome sections of *mespa* expressing embryos

For a more detailed analysis of the involuted mesoderm, vibratome sections of embryos stained for *mespa* gene transcription were performed (Fig. 10).

Examination of the vibratome sections of 30-50μm thickness verified the gene expression of *mespa* to be restricted to the mesodermal layer. Moreover it confirmed the presence of *mespa* positive cells in the leading edge mesoderm, in the anteroventral region of the embryo. This region is located in front of the prechordal plate mesoderm, directly under the layer of ectoderm (Fig. 10 D), and corresponds to the anterior heart forming mesoderm.

The detailed analysis of *mespa* gene expression revealed that *mespa* is expressed in mesodermal regions, which undergo different morphogenetic movements and develop into diverse structures of the embryo (comp. Fig. 3).

On the one hand, it is present in the extending mesoderm, which will give rise to somites. This is in accordance with previous studies, which have described *mespa* gene expression in relation to somitogenesis in *Xenopus* (Moreno, Jappelli et al. 2008; Hitachi, Kondow et al. 2009). On the other hand, it is expressed in the migrating deep mesodermal cells, which develop into heart and visceral arch mesoderm. These findings suggest that *mespa* has additional functions beyond cardiac differentiation.

Starting from this gene expression analysis, which gave a first indication of the possible areas involved, potential downstream target molecules, able to direct the *mespa* expressing cells to adopt different cell fates, were subsequently analysed.

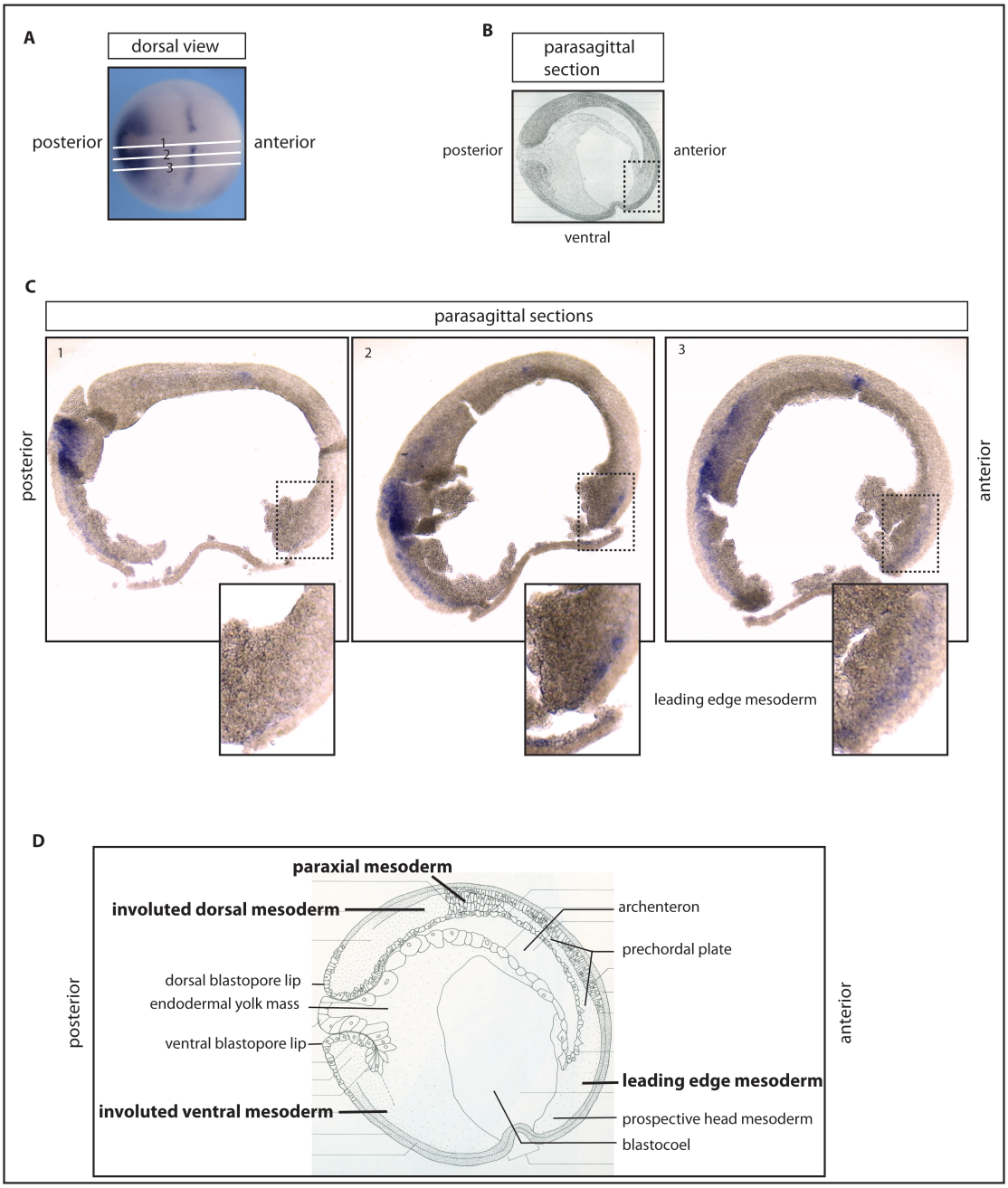

Figure 10: *Mespa* is expressed in the leading edge mesoderm of the gastrula embryo. (A) RNA *in situ* hybridization analysis for *mespa* expression at NF 12.5. Arrowhead indicates blastopore. White lines labelled 1, 2, 3, indicate planes of sections. **(B)** Schematic parasagittal view of an embryo at NF 12.5. Dashed square indicates region of leading edge mesoderm. **(C)** Three exemplary pictures of vibratome parasagittal sections from the medial to the lateral side of the embryo, according to lines in **(A)** (layer thickness 50µm). Dashed squares mark enlarged region of sections showing *mespa* gene expression in the leading edge mesoderm. **(D)** Scheme of a parasagittally sectioned embryo at NF 12.5 showing different parts of the germ layers. **(B, D)** modified from Hausen (1991).

3.2 Cardiogenesis

The above-mentioned analysis of *mespa* expression pattern in *Xenopus laevis* supports a function in cardiogenesis. To further investigate its role in this part of embryonic development, different markers for cardiac differentiation were examined.

3.2.1 *Mespa* is required for *dickkopf1* expression

The Wnt-antagonist Dickkopf1 (Dkk1) was reported to be a direct target of MesP1 in mice (David, Brenner et al. 2008). Moreover inhibition of canonical Wnt-signalling is required to initiate the program of cardiogenesis in *Xenopus* (Schneider and Mercola 2001). Therefore, *dkk1* was initially analysed as a potential signalling partner. Using specifically designed translation-blocking antisense morpholino oligonucleotides (MOs) for different *mesp* homologues, which target sequences that are conserved between the gene pairs, I performed a loss of function analysis for *dkk1* (Fig. 11). Morpholinos are non-toxic, stable and resistant to endogenous nucleases. (Bondue, Lapouge et al. 2008)

The morpholino's efficiency in inhibition of translation had already been tested in our lab. Embryos, injected with a specific morpholino that reduces the synthesis of the target protein, are called "morphants". The first cleavage of the embryo coincides with its midline and separates the embryo into a left and a right body half. Unilateral injections create a manipulated half plus an internal intact control. The second cleavage divides the embryo into two dorsal and two ventral blastomeres, which can be differentiated based on the level of pigmentation. Due to the third cleavage (8-cell stage) the blastomeres are further split into animal and vegetal cells. The progeny of the dorsovegetal blastomeres will later in development contribute mainly to the heart region.

10ng of each MO were injected concurrently with fluorescent dextrane as lineage tracing into one dorsovegetal blastomere. (Fig. 11 A). The injected and control embryos were raised until they reached the early neurula stage (NF15), when they were fixed and subjected to RNA *in situ* hybridization with an antisense *dkk1* pobe. Subsequently, I evaluated the expression of *dkk1* of the diverse injected embryos (Fig 11). Uninjected and control-Morpholino (Co MO) injected embryos showed a symmetric expression of *dkk1* in the anterior heart-forming region (Fig. 11 B, C),

comparable to the *mespb* morphants (Fig. 11 E), and therefore showed no significant alterations upon injection. Whereas injection of *mespa* MO led to a strong down-regulated expression of *dkk1* in the precardiac patches (Fig. 11 D), *mespo* MO had only a mild, but still significant, effect on *dkk1* (Fig. 11 F).

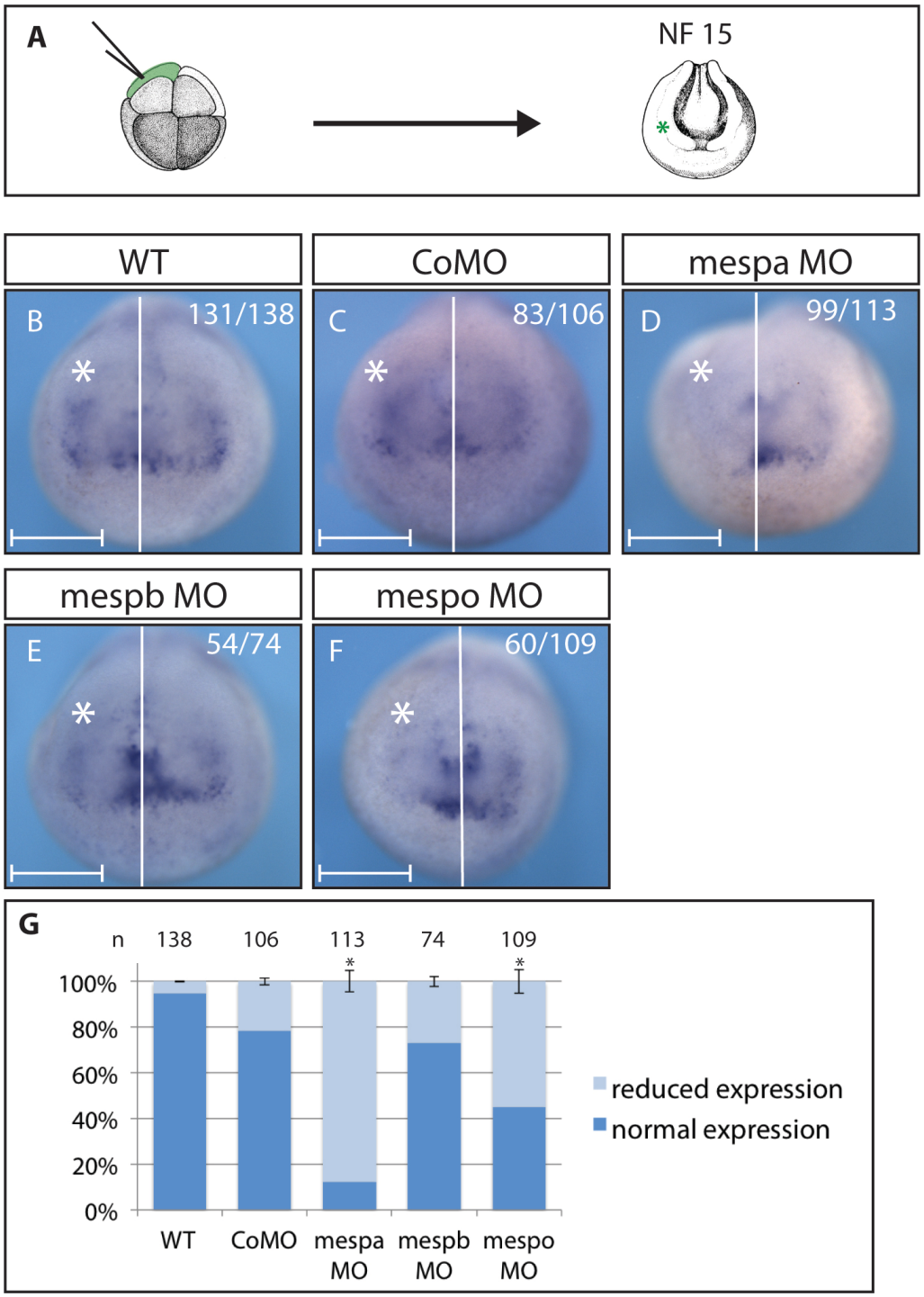

Figure 11: *Mespa* is required for *dkk1* expression. (A) Embryos were injected into one dorsovegetal blastomere at eight-cell stage with 10ng of standardized control morpholino (Co-MO), *mespb* morpholino (*Mespb*-MO), *mespa* morpholino (*Mespa*-MO) or *mespo* morpholino (*Mespo*-MO). **(B)** At NF 15 embryos were analysed by RNA *in situ* hybridization for expression of *dkk1*. Asterisk marks depleted *dkk1* expression. Anterior view. WT- wildtype, uninjected control. **(C)** Distribution of reduced *dkk1* expression phenotypes in three independent biological repeats; *, $p \leq 0.05$. Scale bars: 500 µm.

3.2.2 Induction of *dkk1* in animal cap explants

To test, whether *mespa* is capable of inducing *dkk1*, I took advantage of the animal cap assay (Green 1999), which has been shown to be useful for investigation of heart development (Afouda and Hoppler 2009).

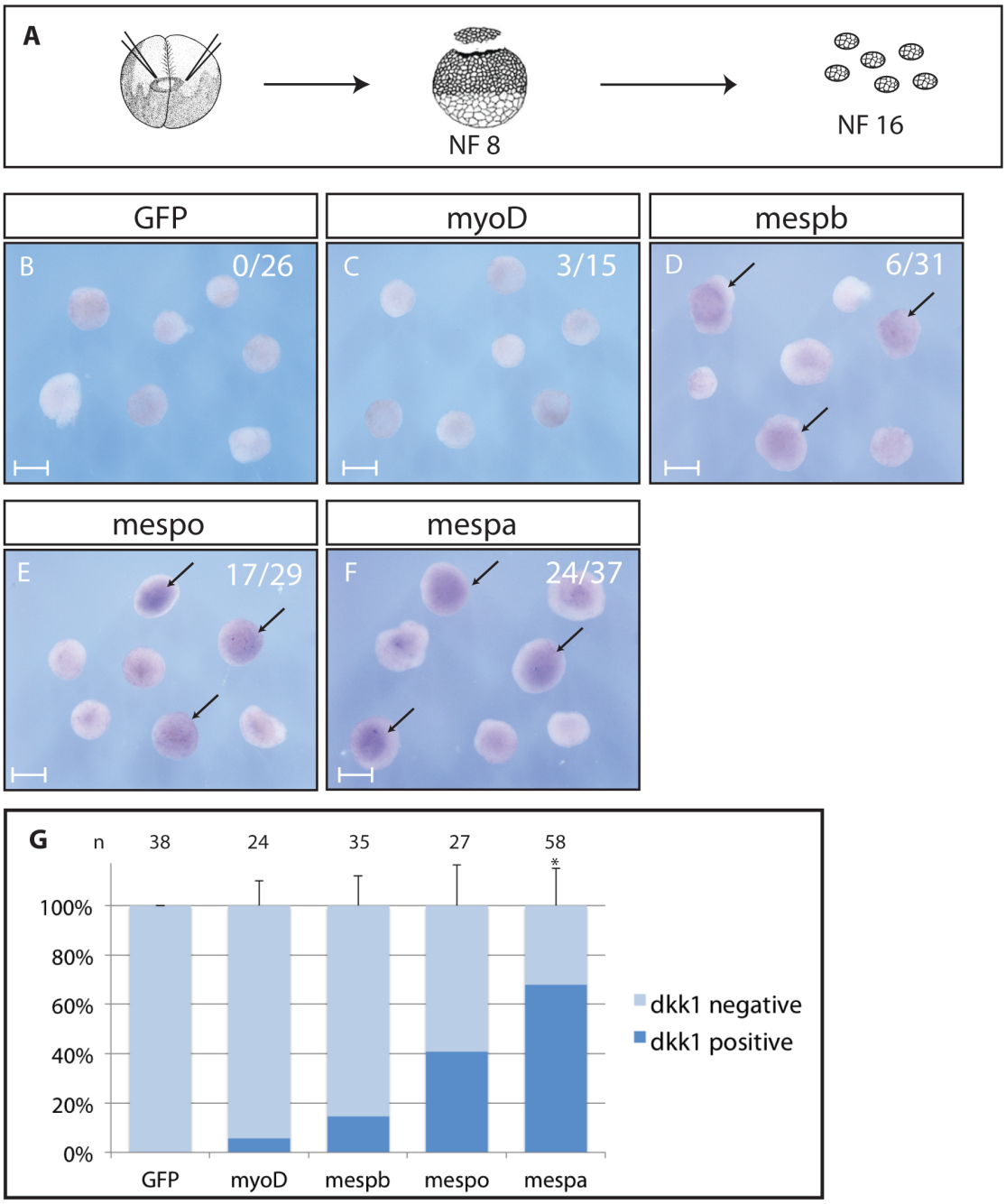

Figure 12: Induction of *dkk1* in animal cap explants. (A) At two-cell stage embryos were injected with 1ng of each mRNA. At NF 8 animal caps were dissected and cultivated until control siblings reached NF 16. **(B)** The Figure shows representative animal caps after RNA *in situ* hybridization for *dkk1*. Arrows mark *dkk1* positive explants. **(C)** Chart displays quantity of *dkk1* expressing animal caps for each condition in three independent biological repeats; *, $p \leq 0.05$. Scale bars: 500µm.

The blastocoel roof at the animal pole of the late blastula embryo is called “animal cap”. This region will differentiate into ectoderm, which will later give rise to skin and nervous system of the tadpole (Keller 1975). When the animal caps are excised and cultured in saline solution they will develop into epidermis. After injection of mRNA of a regulatory protein into the animal region of the two-cell stage embryo, the animal caps are dissected at blastula stage prior to inductive events and cultivated until a specific stage. The ability of the injected protein to induce gene expression in the naïve tissue explant can subsequently be analysed via RNA *in situ* hybridization. The animal cap assay was shown to be an effective and useful tool to study the potency of transcription factors to induce cardiac gene expression, which is comparable to ES cell culture techniques (Warkman and Krieg 2007). As mammalian MesP1 biases ES cells towards a cardiovascular fate (David, Brenner et al. 2008), the animal cap assay was used to test such a function in *Xenopus*.

Following radial injections of 1ng of different mRNA, including *mespa* mRNA, into the embryo’s animal pole at two-cell stage, the embryos were cultured until late blastula (NF 8.5) and the blastocoel roof was dissected. Subsequently, the explants were cultivated until early neurula and analysed for *dkk1* expression by RNA *in situ* hybridization (Fig. 12 A).

Neither *GFP*, nor *myoD* injected explants did express *dkk1* (Fig. 12 B, C). *MyoD* is a bHLH transcriptional regulator for skeletomyogenesis (Rupp, Snider et al. 1994). Upon injection of *mespa* mRNA the animal caps presented an induction of *dkk1* expression (Fig. 12 F), which was less frequently observed by *mespb* or *mespo* injection (Fig. 12 D, E). As neither *mespb* nor *myoD* overexpression could induce *dkk1* in the explants it is likely that these bHLH proteins differ accurately in skeletomyogenic and cardiogenic activities.

In summary, *mespa* is required for *dkk1* expression in the anterior heart-forming region of the embryo and can induce *dkk1* transcription ectopically in tissue explants. The *wnt*-antagonist *dkk1* creates a low *wnt* gradient in the anterior part of the embryo, which was shown to be essential for initiating cardiogenesis in precardiac mesoderm (Schneider and Mercola 2001). Thus, *dkk1* may provide a non-cell-autonomous mechanism for *mespa*-directed induction of cardiogenesis.

3.2.3 *Nkx2.5* gene expression analysis

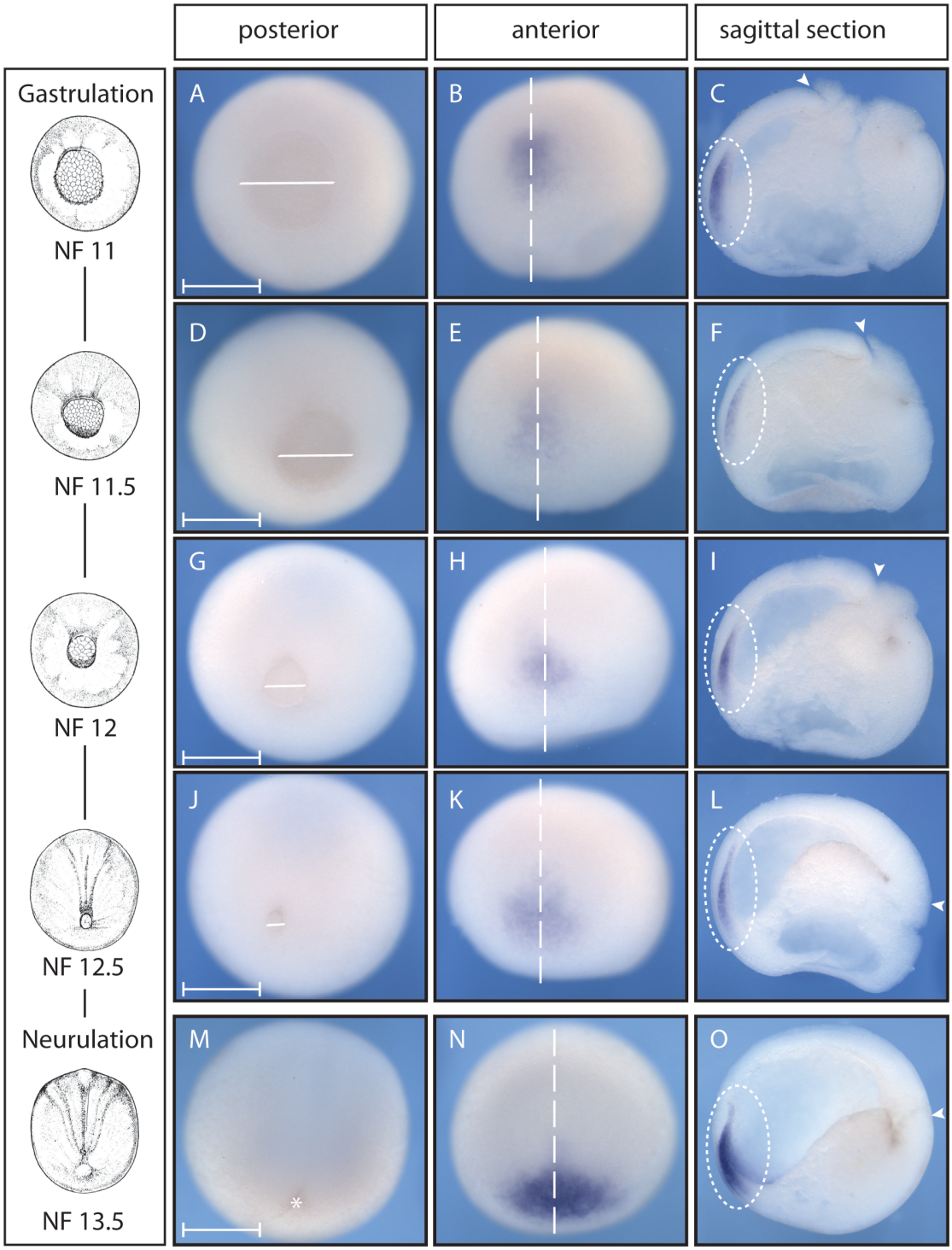

Figure 13: *Nkx2.5* is expressed in early gastrula. *Nkx2.5* expression was detected by RNA *in situ* hybridization at the indicated stages. Panels show different views according to the denotation at the top **(A-O)**. *Nkx2.5* gene expression started at NF 11 in the anterior leading edge mesoderm **(C),** dashed circle. During gastrulation expression in the anterior mesoderm increased **(E-K)**. During neurulation *nkx2.5* was expressed in the precardiac mesoderm in the anteroventral region of the embryo **(L-O)**. Horizontal white lines indicate the blastopore's diameter. Vertical dashed white lines demarcate plane of section. Arrowheads indicate blastopore **(C, F, I, L)** or posterior end of the embryo **(O)**. Asterisk indicates closed blastopore **(M).** Scale bars: 500 µm.

The *wnt*-antagonist *dkk1* is an extrinsic cue, which establishes a certain gradient of signalling molecules in the embryo. However, *dkk1* is not a marker for cardiac progenitor cells itself.

Two transcription factors provide a link between the early specification of cardiac fate during gastrulation and the later onset of cardiac differentiation in tailbud stage. One of them is the homeobox transcription factor Nkx2.5, the vertebrate orthologue of tinman, which is a core cardiac regulator in Drosophila (Sparrow, Cai et al. 2000). While Nkx2.5 is required for early progenitor specification (Prall, Menon et al. 2007; Guner-Ataman, Paffett-Lugassy et al. 2013), it is likewise expressed in late heart tube stages (Mohun, Leong et al. 2000; Gessert and Kuhl 2009). Moreover, its mesodermal expression was found to be essential for cardiac development in mice (Zhang, Nomura-Kitabayashi et al. 2014). Overexpression of Nkx2.5 led to a thickening of the mature myocardium (Cleaver, Patterson et al. 1996). Nkx2.5 gene mutations also predispose for human congenital heart defects (Stallmeyer, Fenge et al. 2010). For these reasons, it was investigated, whether *mespa* is a regulator of *nkx2.5* in *Xenopus laevis*.

Initially, an analysis of *nkx2.5* gene expression was carried out to establish a detail spatial and temporal expression pattern (Fig. 13). Remarkably, *nkx2.5* was already expressed at NF 11 in early gastrula (Fig. 13 C), which was earlier than described before (Gessert and Kuhl 2009). The expression domain is located in the anterior leading edge mesoderm, which could be confirmed via sagital sections. Throughout gastrulation the transcription of *nkx2.5* RNA increased in the anterior region and extended laterally.

During the stage of neurulation *nkx2.5* was expressed in the precardiac mesoderm and moreover visible in the adjacent endoderm (Fig. 13 N,O).

Later on, in tailbud stage, *nkx2.5* mRNA is found in the cardiac crescent (Fig. 14 A). Subsequently, at tadpole stage, *nkx2.5* was expressed in the myocardium of the heart tube (Fig. 14 B, C). The heart tube consists of a spirally looped form at this stage, as chamber formation has not started yet (Mohun, Leong et al. 2000). Moreover, *nkx2.5* was additionally expressed in the splenic anlage of the tadpole (Fig. 14 B), consistent with previous reports (Griffin, Sondalle et al. 2015).

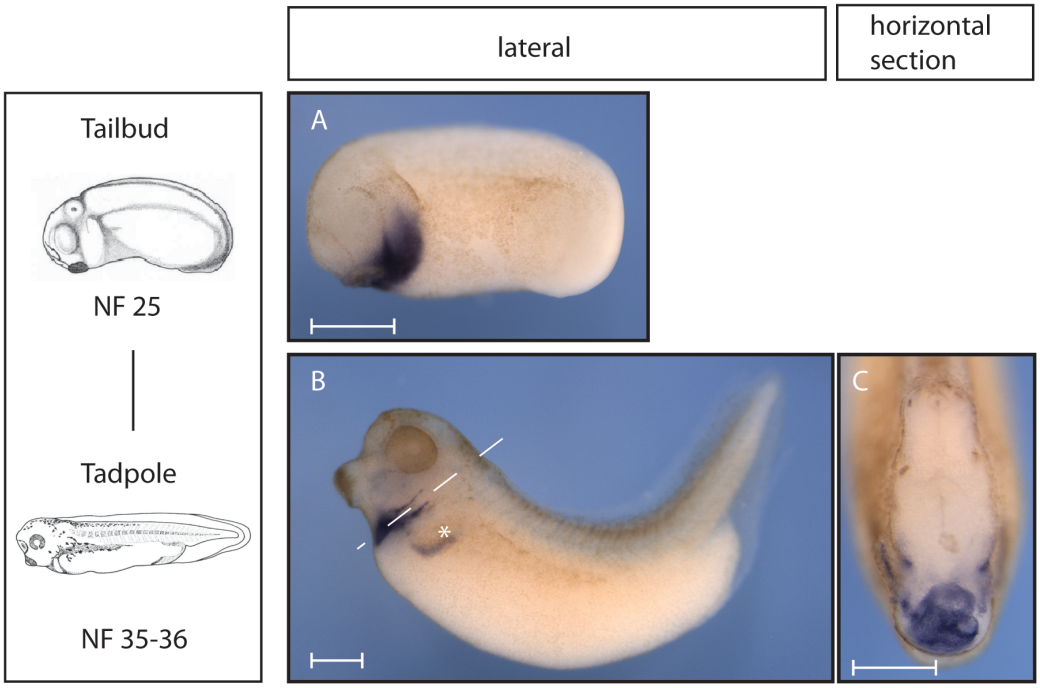

Figure 14: *Nkx2.5* is expressed in the heart tube during tailbud and tadpole stage. (A-C) *Nkx2.5* expression was detected by RNA *in situ* hybridization at tailbud stage. Panels show lateral views. During tailbud stage *nkx2.5* was expressed in the cardiac crescent **(A)** and later in the looping heart tube **(B)**. Caudal to the heart tube, expression in the splenic anlage is shown (asterisk). Horizontal section **(C)** reveals expression in the ventricle, atria and outflow tract. Vertical dashed white line demarcates plane of section. Scale bars: 500 µm.

The time of expression during early gastrulation coincides with *mespa* transcription (compare with Fig. 6) and shows in part a spatial and temporal overlap with *mespa* expression in the sectioned embryo (Fig 15), as both are expressed in the anterior leading edge mesoderm, which will later give rise to the heart anlage. The overlap is only partial, as *nkx2.5* is additionally expressed in the midline region of the embryo, where *mespa* gene transcription is not present (compare with Fig. 6). The partial overlap suggests that *nkx2.5* is expressed in a subset of the *mespa* domain.

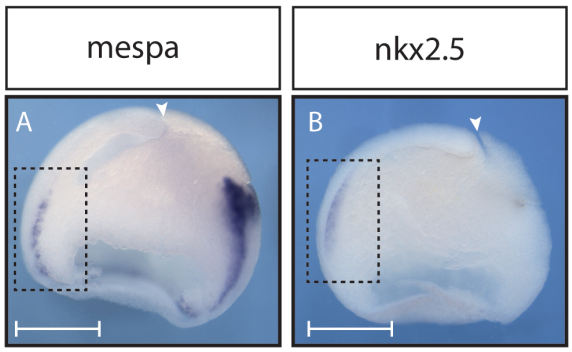

Figure 15: Overlap of *nkx2.5* and *mespa* expression in the early gastrula mesoderm. (A, B) The Figure shows sagittal sections through NF 11 stage embryos, which were subjected to RNA *in situ* hybridization for evaluation of *mespa* and *nkx2.5* gene expression. Comparison of expression shows a spatial and temporal overlap in the leading edge mesoderm (dashed squares). Arrowheads indicate blastopore opening. Anterior to the left, dorsal side up. Scale bars: 500 µm.

3.2.4 Knock down of *mespa* leads to loss of *nkx2.5* expression

In order to evaluate, whether there is not only an overlap in expression, but also a requirement of *mespa* for *nkx2.5* gene transcription, a loss of function study via morpholino-based knockdown of *mespa* was performed. A unilateral knockdown of *mespa* was achieved by injecting 20ng of *mespa* MO into one blastomere at two-cell stage (Fig. 16).

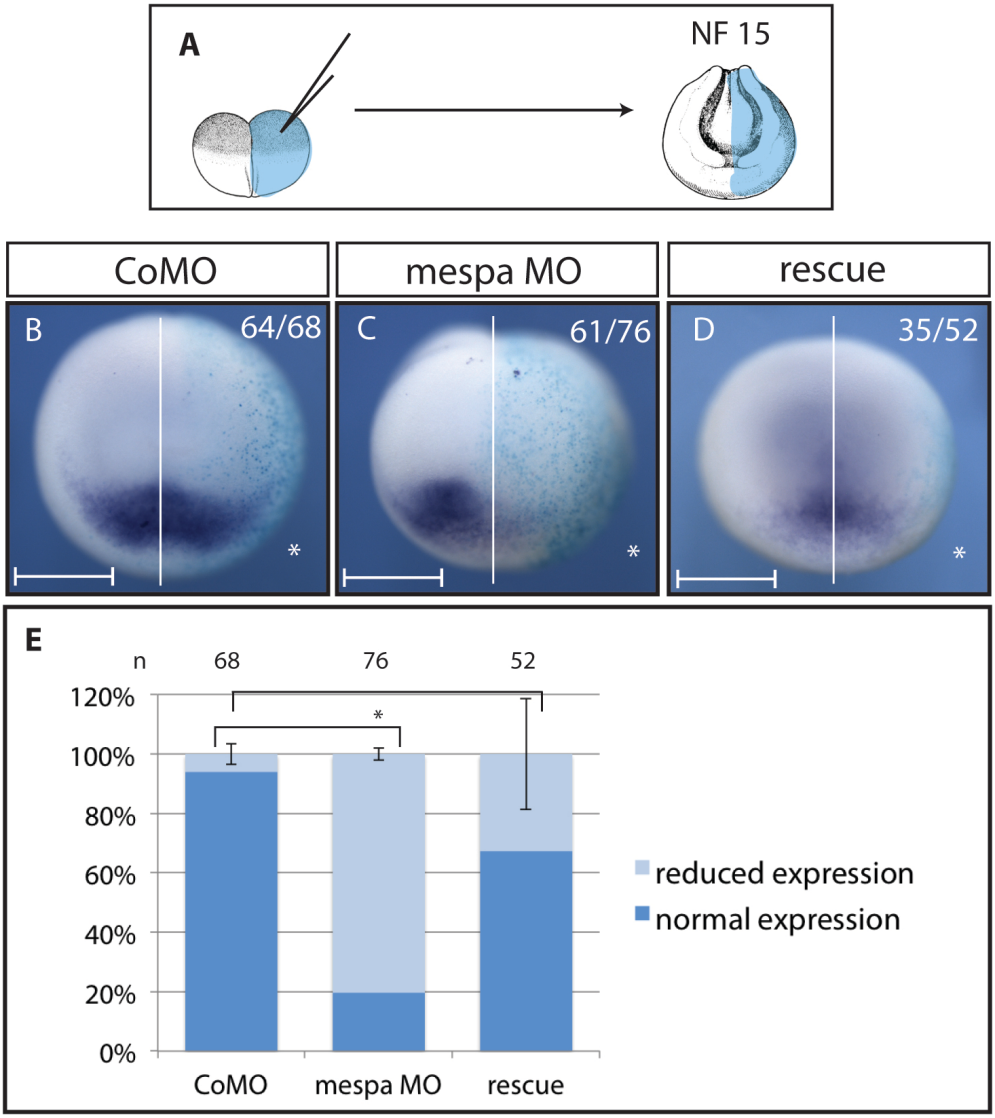

Figure 16. Knockdown of *mespa* leads to loss of *nkx2.5* expression. (A) Embryos were unilaterally injected at two-cell stage, cultivated until NF 15 and analysed by RNA *in situ* hybridization for *nkx2.5* expression. **(C)** Injection of 20ng of *mespa* morpholino together with LacZ as lineage trace causes a downregulation of *nkx2.5* in the injected half. **(B)** The same amount of control morpholino shows no alteration. **(D)** The morphant phenotype was partially rescued by injection of 250pg morpholino insensitive *mespa* mRNA variant. Anterior view. Asterisks mark injected site. **(E)** Phenotypic distribution of *nkx2.5* expression in three independent biological repeats; *, $p \leq 0.05$. Scale bars: 500 µm.

Indeed, a downregulation of *nkx2.5* mRNA was observed by *in situ* hybridization on

the injected side (Fig. 16 C). The loss of gene expression could be rescued by adding 250pg of *mespa*-RNA. This engineered mRNA is depleted for the morpholino recognition site (Fig. 16 D). The morpholino oligonucleotide cannot bind to this mRNA and therefore permits the translation of the injected *mespa* mRNA variant. Hence, the observed downregulation of *nkx2.5* mRNA is a specific consequence of *mespa* depletion Therefore, *mespa* is required (directly or indirectly) for *nkx2.5* gene transcription during gastrula stage.

To answer the question, whether the observed downregulation of *nkx2.5* during gastrulation can be compensated in later stages, the same injections were carried out, except the embryos were cultivated until tailbud stage (Fig. 17).

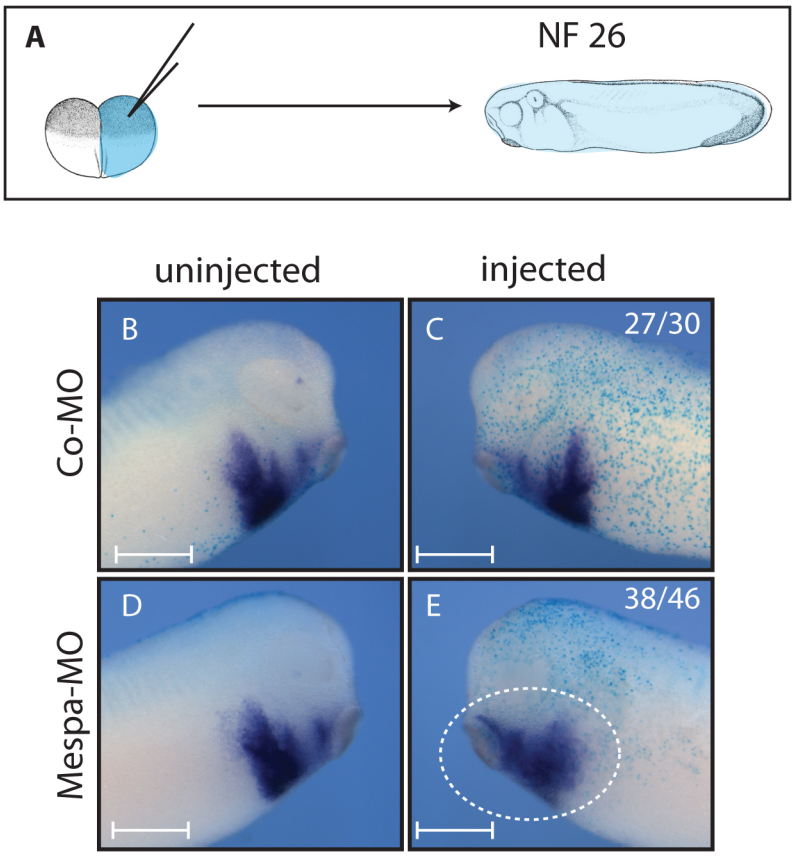

Figure 17: Effects of *mespa* knockdown are not compensated until tailbud stage. (A) Embryos were unilaterally injected at two-cell stage, cultivated until NF 26 and analysed by RNA *in situ* hybridization for *nkx2.5* expression. **(D, E)** Injection of 20ng of *mespa* morpholino together with LacZ as lineage trace causes defects in the proper formation of the cardiac patches (dashed circle) on the injected side. **(B, C)** The same amount of control morpholino shows no alteration (n=3). Lateral views. Scale bars: 500 µm.

By comparison of uninjected and morphant side, *nkx2.5* expression was restored over time in *mespa* morphants, but a defect in the proper formation of the cardiac mesoderm was still observable on the morphant side. Instead of being arranged precisely within the heart region the *nkx2.5* positive cells showed a defective

positioning (Fig. 17 E).

Thus, *nkx2.5* gene transcription is not exclusively dependent on *mespa* in later stages and can partially be compensated, which suggests an additional input for *nkx2.5.* This additional input fits to the missing overlap of gene expression in the midline region of the embryo. However, the proper positioning of *nkx2.5* positive cells remains abnormal until tailbud stage on the *mespa* deficient side. This indicates an essential requirement for *mespa* in the patterning of the heart region.

3.2.5 *Islet1* gene expression analysis

Another factor that provides a link between the early cardiac progenitor specification during gastrulation and the later onset of cardiac differentiation is the LIM homeodomain transcription factor Islet1 (*Isl.1*). *Isl.1* has been described as second heart field marker (Brade, Gessert et al. 2007; Cohen, Miller et al. 2012; Xavier-Neto, Trueba et al. 2012). Arguments against this concept are the neural crest origin of *Isl.1* positive cells in the heart (Engleka, Manderfield et al. 2012) and the early expression of *Isl.1* in the cardiac crescent (Gessert and Kuhl 2009). Therefore *Isl.1* is also seen as a common lineage marker for all cardiac progenitors (Laugwitz, Moretti et al. 2008).

As a consequence, *isl.1* was another potential target gene for *mespa*-induced cardiogenesis in *Xenopus*.

The *Isl.1* gene expression pattern was examined via RNA *in situ* hybridization (Fig. 18). The initiation of *isl.1* mRNA expression started at NF 10 at the very beginning of gastrulation (Fig. 18 C), hence prior to the developmental stages as described before (Gessert and Kuhl 2009) and even earlier than *nkx2.5* (compare with Fig. 13). In the course of gastrulation the intensity of mesodermal expression in the anterior heart forming region increased and *isl.1* appeared additionally in the ectodermal layer in the anterior region of the embryo (Fig. 18 F, I, L). In accordance with reports of *isl.1* mRNA expression in neural crest and neuroectodermal cells of the head (Brade, Gessert et al. 2007), neuroectodermal expression increased during neurulation, when *isl.1* was additionally expressed in the most lateral and medial stripes of primary neurons (Fig. 18 M-O). These lateral primary neurons (Fig. 18 M) are also known as Rohon-Beard sensory neurons (Roberts and Smyth 1974).

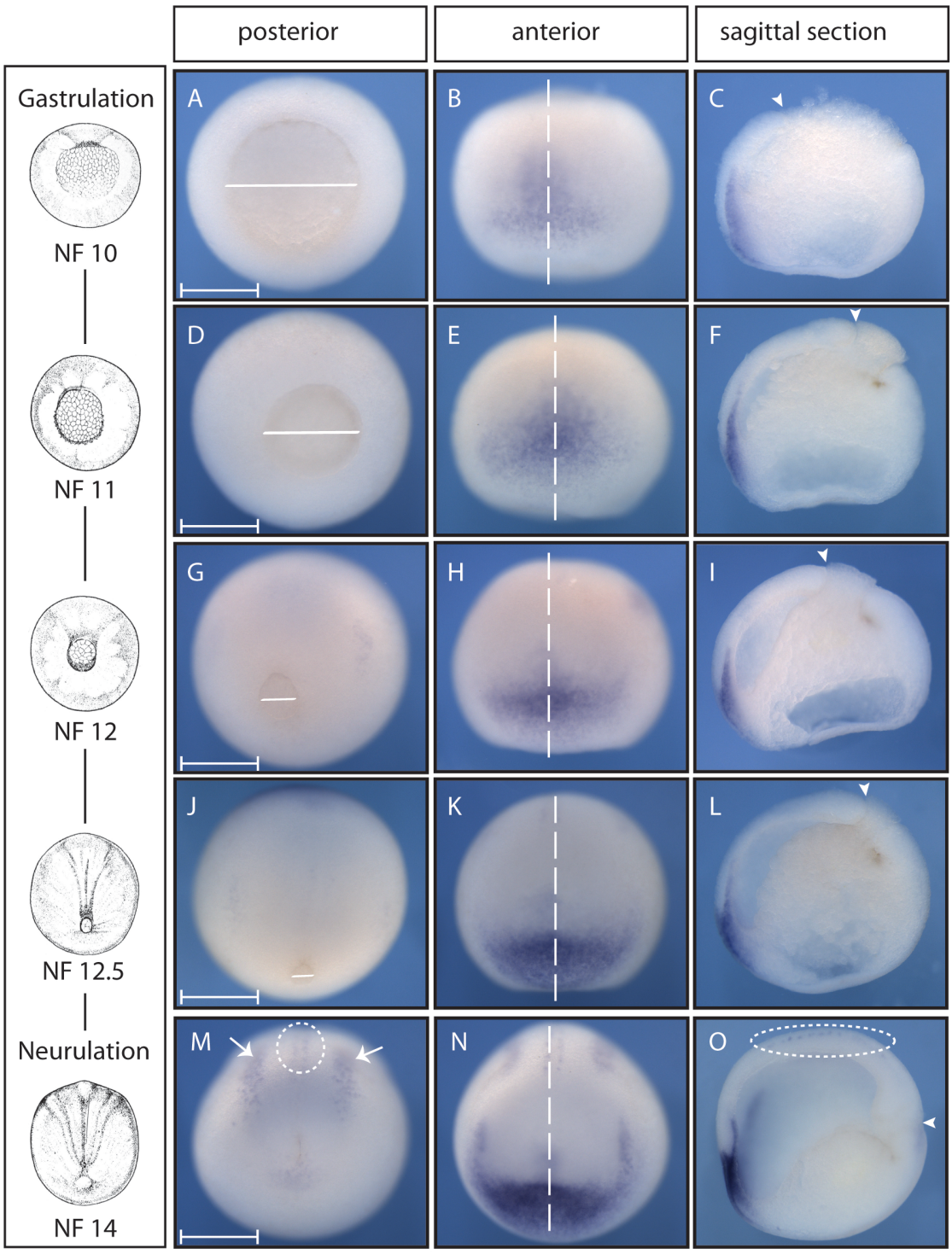

Figure 18: *Isl.1* expression starts in early gastrula. (A-L) *Isl.1* expression was detected by RNA *in situ* hybridization at the indicated stages. Panels show different views according to the denotation at the top. Isl.1 gene expression started at early gastrula **(B, C)** in the anterior leading edge mesoderm. During gastrulation *isl.1* appeared additionally in the ectodermal layer **(I, L)**. At the beginning of neurulation *isl.1* was expressed in the most lateral (arrows) and medial (dashed circles) stripes of primary neurons **(M, O)** and in the anterior precardiac mesoderm **(N, O)**. Horizontal white lines represent the blastopore's diameter. Vertical dashed white lines demarcate plane of section. Arrowheads indicate blastopore or posterior end of the embryo. Scale bars: 500 µm.

Sections of early gastrula stage embryos revealed a comparable expression of *mespa* and *isl.1* in the leading edge mesoderm, which represents a spatial and

temporal partial overlap of expression (Fig. 19). This finding suggests a co-expression of both genes at least in some mesodermal cells, which has not been described before. Hence, an induction of *isl.1* by *mespa* in these cells is formally possible.

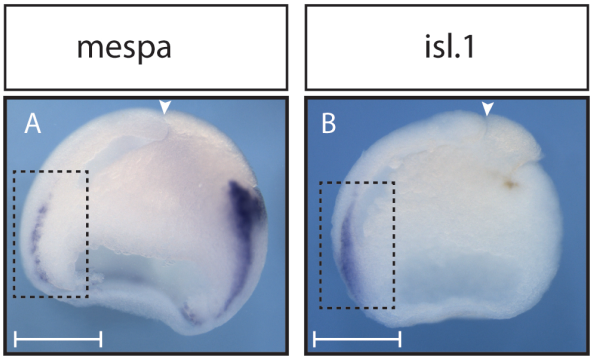

Figure 19: Partial overlap of *isl.1* and *mespa* expression in the early gastrula mesoderm. (A, B) The Figure shows sagittal sections through NF 11 stage embryos, which were subjected to RNA *in situ* hybridization for evaluation of *mespa* and *isl.1* gene expression. Comparison of expression shows a partial spatial and temporal overlap in the leading edge mesoderm (dashed squares). Arrowheads indicate blastopore opening. Anterior to the left, dorsal side up. Scale bars: 500 µm.

In tailbud stage *isl.1* expression was additionally detected in profundal ganglia of cranial nerves and the trigeminal ganglia (Fig. 20 A), (Park and Saint-Jeannet 2010). Subsequently in tadpole stage, *isl.1* was expressed in the eye, in the aortic arches and in the outflow tract of the heart (Fig. 20 B, C).

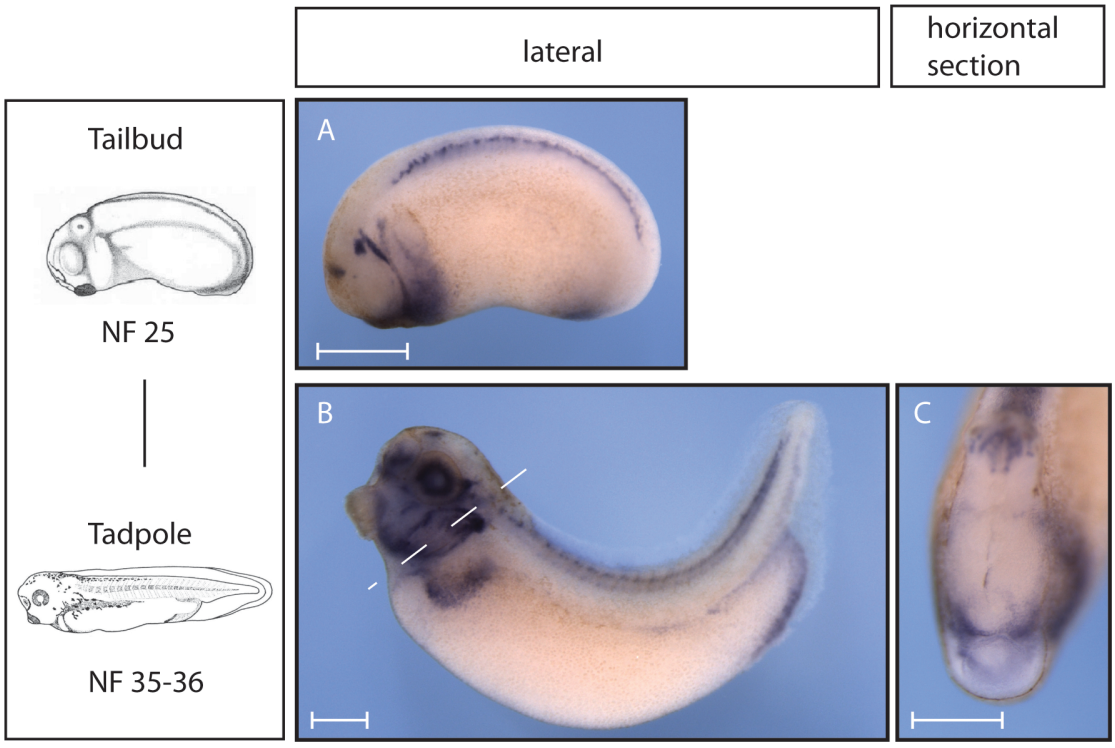

Figure 20: *Isl.1* is expressed in the cranial ganglia, aortic arches and the outflow tract of the heart during tailbud and tadpole stage. (A-C) *Isl.1* expression was detected by RNA *in situ* hybridization. Panels show lateral views. During tailbud stage *isl.1* was expressed in the profundal ganglia of cranial nerves and in

the trigeminal ganglia **(A)**. Later on, during tadpole stage, *isl.1* was expressed in the eye and in the aortic arches **(B, C)**. Horizontal section **(C)** reveals expression in the ventricle and outflow tract of the heart. Vertical dashed white line demarcates plane of section. Scale bars: 500 µm.

3.2.6 Injection of *mespa* morpholino causes loss of *isl.1* expression

Loss of function experiments were conducted to investigate the proposed genetic interaction between *mespa* and *isl.1* (Fig. 21). Upon injection of *mespa* MO into one blastomere at the two-cell stage, the majority of embryos were deficient for *isl1* mRNA expression in early neurula stages (Fig. 21 C). This effect was specific for *mespa*, as co-injection of a morpholino insensitive *mespa* RNA variant rescued the morphant phenotype (Fig. 21 D). Parasagittal sections of morphant and uninjected half uncovered a migratory defect of the involuted mesoderm. Whereas the mesodermal layer of the uninjected half moved anteriorly (Fig. 21 b), the *mespa* morphant mesodermal cells failed to move anteriorly (Fig. 21 a).
Hence, the lack of *isl.1* positive cells in the anterior domain may be due to defective migration of the *mespa*-deficient mesoderm.

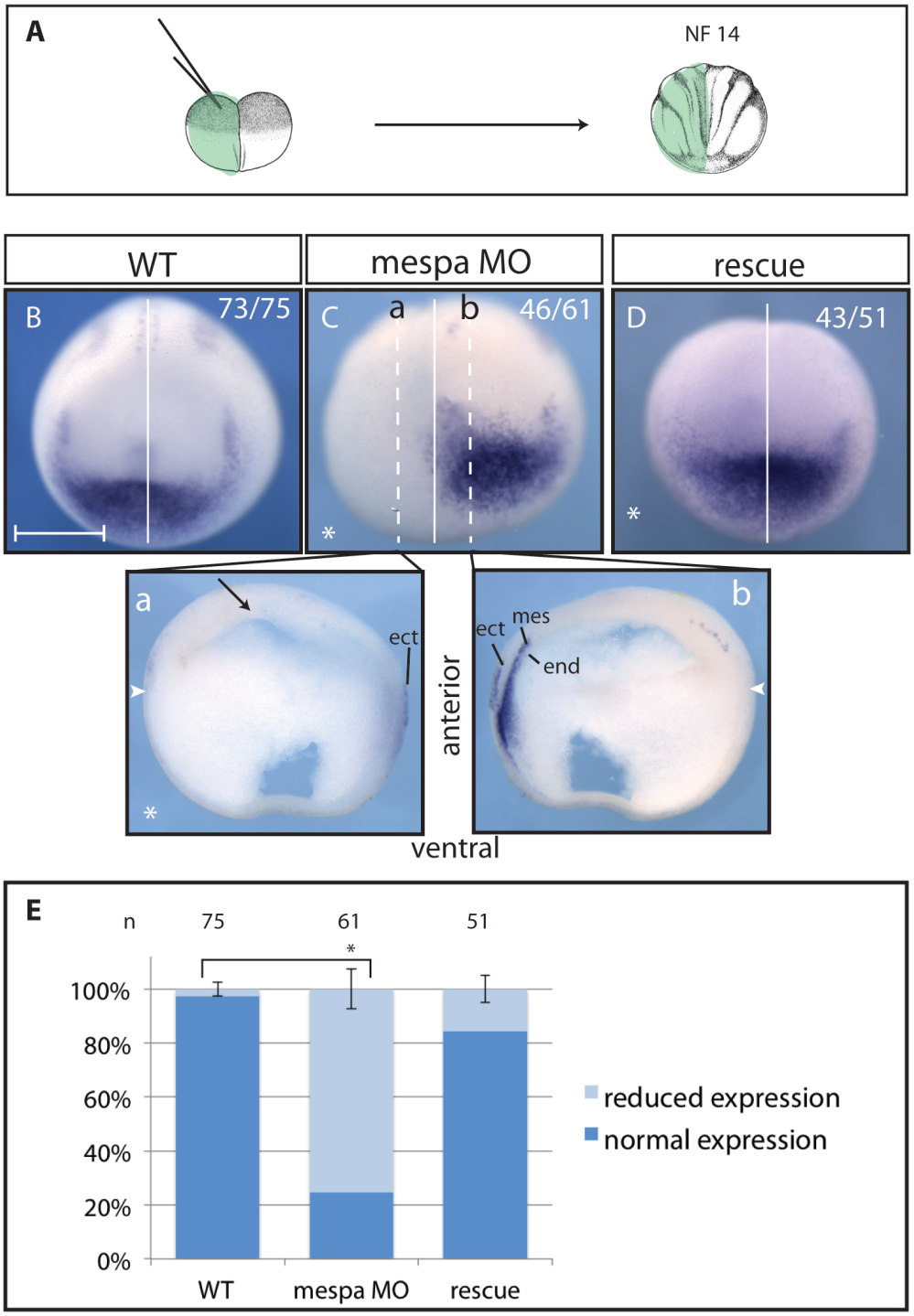

Figure 21: Injection of *mespa* morpholino causes loss of *isl.1* expression. (A) Embryos were unilaterally injected at two-cell stage, cultivated until NF 14 and then analysed via RNA *in situ* hybridization for expression of *isl.1*. **(B)** WT, wildtype embryo. **(C)** Injection of 20ng of *mespa* morpholino causes a downregulation of *isl.1* on the injected side. Dashed lines represent planes of sections through morphant **(a)** and uninjected **(b)** side, depicted beneath. Arrow indicates the anterior border of leading edge mesoderm **(a)**. **(D)** The morphant phenotype was rescued by injection of 150pg morpholino insensitive *mespa* mRNA variant. Anterior view. Asterisks mark injected side. Ect, ectoderm; mes, mesoderm; end, endoderm. **(E)** Phenotypic distribution of *isl.1* expression in three independent biological repeats; *, $p \leq 0.05$. Scale bars: 500 µm.

3.2.7 Induction of *isl.1* in animal cap explants

Figure 22 depicts an animal cap assay, which was performed, to assess *mespa's* inductive function for the transcription of *isl.1.*

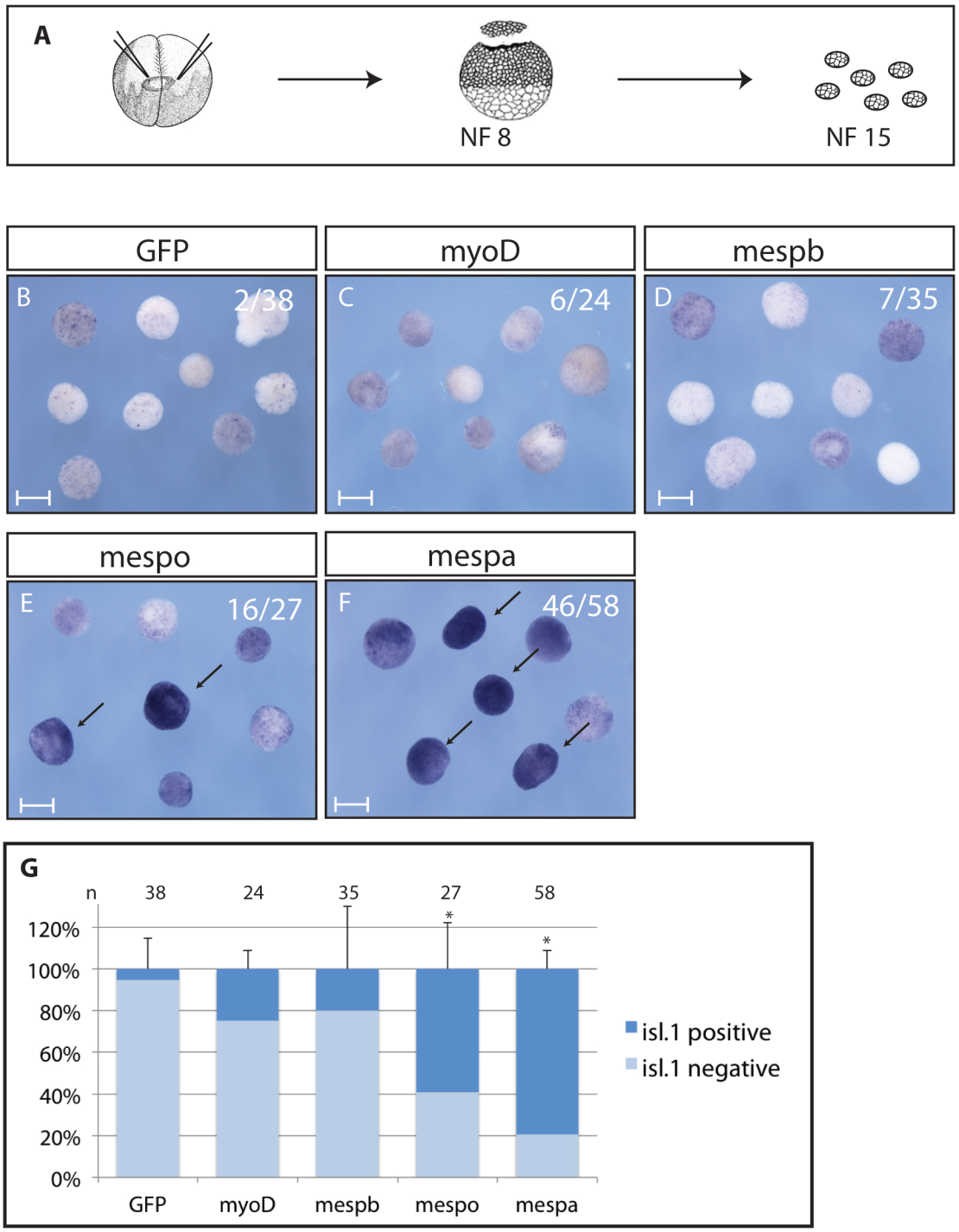

Figure 22: Induction of *isl.1* in animal cap explants. (A) At two-cell stage embryos were injected with 1ng of *GFP, myoD, mespb, mespa* or *mespo* mRNA. At NF 8 animal caps were dissected and cultivated until control siblings reached NF 15. **(B-F)** The Figure shows representative animal caps after RNA *in situ* hybridization for *isl.1*. **(E, F)** Arrows mark *isl.1* positive explants over base level of GFP-injected explants. **(G)** Chart displays quantity of *isl.1* expressing animal caps over base level for each condition in three independent biological repeats; *, $p \leq 0.05$. Scale bars: 500 µm.

Since *isl.1* was also expressed in ectodermal cells (see Fig. 17, 19, 20), the excised animal cap explants contained some *isl.1* positive cells, which were considered as a base level of gene expression. Moreover Brade et al. explained the base level of *isl.1* expression in animal caps as persisting maternal *isl.1* mRNA (Brade, Gessert et al. 2007). Basal *isl.1* mRNA levels were not enhanced by injection of *GFP* mRNA (Fig. 22 B). *MyoD* and *mespb* mRNA enhanced *isl.1* expression not significantly in few animal caps (Fig. 22 C, D), but *isl.1* mRNA was most strongly enhanced by *mespa* (Fig. 22 F). Moreover, *isl.1* was induced by *mespo*, but less frequently (Fig. 22 E, F).
These findings support the hypothesis that *mespa* is not only required for migration of *isl.1* positive cells, but also for induction of *isl.1*.
As the tissue explants responded differently to the introduction of bHLH transcription factors, *mespa* seems to have a unique cardiogenic activity among the bHLH family.

In summary, these results demonstrate that *mespa* is required, first, for gene transcription of definitive cardiac marker like *nkx2.5* and *isl.1* during *Xenopus* gastrulation, but also for the expression of non-cell-autonomous cardiogenic signalling molecules like *dkk1*. In addition, *mespa* is sufficient to activate these genes ectopically in pluripotent cells of animal cap explants.

3.3 Vasculogenesis

MesP1 was found out to be a marker for cardiac, as well as for endothelial precursors (Saga, Miyagawa-Tomita et al. 1999) and major blood vessels seemed to derive from MesP1 expressing cells (Saga, Kitajima et al. 2000) in the mouse embryo. Since MesP1 was also required for the formation of vascular progenitor cells *in vitro* (Saga, Kitajima et al. 2000; Bondue, Lapouge et al. 2008; David, Brenner et al. 2008; Bondue, Tannler et al. 2011; Lescroart, Chabab et al. 2014), another objective of this study was, to investigate *mespa*'s role in vasculogenesis *in vivo* in the *Xenopus* embryo. In order to analyse a function for *mespa* in vasculogenesis, a putative downstream target gene was searched for.

The Apelin receptor (aplnr) is a G protein-coupled receptor, which was identified in 1993 (O'Dowd, Heiber et al. 1993) and subsequently reported to play an important role in vasculogenesis in *Xenopus* (Cox, D'Agostino et al. 2006; Inui, Fukui et al. 2006; Kälin, Kretz et al. 2007; Kidoya and Takakura 2012), in zebrafish (Tucker, Hepperle et al. 2007) and in mice (Kang, Kim et al. 2013). Aplnr double knockout mice died early in development due to cardiovascular malformations, which included defective maturation of the vasculature and abnormal cardiac chamber formation (Kang, Kim et al. 2013). Moreover, the apelin receptor was shown to be involved in sprouting angiogenesis of retinal and tumour cells (Kidoya, Ueno et al. 2008). Because of its importance in vasculogenesis, *aplnr* was subsequently examined in this thesis as a potential target gene of *mespa*.

3.3.1 *Apelin receptor* gene expression analysis

An overview of *aplnr* gene expression has been described before (Devic, Paquereau et al. 1996; Inui, Fukui et al. 2006). In this study, *aplnr*'s temporal and spatial gene expression during early and late *Xenopus* development was analysed in detail. *Aplnr* mRNA was already detected in the involuted mesoderm (Fig. 23) from early gastrula stage on (NF 10). Initially it was expressed in the ventral, dorsal and lateral mesoderm excluding the organizer region. This initial expression was comparable to the *mespa* expression pattern in early gastrula (compare Fig. 4). The broad expression domain at gastrulation is in accordance to an earlier study that both dorsal and ventral blastomeres give rise to the vascular system (Mills, Kruep et al. 1999).

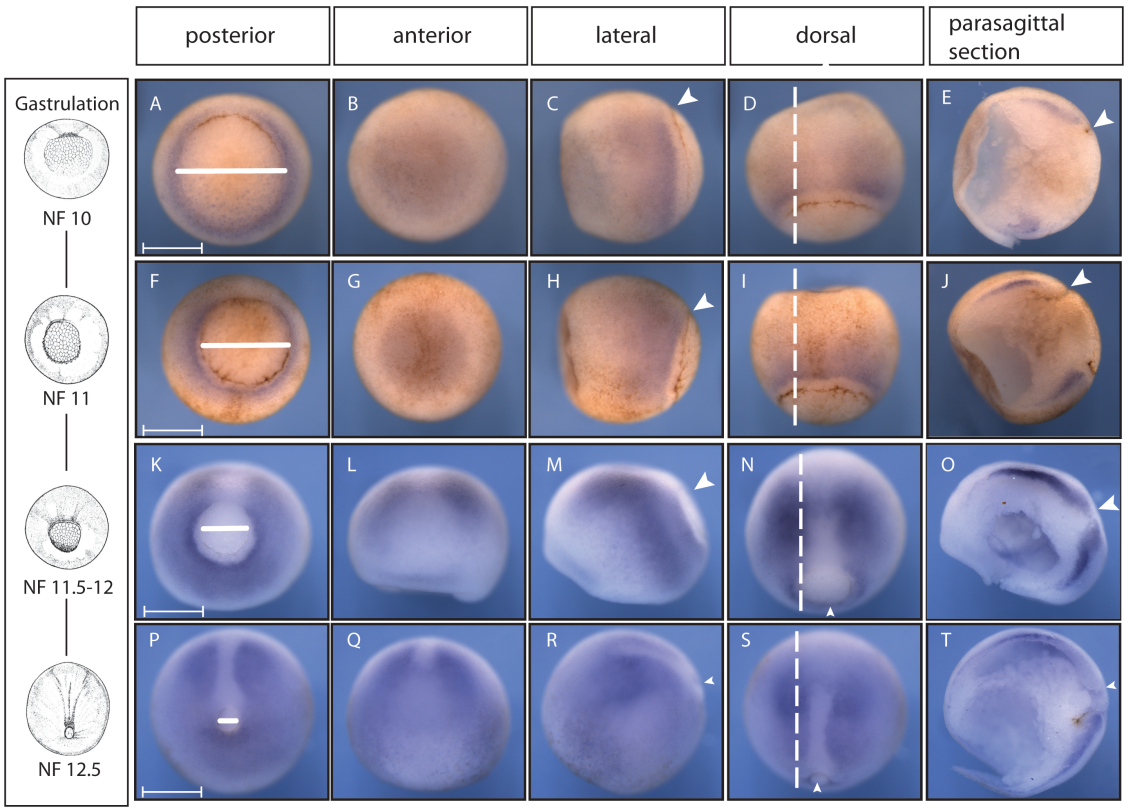

Figure 23: *Apelin receptor* (*aplnr*) gene expression during gastrulation. (A-L) *Aplnr* mRNA expression was detected by RNA *in situ* hybridization at the indicated developmental stages. Panels show different views according to the denotation at the top. *Aplnr* mRNA was expressed from early gastrula stage on **(A-E)** and initially expressed in the ventral and dorsal mesoderm excluding the organizer region **(A)**. Parasagittal sections confirmed that this expression was restricted to the involuted mesodermal layer **(E, J, O, T)**. At the end of gastrulation *aplnr* RNA was additionally present in lateral and anterior regions of the mesoderm **(L, M, Q, R).** Arrowheads indicate blastopore. Horizontal white lines represent the blastopore's diameter. Vertical dashed white lines demarcate plane of section. Scale bars: 500 µm.

During neurulation (Fig. 24), *aplnr* mRNA was still restricted to the mesodermal layer, including the head mesoderm. Sections revealed an expression in the prechordal plate and the paraxial mesoderm (Fig. 24 E, J).

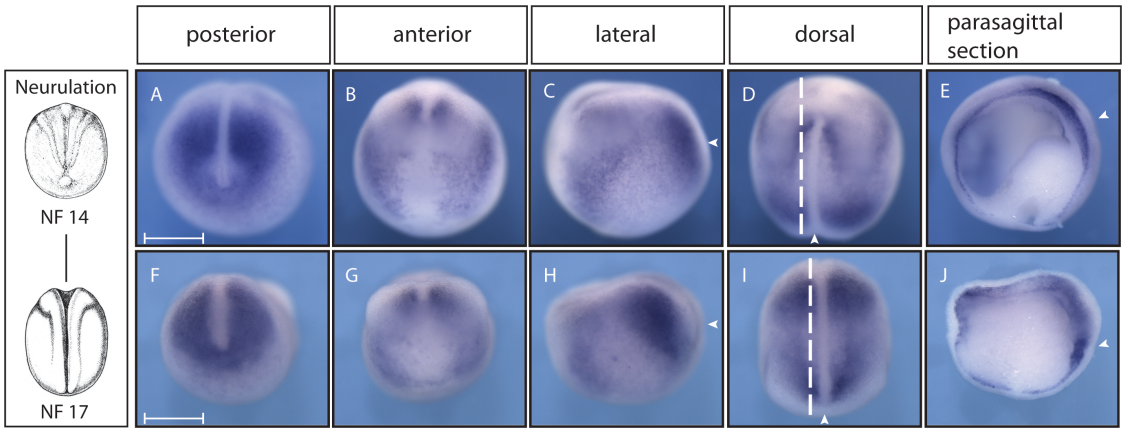

Figure 24: *Aplnr* gene expression during neurulation. (A-J) *Aplnr* mRNA expression was detected by RNA *in situ* hybridization at the indicated developmental stages. Panels show different views according to the denotation at the top. During neurulation *aplnr* was visible in domains next to the anterior neural fold **(B, G)**. Expression in dorsal, ventral and lateral mesoderm continued. Vertical dashed white lines demarcate plane of section. Scale bars: 500 µm.

Later at the tailbud stage, the *aplnr* gene was expressed in forming vascular structures and the tailbud (Fig. 25). Notably, these vascular structures included all of the main existing vessels at this stage. The dorsal aortae run ventral to the notochord and *aplnr* expression in these vessels cannot be seen from the outside (Mills, Kruep et al. 1999). Thus, the *apelin receptor* was confirmed to be a suitable marker molecule, for both early and late vascular development as described before (Devic, Paquereau et al. 1996; Inui, Fukui et al. 2006; Kälin, Kretz et al. 2007).

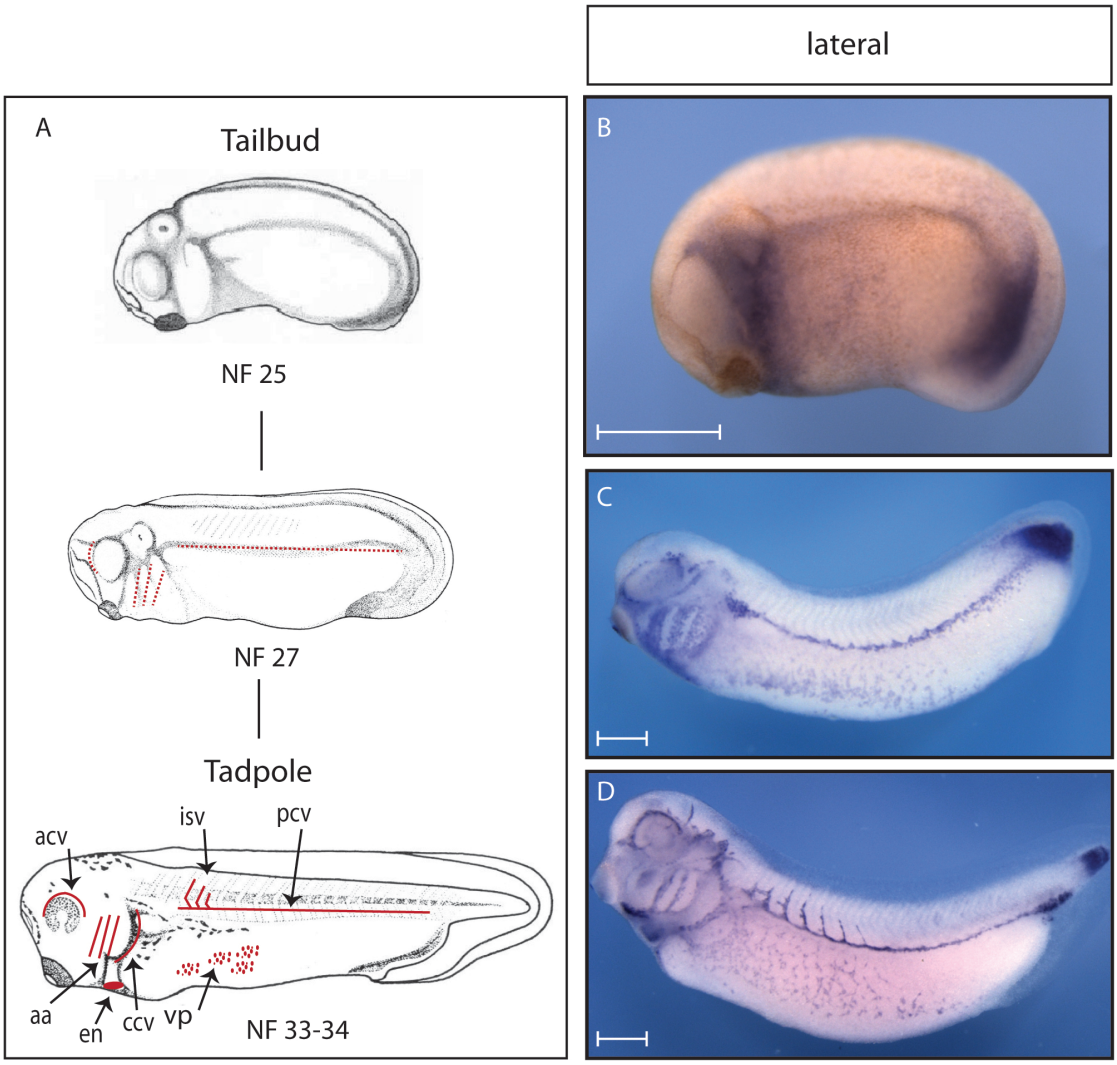

Figure 25: *Aplnr* gene expression during tailbud stage. (A) Scheme of vessels in the tailbud embryo. **(B-D)** *Aplnr* mRNA expression was detected by RNA *in situ* hybridization at the indicated developmental stages. Panels show lateral views, anterior to the left. At tailbud stage *aplnr* RNA was detected in the anterior and posterior cardinal vein (acv and pcv), intersomitic veins (isv), aortic arches (aa), common cardinal vein (ccv), the vascular plexus (vp), endocardium (en) and in the tailbud. (Scheme modified from Mills et al, 1999). Scale bars: 500 µm.

3.3.2 Knockdown of *mespa* causes depletion of *aplnr*

Figure 26 shows loss of function experiments, which were performed, to find out, if *mespa* is required for gene expression of the vasculogenic *apelin receptor*.

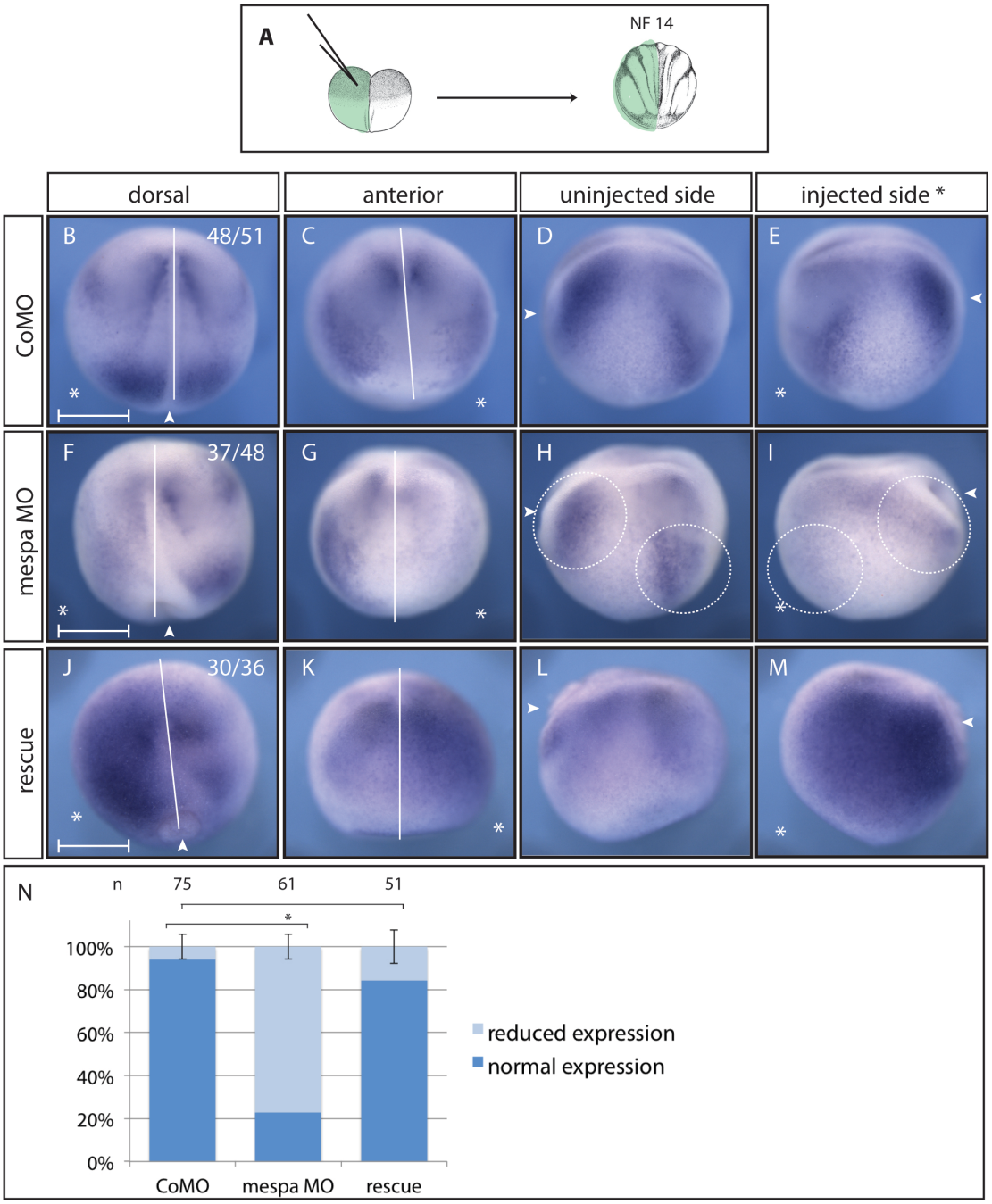

Figure 26: Knockdown of *mespa* causes early depletion of *aplnr* in the lateral and anterior mesoderm. **(A)** Embryos were unilaterally injected at two-cell stage, cultivated until NF 14 and then analysed via RNA *in situ* hybridization for expression of *aplnr*. **(F-I)** Injection of *mespa* morpholino caused a down regulation of *aplnr* in the lateral and anterior region of the injected half (dotted white circles indicate same region of uninjected and injected half). **(B-E)** The same amount of control morpholino showed no alteration. **(J-M)** The morphant phenotype was rescued by injection of morpholino insensitive *mespa* mRNA variant. Panels show different views according to the denotation at the top. Asterisks indicate injected side. Arrowheads mark posterior region. **(N)** Phenotypic distribution of *aplnr* expression in three independent biological repeats; *, $p \leq 0.05$. Scale bars: 500 µm.

The morphants were analysed at an early neurula stage, as differences in *aplnr* gene expression become more distinct at this stage. Unilateral knockdown of

mespa via morpholino injections caused a downregulation of early *aplnr* RNA expression in the anterior and lateral region of the embryo (Fig. 26 F, G, I). This phenotype was fully rescued by adding exogenous *mespa* RNA to the injected morpholino (Fig 26 J, K, M). Injection of control MO caused no alteration of *aplnr* expression (Fig. 26 B, C, E). Hence, the morphant phenotype was specific for *mespa* and *aplnr* gene expression in early neurula is in the anterior and lateral regions dependent on *mespa*.

3.3.3. *Mespa* is required for major vessel formation

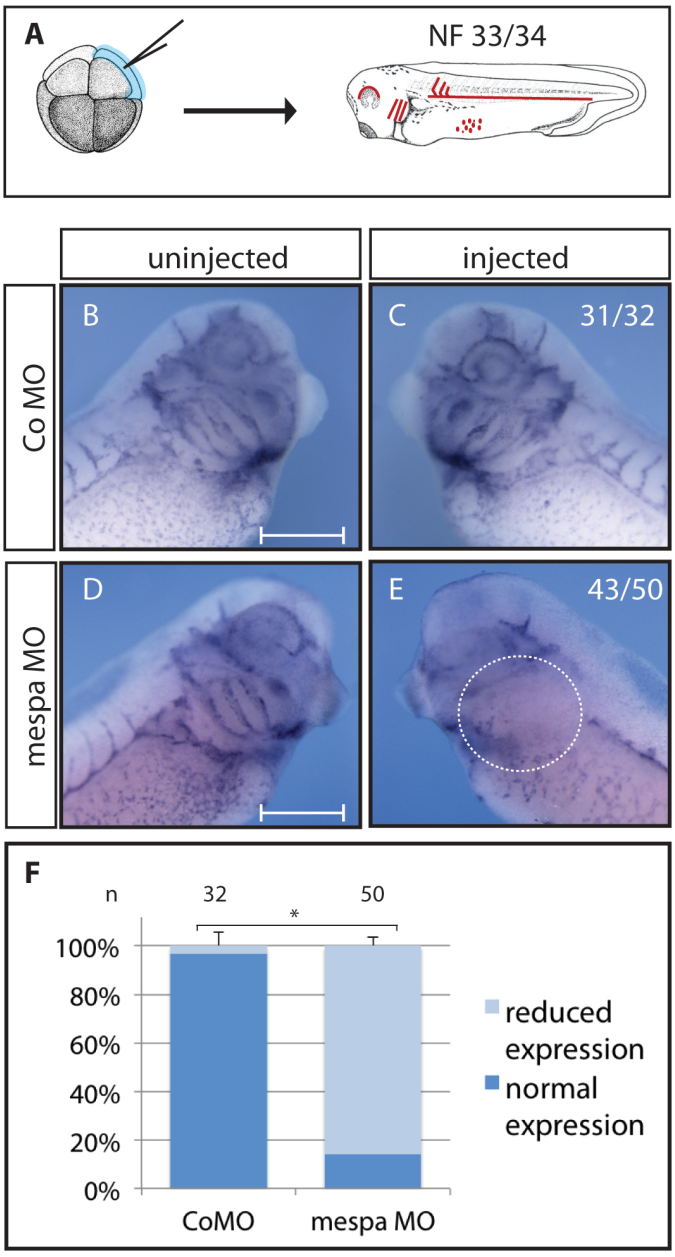

Figure 27: *Mespa* is required for the formation of aortic arches. (A) Embryos were injected into one dorso-vegetal blastomere at eight-cell stage with 10ng of morpholino. **(B-E)** At NF 33-34 they were analysed by RNA *in situ* hybridization for expression of *aplnr*. Panels show lateral views. **(B, C)** Injection of Co-MO

produced no defect in the development of vessels. **(D, E)** Knockdown of *mespa* via morpholino injection led to an absence of the aortic arches. **(F)** Phenotypic distribution of *aplnr* expression in three independent biological repeats; *, $p \leq 0.05$. Scale bars: 500 µm.

To test, whether *mespa* is not only required during early stages for *aplnr* expression, but also affects terminal vascular structures expressing *aplnr*, *mespa* morpholino was injected into different specific blastomeres, according to their contributions to the vascular system (Mills, Kruep et al. 1999).
Subsequently, embryos were analysed at tadpole stage, when vascular structures are established but still dispensable for the supply of oxygen and nutrients.

Knockdown of *mespa* in dorsovegetal cells led to strongly reduced *aplnr* mRNA levels in the aortic arches and the anterior cardinal vein (Fig. 27), whereas ventrovegetal injections led to a reduction of *aplnr* gene transcription in the posterior cardinal vein, intersomitic veins and the vascular plexus (Fig. 28). In summary, depending on the location of *mespa* morpholino injection a site-specific ablation of *aplnr* expression in vascular structures was shown, which suggests an impaired development of the main vessels by *mespa* knockdown.

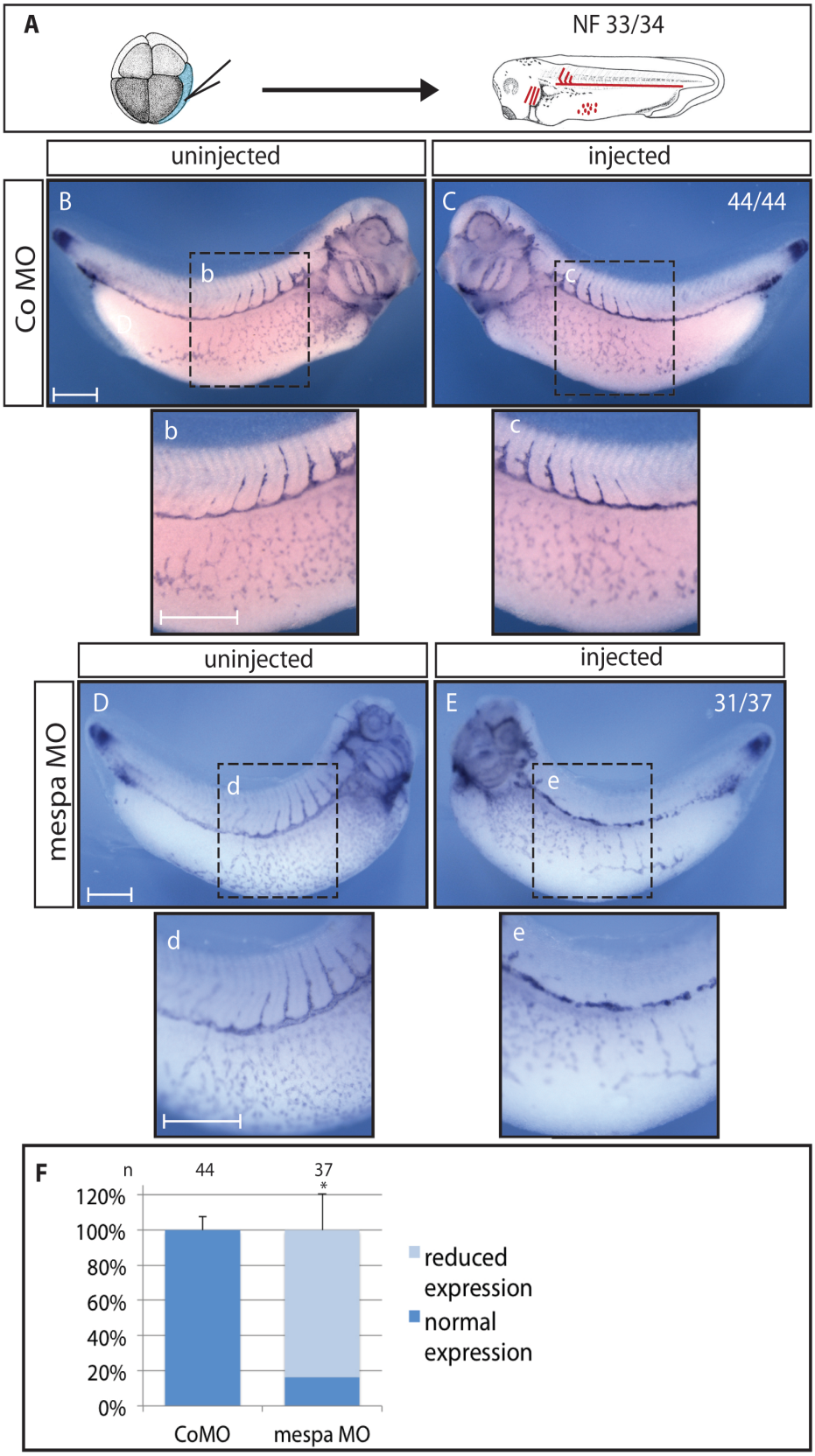

Figure 28: *Mespa* is required for the development of major veins. (A) Embryos were injected into one ventro-vegetal blastomere at eight-cell stage with 10ng of morpholino. **(B-E)** At NF 33-34 they were analysed by *in situ* hybridization for expression of *aplnr*. Panels show lateral views. **(B, C)** Injection of Co-MO produced no defect of vascular structures. **(D, E)** Depletion of *mespa* caused a deficiency in the proper formation of the posterior cardinal vein and intersomitic veins. **(b,c,d,e)** Squares indicate location of enlarged pictures shown beneath **(F)** Phenotypic distribution of *aplnr* expression in three independent biological repeats; *, $p \leq 0.05$. Scale bars: 500 µm.

3.3.4 Induction of *apelin receptor* in animal cap explants

The next question was, if *mespa* induces *aplnr* RNA expression ectopically in animal cap explants.

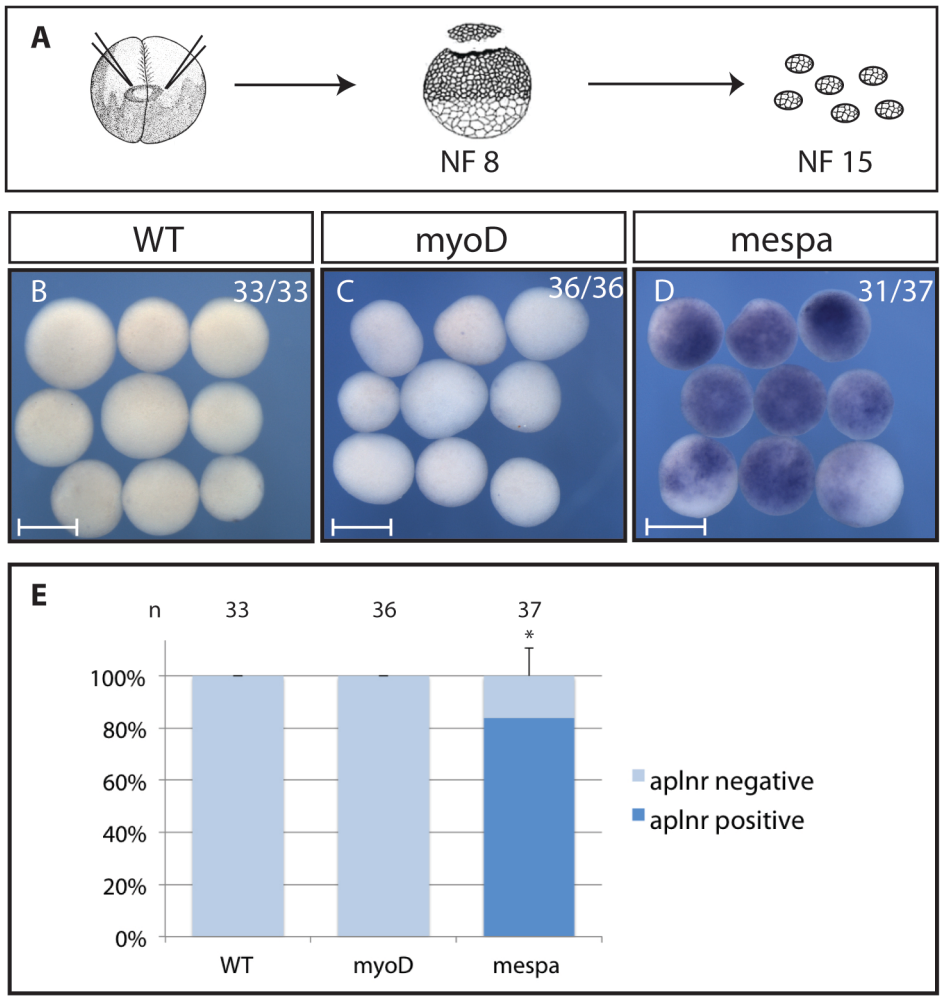

Figure 29: Induction of *aplnr* in animal cap explants. (A) At two-cell stage embryos were injected with 1ng of each mRNA. At NF 8 animal caps were dissected and cultivated until control siblings reached NF 15. **(B-D)** The Figure shows representative animal caps after RNA *in situ* hybridization for *aplnr*. **(B)** Uninjected animal caps (WT, wildtype) showed no expression of *aplnr*. **(C)** Injection of *myoD* mRNA did not induce *aplnr* expression. **(D)** *Aplnr* was only induced by *mespa* mRNA injection. **(E)** Chart displays quantity of *aplnr* mRNA expressing animal caps for each condition in three independent biological repeats; *, $p \leq 0.05$. Scale bars: 500 µm.

The gain of function experiments, depicted in Figure 29, showed a high potency of *mespa* to ectopically activate *aplnr* transcription in prospective ectodermal tissue. In contrast to *mespa*, *myoD* was not able to induce *aplnr* gene expression. Therefore, *mespa* is sufficient to induce the vasculogenic marker *aplnr* in prospective ectodermal cells of the animal caps. Concluding from these results, *mespa* is required and sufficient for *aplnr* expression.

3.4 Migration/Morphogenesis

Since MesP1 knockout mice showed severe cardiac malformations attributed to a migration defect of cardiac precursor cells (Saga, Miyagawa-Tomita et al. 1999), MesP1 was hypothesized to have a morphogenetic function in gastrulation. Moreover, MesP1 was shown to regulate genes involved in epithelial-to-mesenchymal-transition in ES cells, e.g. N-Cadherin, Snail and Twist (Bondue, Lapouge et al. 2008; Lindsley, Gill et al. 2008).

In my study, *mespa* morphant embryos presented a defect in the anterior migration of the mesodermal layer (compare Fig. 21).

3.4.1 Fluorescent labelling shows mesodermal migration defect

In order to assess, whether *mespa* depleted mesodermal cells show a defect in migration during gastrulation, migrating mesoderm was marked via fluorescent dye (Fig. 30). Embryos were injected with control MO and green fluorescent lineage trace on the left side and with *mespa* MO and red fluorescent lineage trace on the right side. These embryos were subsequently photographed under bright and fluorescent light during gastrulation stages (Fig. 30 A).

In contrast to the green Co MO-injected cells, the red *mespa* MO-injected cells failed to converge to the midline and did not migrate anteriorly. Normally, when reaching the endpoint of mesoderm migration, cells of the leading edge spread out and diverge across the blastocoel roof (Keller and Tibbetts 1989). Accordingly, the Co Mo injected green fluorescent mesodermal cells were found in the anterior ventral region (Fig. 30 F, G, L, M). In contrast, the morphant red fluorescent cells stayed behind and concentrated in posterior location (Fig. 30 C, D, I, J). Parasagittal sections through the left and the right side revealed the migratory behaviour of the involuted mesodermal cells. The two surfaces of the central slice are shown in Figure 30 (n-s), presenting the left Co MO- injected side (green) and the right *mespa* MO-injected side (red). In anterior-ventral position no red fluorescent cells, but only green fluorescent cells were found

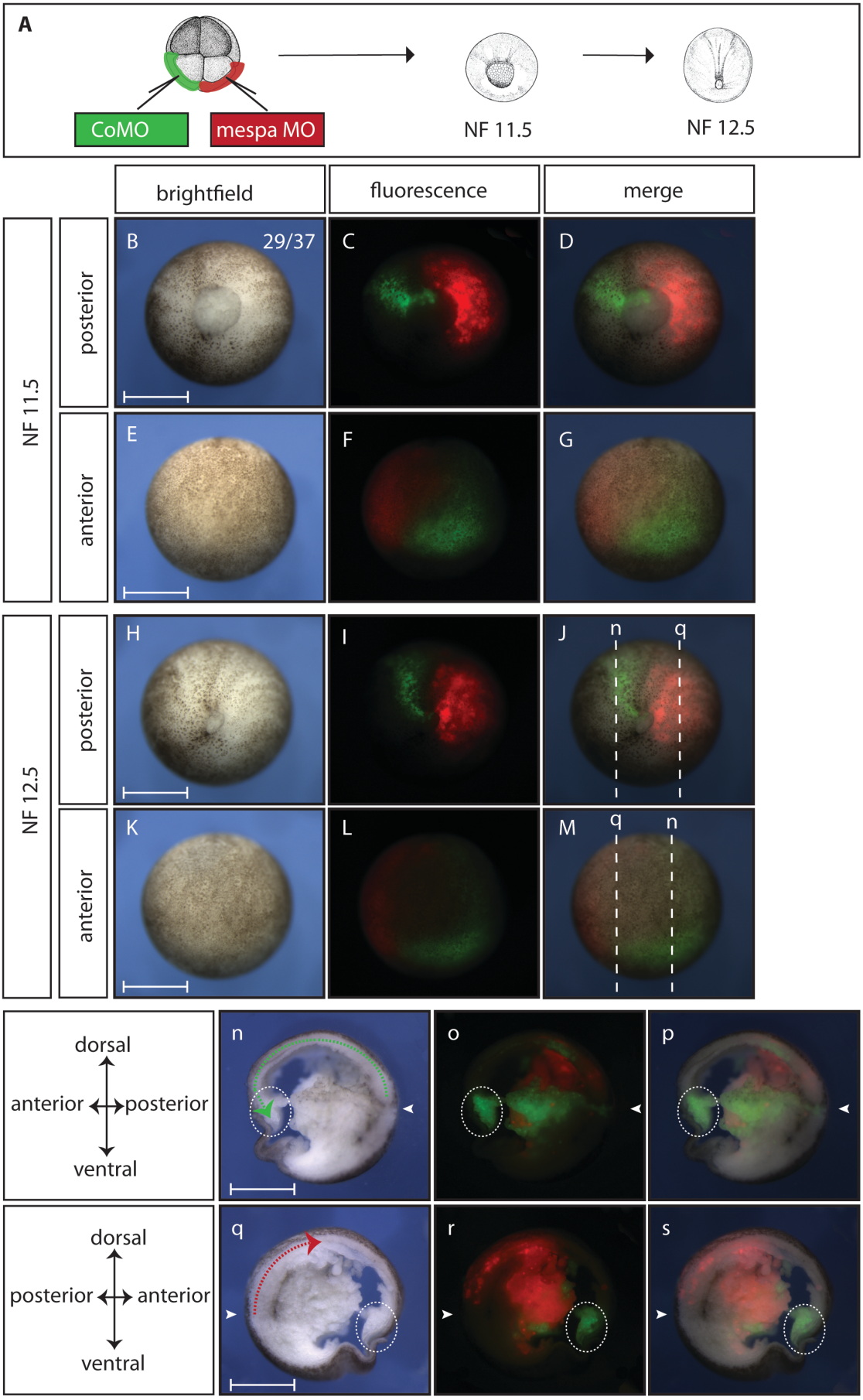

Figure 30: *Mespa* knockdown results in migration defect of leading edge mesoderm. (A) Embryos were injected with 10ng of control morpholino plus green fluorescent dye (Alexa Fluor 488) into the left dorsovegetal blastomere and with 10ng of *mespa* morpholino plus red fluorescent dye (Alexa Fluor 594) into

the right dorsovegetal blastomere at eight-cell stage. **(B-M)** At NF 11.5 and 12.5 they were photographed with a Fluorescence Stereomicroscope. Panels show bright light, fluorescent light and merge, as annotated at the top and anterior and posterior views as annotated on the left; n and q indicate plane of section shown in **(n-s). (n-s)** Parasagittal sections through the left and the right side after fixation at the end of gastrulation revealed the migratory behaviour of the involuted mesodermal cells. In contrast to the green CoMO- injected cells **(n-p)**, the red *mespa* MO-injected cells failed to converge to the midline and did not migrate anteriorly **(q-s)**. Green arrow in **(n)** and red arrow in **(q)** represent distance of migration from the blastopore to the anterior region of mesodermal cells. Dashed circles mark cells in the anterior region. Arrowheads indicate blastopore (n=3). Scale bars: 500 µm.

In conclusion, it was shown that *mespa* function is indeed essential for migratory movements of the mesoderm during gastrulation, as *mespa* depleted cells failed to migrate anteriorly.

This made us look after genes, which control mesoderm morphogenesis, as potential mediators for this *mespa* function.

3.4.2 *Paraxial protocadherin* gene expression analysis

An interesting candidate for the proposed link between the transcription factor mespa and mesoderm migration is *PAPC*, which interacts with the *mesp* family genes during somitogenesis (Kim, Jen et al. 2000; Sawada, Fritz et al. 2000).

Cadherins make up a large group of cell membrane molecules, which are involved in tissue morphogenesis. A considerable subfamily among the cadherins is the group of protocadherins. In comparison to the cadherins, protocadherins have around seven extracellular cadherin repeats in the extracellular domain and an intracellular domain with signaling function, instead of the intracellular catenin-binding sites, of cadherins. The extracellular domain of *PAPC* was found out to function in cell sorting and cell adhesion modifications during gastrulation (Chen and Gumbiner 2006; Kraft, Berger et al. 2012). The intracellular domain is associated with tissue separation and convergence extension movements throughout gastrulation (Kim, Yamamoto et al. 1998; Medina, Swain et al. 2004; Unterseher, Hefele et al. 2004). These movements are regulated via small G-Proteins (Koster, Jungwirth et al. 2010). Moreover, the planar cell polarity pathway is involved in the execution of these functions (Wang, Janicki et al. 2008). Recently, *PAPC* was found to establish tissue identity dependent on Snail1 expression and to modulate cell adhesion during tissue separation (Luu, Damm et al. 2015)

Protocadherins have been investigated in detail in *Xenopus*, and are thought to have conserved roles in other species (Wang and Steinbeisser 2009).

Until now, only the transcription factor lim1 was found out to be required for *PAPC* expression in gastrulation movements in *Xenopus*, as well as in mammals like mice (Hukriede, Tsang et al. 2003).

A spatial and temporal gene expression analysis of *PAPC* during gastrulation is shown in Figure 31. *PAPC* gene expression started at the onset of gastrulation in the dorsal region in the mesodermal layer (Fig. 31 A, D, E). Sections revealed this expression to be confined to the early involuting mesoderm.

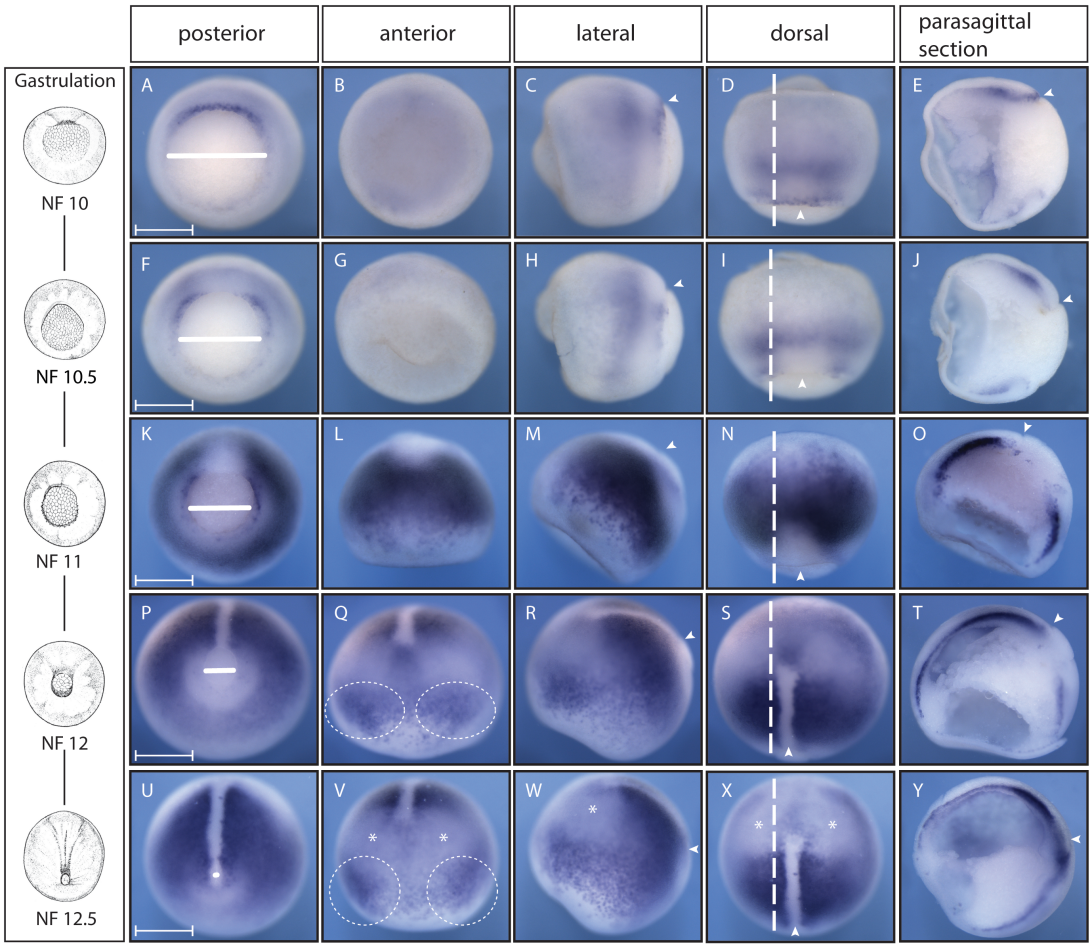

Figure 31: *Paraxial protocadherin* (*PAPC*) gene expression during gastrulation. (A-Y) *PAPC* mRNA expression was detected by RNA *in situ* hybridization at the indicated developmental stages. Panels show different views according to the denotation at the top. **(A-E)** *PAPC* mRNA was discovered from early gastrula stage on (NF 10) and initially expressed in the dorsal region **(A, D)**. Parasagittal sections show that this expression was restricted to the early involuting mesodermal layer **(E)**. From stage NF 10.5 on the notochordal expression was gone and *PAPC* appeared on both sides of the organizer in the paraxial and lateral mesoderm **(F, I)**. Sections showed that expression was located to the involuted dorsal and ventral mesoderm **(J, O, T, Y)**. **(T)** Within the course of gastrulation these *PAPC* positive cells were detected in the anterior part of the embryo, corresponding to leading edge mesoderm (dotted white circles). At the end of gastrulation *PAPC* was present in almost the whole mesodermal layer **(U-Y)** except the head mesoderm (asterisks). Arrowheads indicate blastopore. Horizontal white lines represent the blastopore's diameter. Vertical dashed white lines demarcate plane of section. Scale bars: 500 µm.

As gastrulation proceeded the dorsal expression disappeared and *PAPC* mRNA was present on both sides of the organizer in the paraxial mesoderm (Fig. 31 F, H, I, J). At the end of gastrulation *PAPC* was expressed in almost the whole mesodermal layer (Fig. 31 U-Y), except the head mesoderm (comp. Fig. 9), according to Keller's fate map of the deep mesodermal layer (Keller 1976). Sections confirmed that *PAPC* mRNA was restricted to the mesodermal layer only and spread out until the posterior margin of involuting mesoderm (Fig. 31 E, J, O, T, Y).

During neurula stage, expression of the protocadherin was still detected in the anterior and lateral mesoderm (Fig. 32). Additionally, *PAPC* mRNA levels were enhanced in the forming somites.

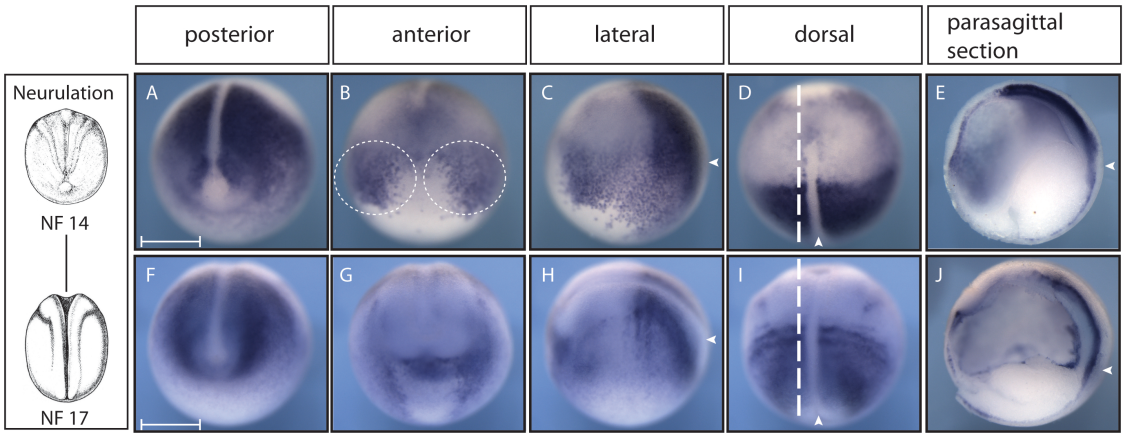

Figure 32: *PAPC* gene expression during neurulation. (A-J) *PAPC* mRNA expression was detected by RNA *in situ* hybridization at the indicated developmental stages. Panels show different views according to the denotation at the top. During Neurulation gene expression was located in the paraxial dorsal somite mesoderm leaving out the notochord, as well as in the anterior and lateral mesoderm. Arrowheads indicate posterior region. Dashed lines indicate plane of horizontal section. Scale bars: 500 µm.

Later on in development during tailbud stage *PAPC* mRNA was detected in the somites, lateral plate mesoderm and the otic placode (Fig. 33). A horizontal section showed continuous expression in the mesodermal layer (Fig. 33 B). During tadpole stages, *PAPC* expression was found in the tail tip, branchial arches and the otic vesicle (Fig. 33 C, D). The expression in the otic vesicle was consistent with a report of *PAPC* to regulate the invagination of the otic placode (Jung, Kohler et al. 2011). By late tailbud stage, expression of *PAPC* has vanished (Fig. 33 E).

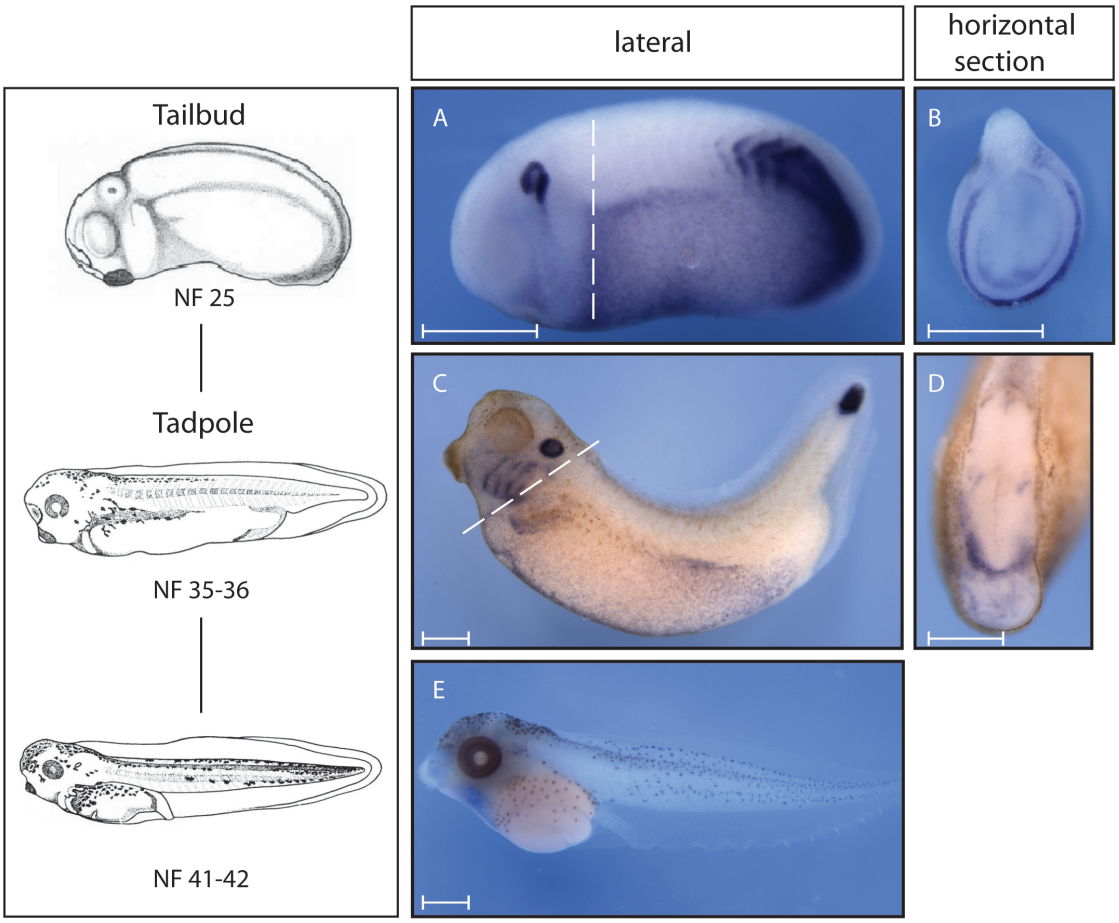

Figure 33: *PAPC* gene expression during tailbud stage. (A-E) *PAPC* mRNA expression was detected by RNA *in situ* hybridization at the indicated developmental stages. Lateral view, anterior is to the left. **(A)** During tailbud stage *PAPC* mRNA was visible in the otic vesicle, in the tailorganizer and in the lateral plate. **(B)** The horizontal section shows detection of *PAPC* in the mesodermal layer of the trunk. **(C, D)** Later on *PAPC* was additionally expressed in the aortic arches. **(E)** Expression disappeared until late tailbud stage. Dashed line indicates plane of horizontal section. Scale bars: 500 µm.

The overlapping expression patterns of *mespa* and *PAPC* during gastrulation are seen best in side by side comparison of sibling embryos (Fig. 34).

Overlapping domains of expression included anterior, heart forming, leading edge mesoderm, as well as lateral and ventral mesoderm, strongly suggesting a regulatory connection. The most anterior dorsal stripe of *mespa* expression appears to coincide with the anterior margin of PAPC expression in the first forming somite, at the border of head and somite mesoderm (Fig. 34 A, B). The somitogenic mesoderm posterior to the first forming somite is a *mespo* expression domain (Kriegmair, Frenz et al. 2013). The highly related bHLH transcription factor *mespo*, involved in somitogenesis, could compensate for a lack of *mespa* expression in that specific region and be an additional input for *PAPC*. Double RNA *in situ* hybridization for a simultaneous staining of *mespa* and *PAPC* RNA

expression in the same embryo, were not successful due to much lower expression levels of *mespa* compared with *PAPC*.

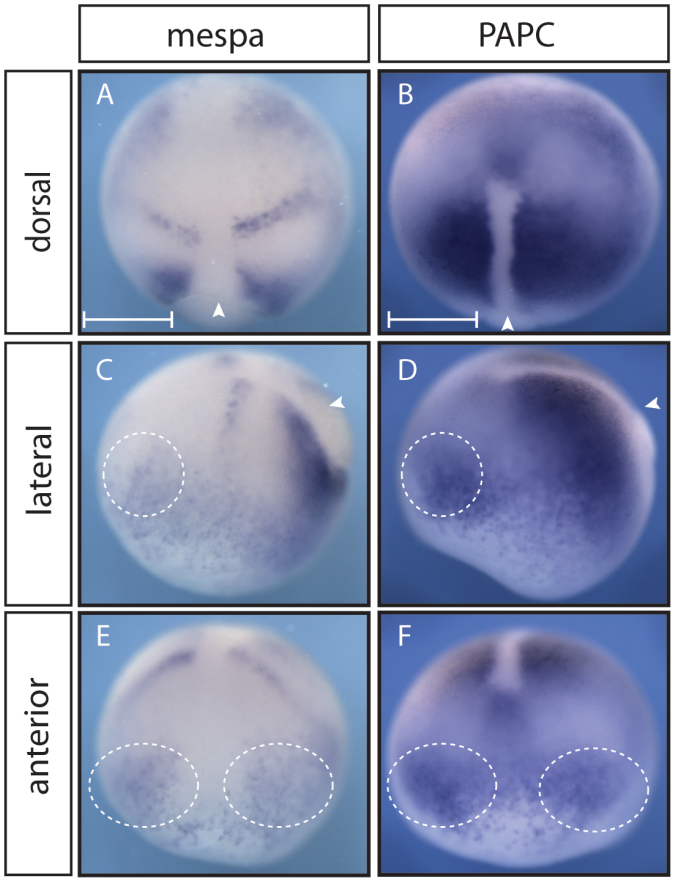

Figure 34: Overlap of *mespa* and *PAPC* gene expression during gastrulation. (A-F) The Figure shows a comparison of *mespa* and *PAPC* expression pattern at NF 12.5 after RNA *in situ* hybridization. Views are described on the left. **(A, B)** The dorsal view shows an overlap of gene expression in the paraxial mesoderm and at the border of head and somite mesoderm. **(C-F)** Lateral and anterior views reveal an overlap in lateral plate and leading edge mesoderm. Arrowheads indicate blastopore. Dashed circles indicate comparable pattern in the anterior region. Scale bars: 500 µm.

3.4.3 *PAPC* mRNA is downregulated in *mespa* depleted embryos

Given this interesting correlation in gene expression patterns, loss of function experiments were performed. Morpholino mediated knockdown of *mespa* reduced *PAPC* mRNA, most prominently in the dorsal, lateral and anterior mesoderm(Fig. 35, F-I). Horizontal sections confirmed depletion of *PAPC* expression in the mesodermal layer on the *mespa* morphant side (Fig. 35 P, Q).

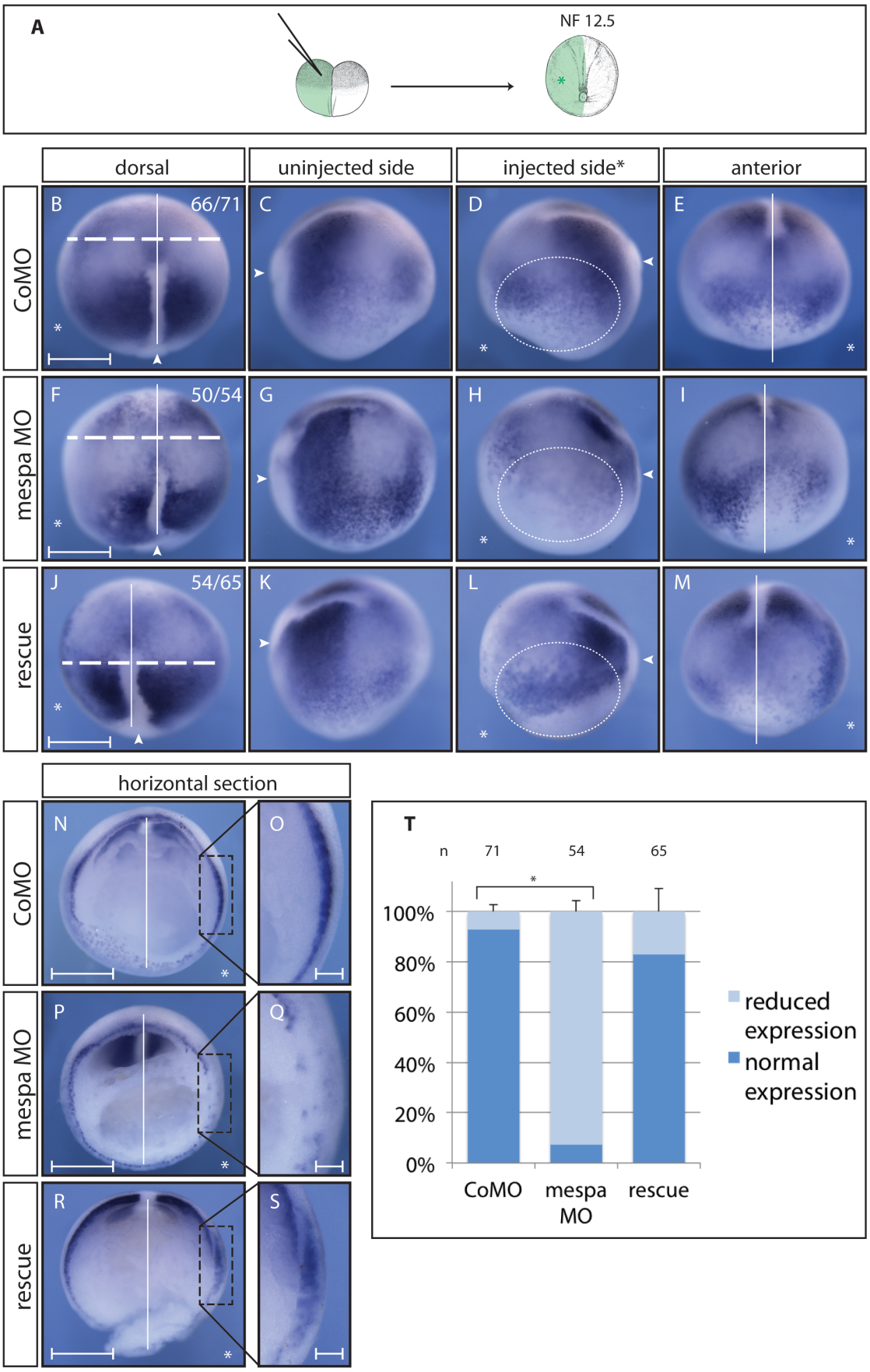

Figure 35: *PAPC* mRNA is down regulated in *mespa* depleted embryos. (A) Embryos were unilaterally injected at two-cell stage, cultivated until NF 12.5 and then analysed via RNA *in situ* hybridization for expression of *PAPC*. **(F-I)** Injection of 20ng of *mespa* morpholino caused a downregulation of *PAPC* in the injected half. **(B-E)** The same amount of control morpholino caused no alterations. **(J-M)** The morphant phenotype was rescued by injection of 250pg morpholino insensitive *mespa* mRNA variant. Panels show

different views according to the denotation at the top. Asterisks mark injected side. **(B, F, J)** Dashed lines indicate plane of horizontal sections shown in **(N-S)**. **(N-S)** Horizontal sections reveal PAPC expression in the mesoderm **(N, O)**, which is down regulated by *mespa* morpholino **(P, Q)** and rescued via *mespa* mRNA injection **(R, S)**. Squares denote enlarged view of mesodermal layer depicted in **(O, Q, S)**. **(T)** Phenotypic distribution of *PAPC* expression in three independent biological repeats; *, $p \leq 0.05$. Scale bars: 500 µm, right column (O, Q, S) 100 µm.

Remarkably, *PAPC* expression was not completely ablated in the morphant half, which implies the existence of additional regulatory inputs for the *PAPC* gene. By combined co-injection of *mespa* mRNA, depleted for the morpholino recognition region, together with *mespa* morpholino, *PAPC* expression was restored (Fig. 35 N-S). However, sections of the rescued morphants still revealed a defect in mesodermal and ectodermal germ layers.

3.4.4 Mosaic knockdown leads to failure of convergence movements

To create a mosaic depletion of the migrating mesoderm, *mespa* MO or control MO was injected together with *ß-Galactosidase* mRNA into the dorsovegetal blastomere at 8-cell stage (Fig. 36).

Co MO-injected embryos presented a normal expression of *PAPC*. The *ß-Galactosidase* targeted cells were recognizable by a light-blue stain and showed an anterior migration according to the dorsovegetal domain of injection (Fig. 36 B-E). By comparison, the *mespa* morphants presented a depletion of *PAPC* expression in the light-blue-targeted cells (Fig. 36 F-I). Cells ablated for *mespa* stayed posteriorly behind and failed to migrate anteriorly (Fig. 36 F-I). This phenotype could be attributed to a defective intercalation during dorsal convergence extension movements of the mesodermal cells. Normally, these cells “actively narrow in one dimension (convergence) and lengthen in the perpendicular dimension (extension)” (Keller, Davidson et al. 2000). In this context, the term “convergence” stands for the dorsal narrowing along the mediolateral axis and extension means lengthening along the anterior posterior axis, rectangular to the narrowing. This is achieved by cell intercalation, which has been defined as „the rearrangement of cells along the mediolateral axis to produce an array that is narrower in this axis and longer in the anteroposterior axis“ (Keller, Davidson et al. 2000). Thereby cells shift in between each other and form fewer rows of cells with a greater length. Convergence and extension movements as a mode of morphogenesis are highly conserved in vertebrates (Keller and Hardin 1987). The morphant embryos showed moreover a blastopore closure defect, which were caused by the

insufficient amount of dorsal convergence, as “the forces of convergence form a hoop stress around the blastopore, which squeezes the blastopore shut” (Keller, Davidson et al. 2000).

Besides this aspect, the observed phenotype suggests an imbalance in adhesion- versus separation processes.

In conclusion, *mespa* knockdown led to a loss of *PAPC* expression and a phenotype of disturbed convergence extension movements and layer formation.

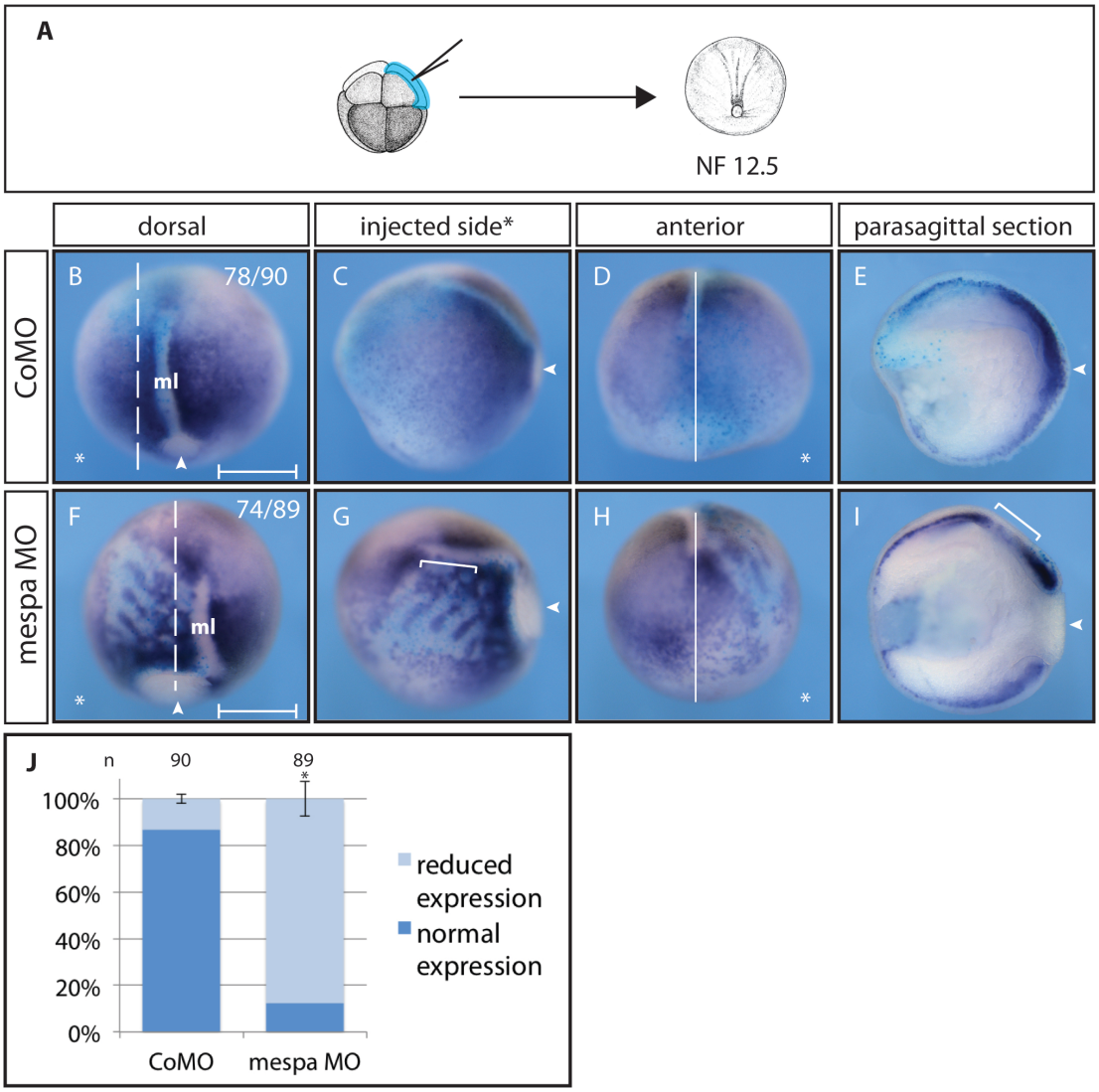

Figure 36: *Mespa* knockdown leads to failure of convergence extension movements. (A) Embryos were injected into one dorsovegetal blastomere at eight-cell stage with 10ng of morpholino and LacZ mRNA as lineage trace. **(B-I)** At NF 12.5 they were analysed by RNA *in situ* hybridization for expression of *PAPC*. Panels show different views indicated at the top. **(B-E)** Injection of Co-MO produced no defects. **(F-I)** Depletion of *mespa* led to failing of dorsal convergence of the injected cells. **(I)** Parasagittal section displayed a deficiency in anterior migration of *mespa* morphant mesoderm. Asterisks mark injected side. Dashed lines indicate plane of parasagittal sections. Ml, midline; bracket marks zone of *PAPC* downregulation; arrow heads in indicate blastopore. **(J)** Phenotypic distribution of *PAPC* expression in three independent biological repeats; *, $p \leq 0.05$. Scale bars: 500 µm.

3.4.5 Overexpression of *mespa* causes ectopic *PAPC* expression

Mespa gain of function in one half of the embryo was achieved by unilateral injection of *mespa* RNA, which is illustrated in Figure 37.

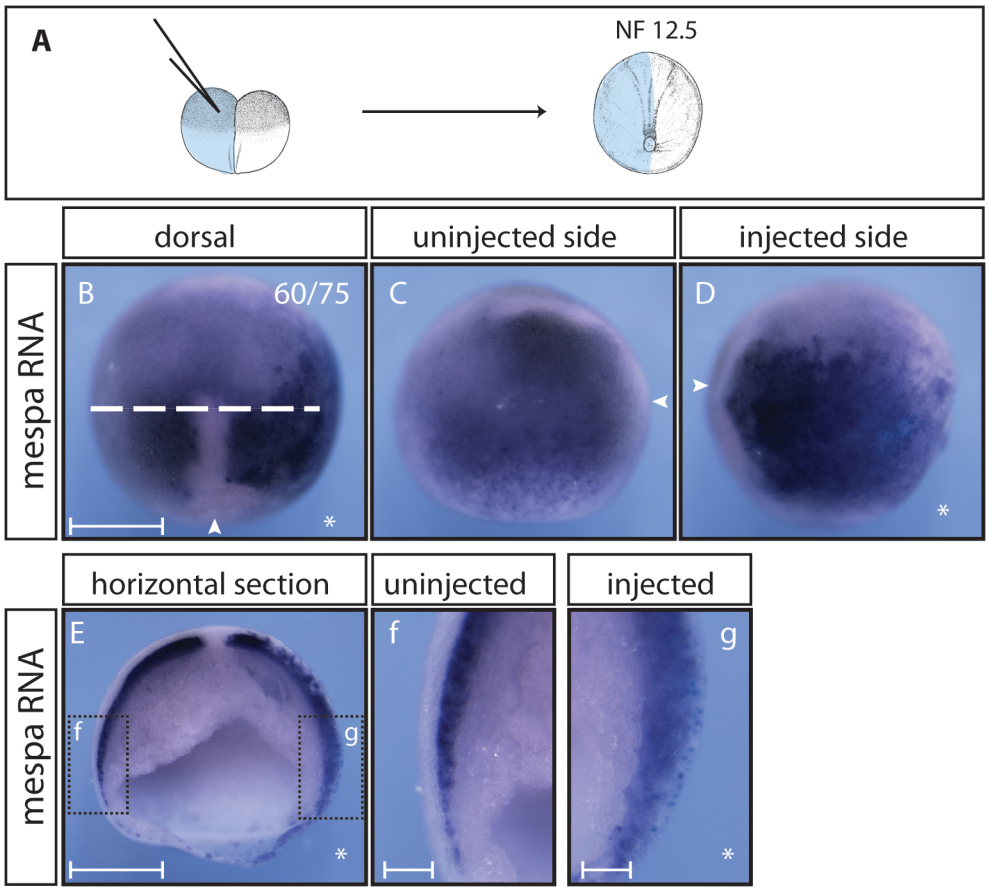

Figure 37: Ectopic *PAPC* expression by *mespa* overexpression. (A) At two-cell stage 250pg of *mespa* mRNA was unilaterally injected into one blastomere. **(B-E)** The embryos were cultivated until NF 12.5 and subjected to RNA *in situ* hybridization for *PAPC*. Panels show different views as denotated at the top. *PAPC* was expressed in the outer cell layer of the injected half **(D, g)**. Dashed line marks plane of horizontal section. Arrowheads indicate blastopore. Asterisks label injected side. Dashed squares indicate region of enlarged view shown in **(f,g)**. Scale bars: 500 µm (B-E) and 100 µm (f,g).

This type of injection preloads mainly prospective ectodermal and mesodermal tissues with the injected mRNA. Since *mespa* expression was not restricted to the mesodermal layer, *PAPC* was induced by *mespa* and ectopically expressed in the outer cell layer of the injected half (Fig. 37 D, E, g). Notably, endodermal cells did not express *PAPC*. Horizontal sections revealed that tissue layer formation seemed to be disturbed upon *mespa* overexpression. There was no clear tissue boundary between the ectodermal and mesodermal layer present, which was indicated by the continuous staining for *PAPC* gene expression in the ectoderm and mesoderm (Fig. 37, g). Remarkably, *PAPC* gene transcription is normally restricted to the mesodermal layer, indicating that *mespa* is sufficient to induce *PAPC* expression in the outer cell layer or even ectopically in the ectoderm, but not in the endoderm.

3.4.6 Induction of *PAPC* in animal cap explants

Subsequently to the gain of function experiments in the whole mount embryo, *mespa* gain of function in tissue explants was carried out.

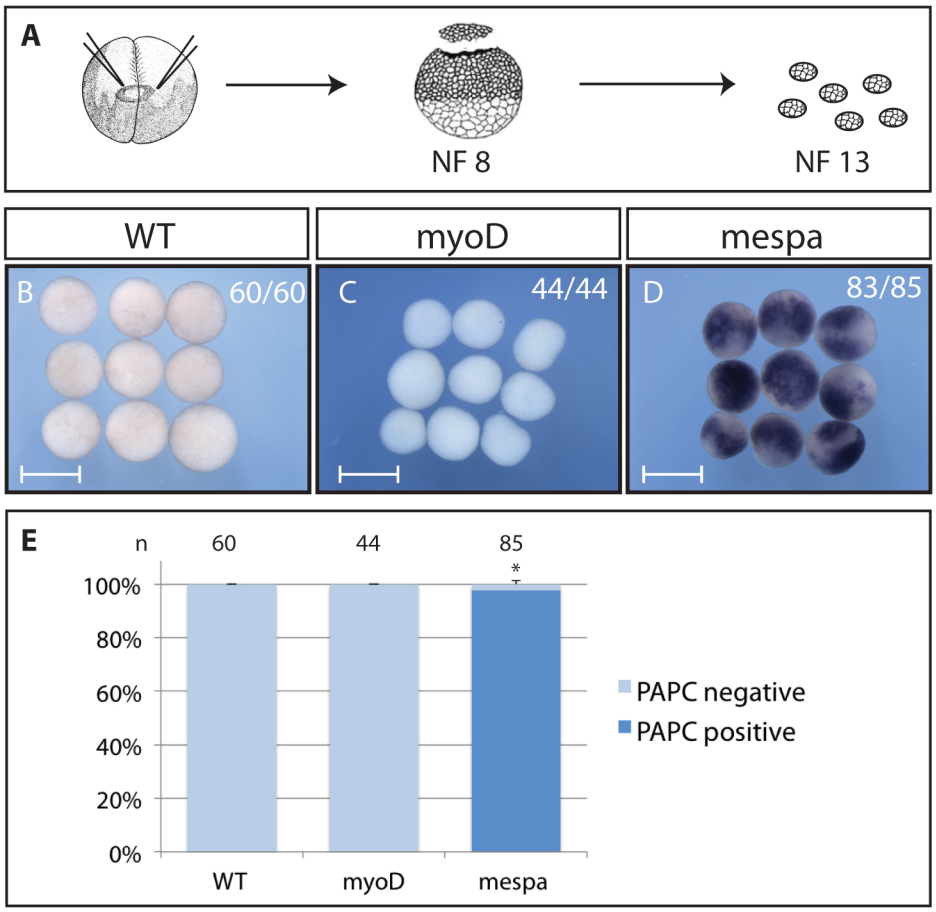

Figure 38: Induction of *PAPC* in animal cap explants. (A) At two-cell stage embryos were injected with 1ng of each mRNA. At NF 8 animal caps were dissected and cultivated until control siblings reached NF 13. **(B-D)** The Figure shows representative animal caps after RNA *in situ* hybridization for *PAPC*. **(B)** Uninjected animal caps (WT, wildtype) showed no expression of *PAPC*. **(D)** Injection of *mespa* RNA induced expression of *PAPC* in animal cap explants. **(C)** This induction was not achieved by *myoD*. **(E)** Chart displays quantity of *PAPC* expressing animal caps for each condition in three independent biological repeats; *, $p \leq 0.05$. Scale bars: 500 µm.

Wildtype animal cap explants do not express the *PAPC* gene (Fig. 38, B). Exogenous *mespa* mRNA induced the transcription of *PAPC* in uncommitted cells of the animal cap explants in a highly penetrant number (Fig. 38, D). Although *myoD* overexpression was shown to initiate gene transcription of mesodermal genes like *cardiac actin* in animal cap explants (Rupp, Snider et al. 1994), induction of *PAPC* could not be achieved by *myoD* mRNA injection (Fig. 38, C).

In conclusion, the presented results suggest a function for mespa in the anterior migration of the mesoderm. *PAPC* was shown to be most likely a downstream

target gene of *mespa* in morphogenesis, as *mespa* knockdown led to a partial loss of *PAPC* gene expression and *mespa* overexpression induced *PAPC* ectopically. Morevore, *mespa* and *PAPC* showed a spatial and temporal overlap of gene transcription in significant mesodermal domains, as the anterior heart forming mesoderm.

3.5 Mesoderm formation/Skeletomyogenesis

A retrospective clonal analysis of mice embryos showed that cardiovascular and head muscle progenitors originate from a common precursor (Lescroart, Kelly et al. 2010). Furthermore, a study in ES cells demonstrated that Mesp1 could induce ES cells to adopt hematopoietic, skeletomyogenic or cardiac fates, depending on the state of differentiation and signalling environment (Chan, Shi et al. 2013).

Since my experiments showed moreover multiple functions for *mespa* for mesodermal genes, I hypothesized a more general role for *mespa* in the formation of the mesodermal germ layer.

3.5.1 Overlapping expression of *mespa*, *brachyury*, *myoD* and *myf5*

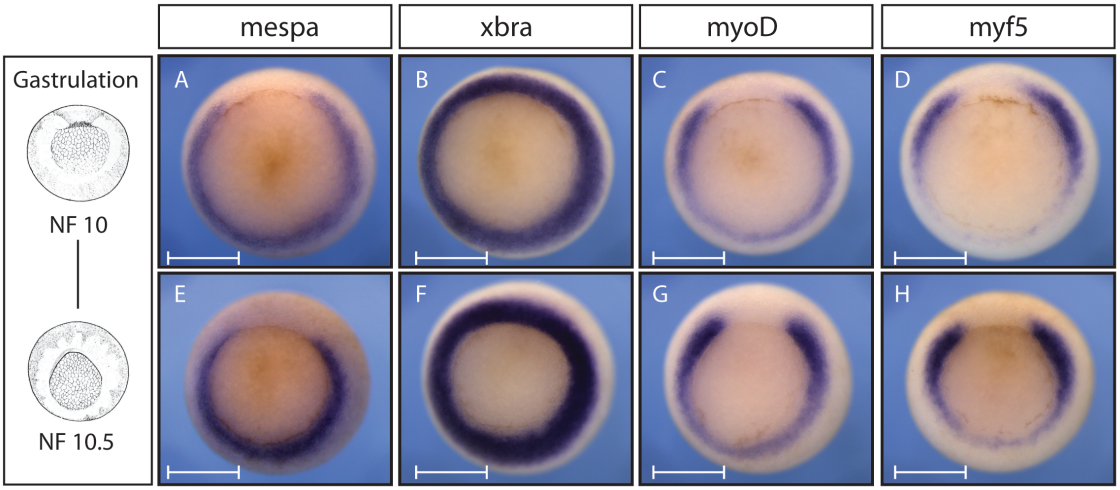

Figure 39: Overlapping expression of *mespa*, *xbra*, *myoD* and *myf5*. (A-H) Embryos were cultivated until NF 10 **(A-D)** and NF 10.5 **(E-H)** and subjected to RNA *in situ* hybridization for expression of *mespa*, *brachyury*, *myoD* and *myf5.* A comparable expression pattern of *mespa*, *brachyury* (*xbra*), *myoD* and *myf5* was visible in the blastoporal collar of mesoderm. *Xbra* was additionally expressed in the dorsal organizer region. Posterior view. Scale bars: 500 µm.

In situ hybridization revealed that the *mespa* expression pattern in the blastoporal collar of the gastrula stage embryo resembled the expression of *brachyury* (*xbra*) (Fig. 39 B, F), an essential mesodermal inductive T-box transcription factor, which was shown to induce MesP1 expression in ES cells (David, Jarsch et al. 2011). Furthermore, the early *mespa* expression pattern overlapped with the expression of *myoD* and *myf5* (Fig. 39 C, D, G, H), which are expressed during early gastrula (Steinbach, Ulshöfer et al. 1998). *MyoD* and its paralogue *myf5*, are bHLH transcription factors, which control the determination and differentiation of skeletal muscle cell lineages (Penn, Bergstrom et al. 2004)

Figure 39 depicts embryos at the beginning of gastrulation, which were stained by RNA *in situ* hybridization for expression of *mespa*, *xbra*, *myoD* and *myf5*. The pictures show a vegetal view of the blastopore. All of these transcription factors were expressed in a circular manner, surrounding the blastopore. The dorsal gap of expression for *mespa*, *myoD* and *myf5* represents the organizer region, which will later become notochord mesoderm. In comparison, *xbra* expression included the dorsal organizer region. Notably, the *mespa d*omain was moreover smaller than the ring of *xbra* expression (Fig. 39 A, B, E, F).

The somitogenic mesoderm (comp. Fig. 3) converges posteriorly to form a thick ring surrounding the blastopore and will be added to posterior, dorsal structures (Keller 1976; Wilson, Oster et al. 1989). Therefore, *MyoD* and *myf5* expression was slightly more intense in the dorsal paraxial mesoderm just next to the organizer (Fig. 39 C, D, G, H). The myotomal compartment of the somites will later generate striated skeletal muscle (Buckingham 1992).

In contrast, *mespa* expression was concentrated in the ventral mesodermal region opposite to the organizer (Fig. 39 A, E). *Xbra* expression was condensed and extended more laterally, than *mespa*, *myoD* and *myf5* at this early gastrula stage. The spatial and temporal overlap of expression domains indicated a corresponding co-expression of these genes in most ventrolateral mesodermal cells. Thus, an interaction between *mespa* and *xbra* for mesodermal induction and between *mespa* and *myoD and myf5* for skeletomyogenic regulation are formally possible.

3.5.2 Knockdown of *mespa* causes downregulation of mesodermal and skeletomyogenic gene expression

To test, whether *mespa* is required for gene expression of *xbra*, *myoD* and *myf5* at early gastrula, loss of function experiments were performed (Fig. 40).

Unilateral injections of *mespa* MO led to a substantial decrease of *xbra*, *myoD* and *myf5* transcription on the injected side, as detected by RNA *in situ* hybridization (Fig. 40 D, H, L). While *myoD* and *myf5* expression was nearly abolished, *xbra* gene transcription was reduced by *mespa* knockdown. In contrast, injection of control MO, as well as injection of *mespo* MO, had no effect on gene expression (Fig. 40 B, C, F, G, J, K).

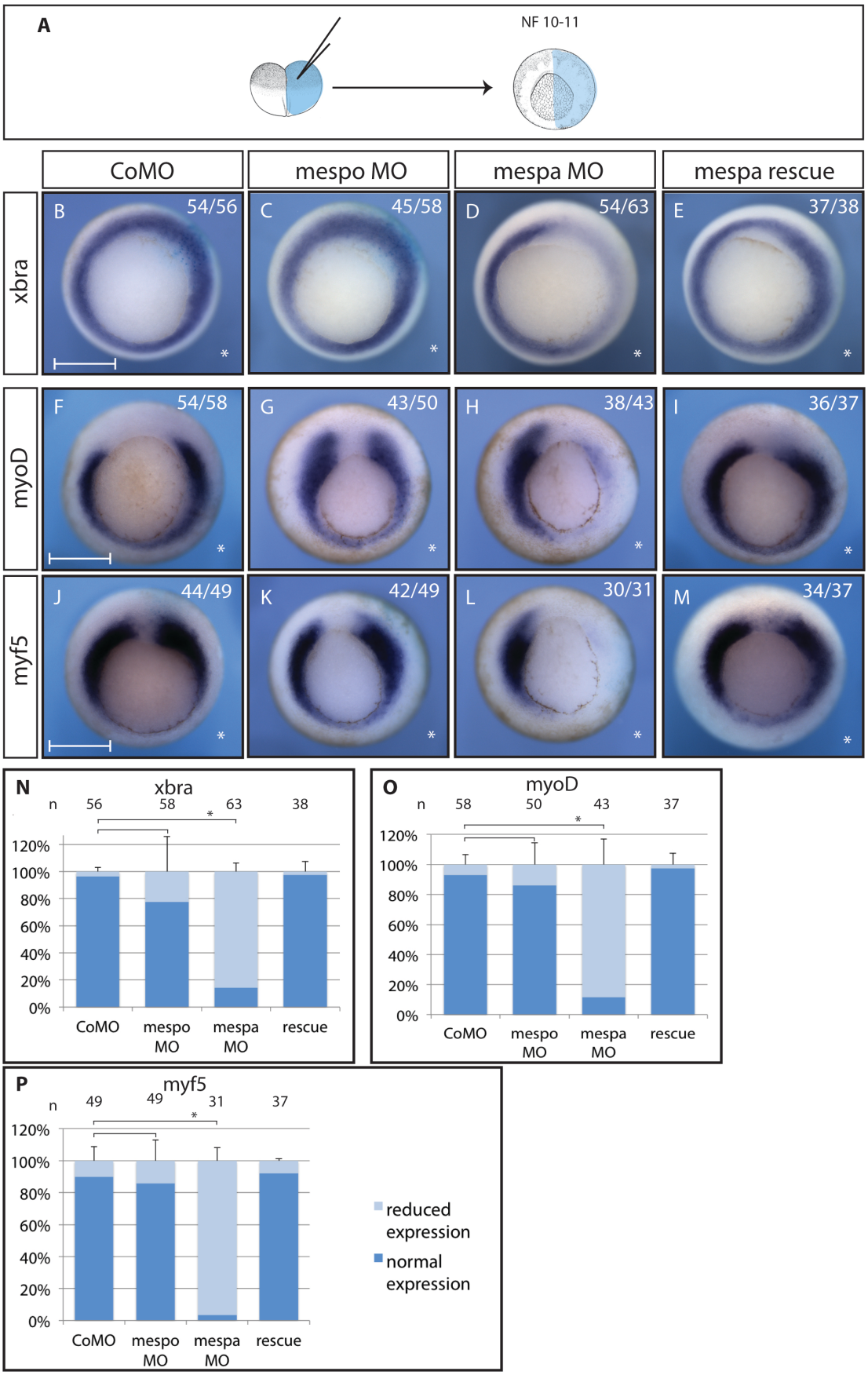

Figure 40: Knockdown of *mespa* causes downregulation of mesodermal and skeletomyogenic gene expression. (A) Embryos were unilaterally injected with 20ng of morpholino at two-cell stage und cultivated until NF 10 (*xbra*), or NF 11 (*myoD*, *myf5*), respectively. **(B-M)** By RNA *in situ* hybridization expression of *xbra*, *myoD* and *myf5* was analysed. **(C, G, K)** *Mespo*-MO caused only slight alterations in gene expression. **(D, H, L)** Injection of *mespa*-MO led to a strong downregulation of marker gene expression. **(E, I, M)** This morphant

phenotype was rescued by injection of 250pg morpholino insensitive *mespa* mRNA variant. Panels show posterior views. Asterisks mark injected side. Scale bars: 500 µm. **(N, O, P)** Phenotypic distribution of *xbra, myoD* and *myf5* expression in three independent biological repeats; *, $p \leq 0.05$.

The *mespa* morphant phenotypes could be rescued by co injection of a morpholino insensitive *mespa* mRNA variant and were therefore specific for knockdown of *mespa* (Fig. 40 E, I, M).

The strong impact of *mespa* knockdown on the skeletomyogenic regulators suggests the existence of common muscle field at the beginning of gastrulation, which will only later separate into cardiovasculogenic and skeletomyogenic progenitor cells. Moreover, it could be concluded that *mespa*, but not *mespo* is required for initiating gene transcription of these mesodermal genes. As *xbra* was only incompletely decreased, the hypothesis of a positive reinforcement loop by *mespa*, which sustains *xbra* expression, but is not required for initiation of *xbra* transcription, is likely.

4. Discussion

A clear understanding of the precise transcriptional orchestra that organizes early embryonic development of multipotent progenitor cells to cardiovascular cells still remains elusive. Approaching the early embryos *in vivo* or simulating surrounding conditions *in vitro* often form obstacles, which prevent close study of these crucial steps in development.

Contrary to mammalian embryos that die early in development without a functional circulatory system (Saga 1998), amphibians can develop to tadpole stage in the absence of a functional heart. Hence, cardiovascular phenotypes can be investigated until the end of embryogenesis (Knower 1907; Copenhaver 1926).

Due to its numerous advantages *Xenopus laevis* is a very suitable model organism to study cardiovascular development *in vivo.*

In this study, functions and potential new target genes of *mespa*, the *Xenopus* homologue of MesP1, were investigated with regard to early steps in cardiogenesis, vasculogenesis, morphogenesis and mesoderm induction.

In order to characterize a possible involvement of *mespa* in the broader context of mesoderm specification and patterning, I have devised experiments to demonstrate: i) an overlap of expression domains as prerequisite for genetic interaction: ii) requirements for potential target gene activation by *mespa* protein knockdown; and iii) sufficiency to induce target genes by overexpression of *mespa* in broad regions of the embryo and animal cap explants as a proxy for naïve, unprogrammed embryonic cells.

4.1 Cardiogenesis

Two essential members of the core transcriptional network that determine the cardiovascular progenitor cells in vertebrates were analysed for regulation by *mespa.* The transcription factors Nkx2.5 and Islet1 are known to be a target gene of MesP1 in ES cells (Bondue, Lapouge et al. 2008; David, Brenner et al. 2008; Lindsley, Gill et al. 2008; Bondue, Tännler et al. 2011; Chan, Shi et al. 2013).

RNA *in situ* hybridization assigned the early expression of *nkx2.5* to a specific region in the anterior leading edge mesoderm, where *nkx2.5* transcription was

already detected at the beginning of gastrulation, thus sharing a partially overlapping expression region with *mespa* (Fig. 15).
Transcription of *isl.1* was detectable, even earlier, from stage NF 10 onwards at the initiation of gastrulation. Remarkably, this start of transcription was for both genes earlier than reported before (Brade, Gessert et al. 2007; Gessert and Kuhl 2009) The early beginning of transcription indicates that *isl.1* and *nkx2.5* not only mark later heart field progenitor cells, but are also expressed in very early cardiovascular progenitors in *Xenopus laevis*, which underlines the hypothesis that cardiac mesoderm is already determined at the beginning of gastrulation (Keller 1976). Further experiments will have to be performed to confirm these results quantitatively via qPCR.

Subsequently, my results show that *mespa* knockdown led to loss of *nkx2.5* gene transcription during gastrulation (Fig. 16), which was not fully compensated even until tailbud stage (Fig. 17). Although *nkx2.5* gene expression was restored in the morphant half, there were remaining defects in the formation of the heart anlage (Fig. 17). On one hand, this points to a second pathway which induces *nkx2.5* and is able to re-establish *nkx2.5* gene expression, on the other hand, it emphasizes an essential position for *mespa* in the proper formation of the heart anlage even in later stages.
Correspondingly, injection of *mespa* morpholino caused loss of *isl.1* expression in the cardiac mesoderm, whereas *isl.1* mRNA in the sensorial layer of the neuroectoderm was not affected (Fig. 21). Thus, *mespa* is required for induction of *isl.1* gene transcription in the mesoderm. Sections of morphant embryos revealed a delayed movement of the mesodermal cell layer to the anterior pole of the embryo (Fig. 21 a), which could also account for the loss of *isl.1* expression in the anterior cardiac mesoderm. A delayed movement of *mespa* deficient mesodermal cells could also be a reason for the diminished *nkx2.5* expression in the anterior region. However, considering that *mespa* overexpression was sufficient to induce gene expression of *isl.1* in animal cap explants (Fig. 22), it is unlikely that the strong phenotype, seen in the *mespa* knockdown experiment, was only based on a migration defect.
Since the *isl.1* knockdown in *Xenopus* leads to downregulation of early and late cardiac markers and smaller hearts with looping defects (Brade, Gessert et al.

2007), the cardiac malformations in MesP1 knockout mice, ranging from separated heart tubes to randomized looping (Saga, Miyagawa-Tomita et al. 1999), could be based partially on a subsequent loss of Isl.1 expression. Nevertheless, overexpression of *isl.1* was not sufficient for induction of cardiac markers in ventral marginal zone explants (Brade, Gessert et al. 2007), while *mespa* was shown to induce definitive cardiac markers like *troponin I type 3* and *tbx20* (Kriegmair, Frenz et al. 2013). Thus, *mespa* appears to be indispensable for induction of a set of genes responsible for cardiac induction independently from *isl.1*.

Since *mespa* is only transiently expressed in a defined region in the embryo, it can be assumed that it exerts its broad range of function additionally through a non-cell-autonomous mechanism, although others claimed that MesP1 acts only cell-autonomously (Bondue, Lapouge et al. 2008). The Wnt-antagonist Dkk1 is a direct target gene of mammalian MesP1 in ES cells (David, Brenner et al. 2008). The question was, whether *dkk1* is a potential target gene of *mespa* in *Xenopus*.

Here, it has been shown that *dkk1* mRNA expression in the anterior cardiac mesoderm was *mespa* dependent and that *mespa* was able to induce *dkk1* mRNA in animal caps, while other bHLH transcription factors were not. These results are in line with previous reports of *wnt*-antagonism by *dkk1* to initiate cardiogenesis in *Xenopus* (Schneider and Mercola 2001).

Adding up to this, the salt-and-pepper like pattern of *mespa* expression in the anterior cardiac crescent hints at the existence of a non-cell-autonomous mechanism, through which *mespa* positive cells could induce adjacent *mespa* negative cells to adopt a cardiac fate. The observation that *mespa* is sufficient and required to activate *dkk1* in *Xenopus* supports the model that non-autonomous mechanisms of mespa function are conserved in vertebrates.

In conclusion, my results showed for the first time in an *in vivo* organism that *nkx2.5, isl.1* and *dkk1* lie downstream of *mespa* in mesodermal cells.

4.2 Vasculogenesis

Cardiogenesis is closely linked to vasculogenesis, i.e., the development of blood vessels during embryogenesis (reviewed in Drake 2003).

Xenopus laevis is a very appropriate model to study vasculogenesis, as it shares a comparable type of circulatory system with mammals (Mohun, Leong et al. 2000).
To evaluate *mespa*'s requirement for vasculogenesis a crucial receptor in vascular development was analysed. The G-Protein coupled Apelin receptor, also termed APJ, was first identified in humans in 1993 (O'Dowd, Heiber et al.).
In *Xenopus* the *apelin receptor* (*aplnr*) was first described in 1996 and named *Xmsr* for *mesenchyme associated serpentine receptor*, based on the finding that the receptor was found in endothelial and cardiac precursor cells (Devic, Paquereau et al. 1996).
The role of MesP1 in vasculogenesis has not been studied extensively in an *in vivo* context yet. However, derivatives of MesP1 expressing cells were found in the dorsal aorta and intersomitic vessels of the mouse embryo (Saga, Kitajima et al. 2000). This is in line with my findings that *mespa* knockdown led to absence of *aplnr* mRNA expression in major vessels of the frog embryo (Fig. 27, Fig. 28). *Mespa* morpholino injection into one blastomere at the 8-cell stage creates a mosaic knockdown, which allows a local downregulation of *mespa* protein expression in specific regions of the embryo. Thereby, different targeted injections showed a specific effect of *mespa* knockdown, according to ventral or dorsal injections, as vascular endothelial cells do not derive from a single embryonic source, but from different blastomeres (Mills, Kruep et al. 1999). Thus, *mespa* knockdown caused a lack of *aplnr* expression, either the in the aortic arches (Fig. 27), which will later form the dorsal aorta, or in the intersomitic veins (Fig. 28). Hence, early knockdown of *mespa* resulted in specific impairment of crucial vascular structures, which could not be compensated even in late stages of development. As a conclusion from this finding, vascular progenitor cells are already determined during gastrulation and therefore early interfering effects lead to vascular malformations in later stages.
MesP1 transfected ES-cell clones showed vascular sprouting from embryoid bodies (David, Brenner et al. 2008) and others observed an upregulation of vascular markers in ES-cells by MesP1, e.g. CD31, VE-Cadherin and smooth muscle actin (Bondue, Lapouge et al. 2008; David, Brenner et al. 2008; Bondue, Tannler et al. 2011). Accordingly, *mespa* RNA overexpression was sufficient to induce strong expression of *apelin receptor* mRNA in naïve tissue explants (Fig. 29). Remarkably, no additional mesodermal signalling inputs besides *mespa* are required to initiate

apelin receptor transcription in naïve animal cap explants, which leads to the hypothesis that *aplnr* is a direct target gene of *mespa* in *Xenopus*. This assumption is supported by a study, which showed direct binding of MesP1 to the Aplnr gene in ES cells (Lescroart, Chabab et al. 2014). Finally, supplementary data of two studies presented an upregulation of Aplnr gene transcription by MesP1 in microarrays of ES cells (Bondue, Tannler et al. 2011; Lescroart, Chabab et al. 2014), which was not commented on in the papers, but corroborates the results described in this thesis.

The apelin receptor was additionally described to be involved in cardiac development in different model systems, which underlines the above-mentioned close relation between development of heart and vessels. In zebrafish the apelin receptor and its ligand apelin, were found to control heart field formation. Morpholino mediated knockdown of aplnr led to reduced expression of the cardiac myosin light chain gene (cmlc2) in cardiac precursors and to absence of a functional heart (Zeng, Wilm et al. 2007). Others showed an upregulation of nkx2.5 and tbx5 by aplnr expression in embryoid bodies (D'Aniello, Lonardo et al. 2009). Moreover, Aplnr double knockout mice died very early during development around day 10.5 p.c. and showed cardiac malformations and vascular defects (Kang, Kim et al. 2013). In *Xenopus*, *aplnr* morpholino injection into dorsovegetal blastomeres led to shrunken hearts and attenuated gene expression of terminal cardiac markers like *myosin heavy chain α* and *troponin I type 3*. However, expression of *nkx2.5* was not affected upon *aplnr* knockdown (Inui, Fukui et al. 2006).
In this study, the *aplnr* has been revealed to have a broad domain of expression at the beginning of gastrulation (Fig. 23), which is similar to *mespa* expression pattern at this time. During late gastrula and early neurula stages, *aplnr* is additionally expressed in the anterior heart-forming mesoderm. In later stages, *aplnr* is mainly restricted to expression in vascular structures (comp. Fig. 23, Fig. 24 and Fig. 25). Knockdown of *mespa* caused partial depletion of *aplnr* expression in early neurula (Fig. 26). As *aplnr* gene expression in the anterior heart-forming mesoderm was diminished, this expression domain could correspond to the fraction of *aplnr* positive cells involved in cardiogenesis. Hence, it can be assumed that *aplnr* acts downstream of *mespa* in cardiac development, as well as in vascular

development. An interesting approach to test this hypothesis would consist in co-injecting *mespa* morpholino and *aplnr* mRNA and subsequent analysis via RNA *in situ* hybridization, whether the co-injected *aplnr* mRNA can rescue, e.g., the downregulation of *isl.1* and *nkx2.5* in this context.

In summary, I could show for the first time *in vivo* that *mespa* is mandatory for *aplnr* gene expression in cardiovascular development.

4.3 Cell migration and embryonic morphogenesis

During embryonic development, the accurate migration of progenitor cells is an essential process to form tissues and organs of the vertebrate body. Crucial steps in organogenesis, like cardiogenesis, depend highly on morphogenetic movements, which are predominantly performed during gastrulation (Scarpa and Mayor 2016). Defective progenitor migration can cause profound congenital malformations of different tissues and organs (Herion, Salbaum et al. 2014).

Transcription factors have been shown to be required for migration of progenitor cells in various organs, such as liver (Sosa-Pineda, Wigle et al. 2000) and brain (de la Torre-Ubieta and Bonni 2011). Previous studies have indicated that progenitor cell specification and migration are possibly linked by common transcriptional regulators (Brand 2003; Christiaen, Davidson et al. 2008). Recently, Chiapparo et al. (2016) confirmed by *in vitro* experiments that Mesp1 coordinates as a transcriptional regulator cardiovascular progenitor migration and specification in ES cells, in line with a prior study of the Mesp homolog in Ciona intestinalis (Christiaen, Davidson et al. 2008). Moreover, the cardiac malformations in MesP1 knockout mice embryos were partially attributed to a migration defect of early mesodermal progenitors (Saga, Miyagawa-Tomita et al. 1999; Kitajima, Takagi et al. 2000).

In this study, the migratory function of *mespa* during gastrulation was examined. Via fluorescent labelling of *mespa* morphant cells, it was shown that *mespa* is necessary for mesodermal migration during gastrulation (Fig. 30). Moreover, sections of gastrula stage embryos, in which *mespa* was unilaterally down regulated, exhibited a delayed anterior migration of *mespa* deficient cells (compare Fig. 21 a). In accordance with the findings above, Mesp1 deficient mesodermal cells

failed to migrate anteriorly at the start of gastrulation in mice (Saga, Miyagawa-Tomita et al. 1999).

These observations suggested that *mespa,* as MesP1 in mice and ES cells, is required for mesodermal migration in *Xenopus laevis*. Therefore, further research was concentrated onto finding a downstream target gene involved in morphogenetic movements in *Xenopus*.

Paraxial Protocadherin (PAPC) was found to be a potential target gene. *PAPC* has been demonstrated to play a role in several aspects of *Xenopus* embryonic morphogenesis like convergence extension movements (Kim, Yamamoto et al. 1998; Unterseher, Hefele et al. 2004; Wang, Janicki et al. 2008), tissue separation and planar cell polarity pathway (Kim, Jen et al. 2000; Medina, Swain et al. 2004; Chen and Gumbiner 2006). A connection between the *mesp*-family of transcription factors and *PAPC* has been identified in somitogenesis, where *mespb*, also known as *thylacine1*, and *mespo* were required for *PAPC* expression in the presomitic mesoderm of the *Xenopus* and Zebrafish embryo, respectively (Kim, Jen et al. 2000; Sawada, Fritz et al. 2000). A link between *mespa* and *PAPC* during cardiovascular development has not been demonstrated so far.

Partial overlap of *mespa* and *PAPC* gene expression in the mesoderm during gastrulation pointed to a potential relation between both genes. Therefore, experiments to evaluate gain and loss of function were carried out.

Remarkably, *mespa* induced *PAPC* expression in a highly significant manner in naïve tissue explants (Fig. 38), as well as in the ectoderm (Fig. 37), which suggests that *PAPC* is most likely a downstream target gene of *mespa.*

In accordance with this hypothesis, the mammalian homologue of *PAPC,* termed Protocadherin8 (pcdh8) was upregulated in MesP1 expressing ES cells (Supplementary Data in Lescroart, Chabab et al. 2014). To demonstrate a direct regulatory role for *mespa,* the *PAPC* gene could be screened *in silico* for the presence of *mespa* DNA binding sites.

Loss of function experiments indicate that *PAPC* expression in the dorsal paraxial and anterior ventral mesoderm is dependent on *mespa*, as knockdown of *mespa* leads to downregulation of *PAPC* in these regions (Fig. 35). Since *PAPC* expression was not completely abolished in *mespa* morpholino injected embryos (Fig. 35), *mespo* could be accountable for the remaining *PAPC* expression. While *mespo* is

only expressed in the somitogenic mesoderm (Kriegmair, Frenz et al. 2013), where *PAPC* gene transcription was present, but *mespa* was not, *mespo* could compensate for the restricted overlap of *mespa* and *PAPC* expression in this region. It was found out that *mespo* probably activates expression of *PAPC* in somitomeres in later stages of *Xenopus* development (Kim, Jen et al. 2000), consistent with the hypothesis of *mespo* to compensate for the loss of *mespa*.

For a more specific functional analysis, mosaic knockdown of *mespa* was performed. The mosaic knockdown of dorsovegetal blastomeres caused defects in gastrulation movements, such as impaired extension convergence movements of the injected cells (Fig. 36). Correspondingly, a dominant negative form of *PAPC* was shown to lead to deficiency in anterior extension of the paraxial mesoderm (Kim, Yamamoto et al. 1998).

As *PAPC* exhibits a complex role in cell adhesion - that is, both promoting (Kim, Yamamoto et al. 1998) and reducing adhesion (Kraft, Berger et al. 2012)- *mespa* might act via *PAPC* to move the mesodermal layer as a cohesive sheet. RNA in situ hybridization revealed a salt and pepper like pattern of *PAPC* positive and *PAPC* negative cells in the anterior region of the embryo (Fig. 31 Q, V). This suggests the existence of adhesive, yet flexible cell contacts between positive and negative cells, which enable cells to slide past each other.

Additionally, *PAPC* has recently been shown to form cleft like contacts at the mesoderm-ectoderm boundary in gastrulation and thereby creating a self/non-self recognition mechanism (Luu, Damm et al. 2015). Correspondingly, overexpression of *mespa* caused defects of the ectodermal-mesodermal boundary (Fig. 37), which suggests that a balanced *mespa* expression and consequently a balanced *PAPC* regulation, is required for tissue separation and association.

The human *PAPC* homologue, Protocadherin8, has been reported to act as a tumour suppressor gene in breast cancer cells by inhibiting cell migration and proliferation (Yu, Koujak et al. 2008). Whether Protocadherin8 may also be able to promote cell migration in human development, still needs to be addressed. However, this finding emphasizes the protocadherin's evolutionary conserved importance for tissue integrity.

In conclusion, I could demonstrate for the first time *in vivo* in a vertebrate organism that *mespa* promotes mesodermal cell migration, concomitantly to progenitor specification during gastrulation. My results show an important function of *mespa* in regulating mesodermal cell migration by regulating *PAPC* expression, thereby identifying a component of the intrinsic molecular machinery that executes morphogenetic movements during gastrulation. The exact molecular mechanisms promoting migration of cardiovascular progenitor cells are still poorly understood and require further investigation.

4.4 Mesoderm formation

Furthermore, the question has been addressed, whether *mespa* is required for the induction of other mesodermal genes, based on its timing of transcriptional activation in a broad domain of preinvoluted mesoderm.

Different families of extrinsic signalling molecules are involved in mesoderm induction. In short, the Nodal family is included in starting mesoderm formation, FGFs and Wnt proteins maintain mesoderm formation and members of the BMP family are included in mesodermal patterning (Kimelman 2006).

Mesoderm induction is controlled by a complex network of regulatory genes (Davidson, Rast et al. 2002). Several upstream regulators of MesP1 have been identified. Among them are the T-box transcription factors Eomesodermin (Costello, Pimeisl et al. 2011; van den Ameele, Tiberi et al. 2012) and Brachyury (T) (David, Jarsch et al. 2011).

FGF signalling establishes and maintains the expression of *xbra*, the *Xenopus laevis* homologue of Brachyury (T) (Fletcher and Harland 2008). Subsequently, *xbra* forms the mesoderm progenitor niche via establishment of high *wnt* signalling and low *retinoic acid* signalling (Martin and Kimelman 2010).

In murine embryogenesis, knockout of Brachyury (T), led to accumulation of cells in and ventral to the primitive streak (Wilson, Manson et al. 1995), in a manner resembling MesP1 knockout mice. Whereas Brachyury gene expression was not affected by MesP1 knockout only (Saga, Miyagawa-Tomita et al. 1999), knockout of both, MesP1 and MesP2, led to a defect in embryonic mesodermal layer formation associated with reduced anterior extension of Brachyury expression (Kitajima,

Takagi et al. 2000). In addition, others showed that MesP1 expression promotes induction of several mesodermal markers in ES cells (Lindsley, Gill et al. 2008).

In my study, it was demonstrated that *mespa* was able to induce mesodermal genes in naïve tissue explants. These results strengthened the hypothesis of *mespa* to be highly competent in mesodermal induction. From these observations, it was hypothesized that *mespa* could be required for induction or maintenance of *xbra*, the Brachyury (T) homologue in *Xenopus*.

Expression pattern of *mespa* and *xbra* were compared via RNA *in situ* hybridization, depicting a spatial and temporal overlap at the beginning of gastrulation (Fig. 39). Yet, *xbra* is additionally expressed in the dorsal organizer region, where *mespa* is not present. In addition, the annular *xbra* expression domain is broader than the corresponding *mespa* expression domain at this time (comp. Fig. 39).

Remarkably, loss of function experiments revealed that *xbra* expression was partially diminished upon *mespa* knockdown (Fig. 40). Hence, it can be assumed that *mespa* is required for induction of *xbra* during gastrulation. As *xbra* expression was still observable and not completely abolished, it is most likely that *mespa* strengthens *xbra* expression in the mesoderm, once *xbra* expression has already been initiated by other factors. Moreover, the expression pattern analysis showed that *xbra* expression in the dorsal organizer region must be independent from direct *mespa* activity, as *mespa* is not expressed in this domain. In conclusion, it can be assumed that *mespa* is a supportive factor, which reinforces *xbra*-directed mesodermal induction.

In ES cells, Brachyury (T) was found to bind directly to the MesP1 promoter region and to enhance MesP1 expression (David, Jarsch et al. 2011). Whether *xbra* induces *mespa* in *Xenopus* still needs to be addressed.

4.5 Skeletomyogenesis

The existence of a common myogenic progenitor field for heart and cranial skeletal muscle has been described before (Tzahor 2009; Kelly 2012).

Mespa target genes, like *isl.1* and *nkx2.5,* have been reported to be additionally expressed in branchiomyogenic progenitor cells (Grifone and Kelly 2007; Nathan, Monovich et al. 2008). Furthermore, isl.1 was shown to promote cardiac

differentiation and inhibit skeletal muscle differentiation in the chick embryo (Harel, Nathan et al. 2009).

However, in Ciona intestinalis, isl.1 expressing cells derived from a common mesp lineage did not have a cardiac fate. These isl.1-positive cells migrated dorsally and differentiated into atrial siphon and skeletal muscle. The authors proposed that rearrangement of multipotent cardiopharyngeal muscle progenitor cells in chordate ancestors might have assisted in development of the vertebrate second heart field (Stolfi, Gainous et al. 2010).

Chan, Hagen et al. (2016) have recently reported that MesP1 positive ES cells promote formation of bipotent progenitor cells, which have the potential to develop into both cardiac and skeletal muscle. This is consistent with another study, where lineage-tracing experiments in mice suggested that MesP1 induced cardiovascular and head muscle progenitors from common precursor cells. It was proposed that the right ventricular myocardium shares a clonal relationship with skeletal muscles, derived from pharyngeal mesoderm (Lescroart, Kelly et al. 2010). Consequently, the concept of a cardiopharyngeal field has recently developed. This developmental domain consists of pharyngeal mesoderm, which gives rise to the right ventricle and the outflow tract of the heart and branchiomeric skeletal muscles, reviewed in Diogo, Kelly et al. (2015).

In the present study, a spatial and temporal overlap of expression of the myogenic bHLH transcription factors *myoD* and *myf5* with *mespa* was demonstrated via RNA *in situ* hybridization (Fig. 39). A following loss of function experiment revealed that *mespa* is required for *myoD* and *myf5* expression, as those are depleted upon *mespa* knockdown (Fig. 40). Hence, here it was shown for the first time that *mespa* is mandatory for myogenesis in the early gastrula stage embryo.

Taken together, these discoveries suggest the existence of a *mespa* expressing common myogenic field of progenitor cells at the beginning of gastrulation, which will later differentiate into skeletal muscle and cardiac muscle cells, respectively.

The question remains on what influences the decision, whether the cells become muscle or heart. There are several answers to this question.

First, *mespa* could act, like other mesoderm inducing factors (Steinbach, Ulshöfer et al. 1998), via an autocatalytic dominant regulatory mechanism, which restricts onset of *myoD* induction to early gastrula. *Mespa* may locally upregulate and

stabilize basal *myoD* transcription by establishing a positive autoregulatory loop (Weintraub, Davis et al. 1991).

Secondly, it has been established that *myoD* and *myf5* function via heterodimerizing with E-proteins (Murre, McCaw et al. 1989; Weintraub, Davis et al. 1991). Hence, differences in cell determination could additionally be based on the amount of dimerization partners in each cell. The lack of dimerization partners would explain the dominant function of *mespa* in loss of function experiments (comp. Fig. 40) and the limited activity *of mespa* for *xbra*, *myoD* and *myf5* in gain of function conditions (own data).

Factors, which may determine cardiac muscle, are the above-mentioned transcription factors nkx2.5 and isl.1. In chick embryo, for example, isl.1 was shown to inhibit skeletal muscle differentiation (Harel, Nathan et al. 2009).

4.6 Model for integrating diverse functions

Taken together, work presented in this thesis strengthens the postulation that *mespa* functions in cardiovascular development, but furthermore in vasculogenesis and morphogenesis and remarkably also in mesodermal induction and skeletomoyogenesis. Hence, *mespa* possesses an essential function in mesodermal cell determination and mesodermal patterning.

My experiments indicate much broader functions for *mespa*, which exceed a hypothesized role as promoter of cardiac differentiation. These additional functions relate to mesoderm formation, vasculogenesis, skeletomyogenesis and regulation of morphogenesis.

The main question arising from my results was, how can these diverse functions be prioritized and coordinated?

There are a number of potential answers to this. As Gerhart and Keller postulated already in 1986: “Ultimate cell fate is determined by the gastrulation processes that place the cell in its ultimate position. The early gastrula may be determined just enough to engage in the gastrulation processes that establish the next stage and its processes. Individual cells of the early gastrula can still follow a wide variety of developmental paths depending on their interactions with other cells.”

Thus, *mespa* establishes certain progenitor cells in different regions of the embryo at the beginning of gastrulation, which will then be determined further over time

according to their specific surroundings. These surroundings imply direct cell-cell interactions, as well as gradients of extrinsic signalling molecules or via *PAPC* for final determination through coordinated migration

There are different lines of evidence, which support this hypothesis. For example, Wnt/beta catenin-signalling was found to promote cardiogenesis at the beginning of gastrulation, while inhibiting it later on (Cohen, Miller et al. 2012). In *Xenopus* there is a gradient of *wnt* molecules, secreted by the dorsal and posterior organizer region, which results in a low amount of *wnt* signalling in the anterior and ventral region, where the heart is going to be formed. By induction of the *wnt*-antagonist *dkk1*, *mespa* adds to inhibit canonical *wnt* influence on heart progenitor cells.

There are other hints that the signalling environment is essential for directing the common precursors to different cell fates.

Kinetic analysis of ES cell differentiation under the influence of an inducible Mesp1 protein indicated different functions for this protein, which are elicited at different time points and stimulation by environmental factors (Chan, Shi et al. 2013). The MesP1 positive ES cells developed differently depending on the cell culture medium: By addition of serum-derived factors to the medium the cells underwent cardiac or haematopoietic differentiation, whereas without serum-derived factors they differentiated into skeletomyogenic cells. The serum-derived factors may mimic local environmental cues of the embryo.

Another model consists of a *mespa* feed-forward-loop (Fig. 41), as it has been described for MyoD in skeletomyogenesis (Penn, Bergstrom et al. 2004). This kind of transcriptional regulatory network contains a master regulator, which controls a second regulator while both bind a common target gene (Lee, Rinaldi et al. 2002).

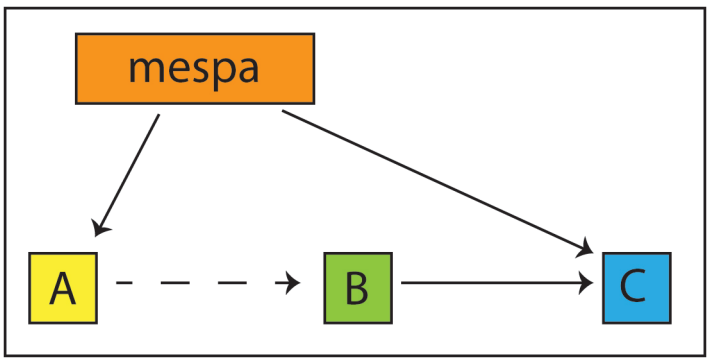

Fig. 41 Feed-forward loop. Model of a feed-forward circuitry with *mespa* as a master regulator, which induces target gene A. Target gene A activates target gene B and hence B and *mespa* induce target gene C.

The feed-forward loop may present a model, wherein factors induced by *mespa* – for example, *isl.1* and *nkx2.5* – regulate *mespa* activity at subsequent target genes, thereby creating a temporally patterned gene expression during mesodermal specification. Hence, transient *mespa* expression during gastrulation and concomitant latent binding to promoter regions of target genes may provide a mechanism to control different developmental processes (Penn, Bergstrom et al. 2004). Ultimately, expression of the final target gene depends on the adequate amount of *mespa* and secondary regulators controlled by *mespa* at the promoter site. Slight changes in the amount of *mespa* would lead to an amplified effect at the common target gene within the regulatory network (Lee, Rinaldi et al. 2002). Consistent with this hypothesis, microarray analysis of early and late MesP1 expressing progenitor cells in mice showed differential expression of important transcription factors (Lescroart, Chabab et al. 2014). These features of a feed-forward motif may offer a model, by what means *mespa* can act as a single transcriptional regulator of such different types of progenitor cells, as mesodermal, cardiogenic, vasculogenic and skeletomyogenic progenitor cells.

4.7 Outlook

Here, I have shown that *mespa* specifies mesodermal progenitor cells during gastrulation and directs the morphogenetic movements of these cells, which will ultimately give rise to distinct cell types.

Further work is needed to resolve the regulatory network of *mespa* target genes *in vivo* to define the differentiation processes of various progenitor cells. The mechanisms how extrinsic and intrinsic signals are integrated leading to differentiation and migration of mesodermal cells during gastrulation remain poorly understood. Future studies will be required to further corroborate the results presented in this study by techniques like quantitative PCR or microarray analysis.

There remains an open question as to what extent *mespa* is also involved in developmental processes of haematopoiesis. Different lines of evidence exist that MesP1 can direct ES cells to adopt a haematopoietic fate (Cai, Langer et al. 2012; Chan, Shi et al. 2013). In *Xenopus,* a close association between haematopoietic and vascular development has been described, which has led to the concept of a

common precursor cell, the haemangioblast. Arising from a mesodermal region called ventral blood islands during neurula stage this common precursor cell has been shown to develop into embryonic blood and endothelial cells (Walmsley 2002). Therefore, it is conceivable that *mespa* may also regulate certain haematopoietic factors.

Furthermore, the question, which effects are controlled by direct binding of *mespa* and which are indirect, including non cell autonomous effects, still needs to be addressed. Therefore, chromatin immunoprecipitation coupled to next generation sequencing (ChIP-Seq) of *mespa* binding sites should be applied.

Finally, these results provide important insights for a better understanding of the mechanisms underlying cardiovascular differentiation during embryonic development.

5. Abbreviations

bHLH	basic helix-loop-helix
bp	base pair
cDNA	complementary DNA
Co	Control
ddH_2O	double-distilled water
DEPC	diethylpyrocarbonate
dig	digoxigenin
DNA	desoxyribonucleic acid
dNTPs	mixture of all four desoxribonucleotides
EDTA	ethylenediaminetetraacetic acid
e.g.	exempli gratia, for example
EGTA	ethylene glycol tetraacetic acid
ES	Embryonic stem
et al.	et alii, and others
g	gram
GFP	green fluorescent protein
h	hour/hours
hES cell	human embryonic stem cell
hpf	hours post fertilization
i.e.	id est, that is
iPS cell	induced pluripotent stem cell
kb	kilobases
kDa	kilodaltons
l	liter
M	molar
MBT	mid-blastula transition
min	minute
ml	mililiter
mm	milimeter
mM	milimolar
MO	Morpholino
mRNA	messenger ribonucleic acid

NF	developmental stage of *Xenopus* laevis according to Niewkoop and Faber, 1994
ng	nanogram
nm	nanometer
nmol	nanomol
PBS	phosphate buffered saline
PCR	polymerase chain reaction
Pol	RNA- polymerase II
qPCR	quantitative polymerase chain reaction
RNA	ribonucleic acid
RT	room temperature
SDS	sodium dodecyl sulphate
sec	second/seconds
U	unit/units
UV	ultraviolet
V	Volt
WT	wild type
Wnt	wingless
µg	microgram
µl	microliter
µM	micromolar

6. References

Afouda, B. A. and Hoppler, S. (2009). "Xenopus Explants as an Experimental Model System for Studying Heart Development." Trends Cardiovasc Med **19**(7): 220-226.

Bergmann, O., Bhardwaj, R. D., Bernard, S., Zdunek, S., Barnabé-Heider, F., Walsh, S., Zupicich, J., Alkass, K., Buchholz, B. A., Druid, H., et al. (2009). "Evidence for Cardiomyocyte Renewal in Humans." Science **324**(5923): 98-102.

Bondue, A., Lapouge, G., Paulissen, C., Semeraro, C., Iacovino, M., Kyba, M. and Blanpain, C. (2008). "Mesp1 acts as a master regulator of multipotent cardiovascular progenitor specification." Cell Stem Cell **3**(1): 69-84.

Bondue, A., Tannler, S., Chiapparo, G., Chabab, S., Ramialison, M., Paulissen, C., Beck, B., Harvey, R. and Blanpain, C. (2011). "Defining the earliest step of cardiovascular progenitor specification during embryonic stem cell differentiation." J Cell Biol **192**(5): 751-765.

Brade, T., Gessert, S., Kuhl, M. and Pandur, P. (2007). "The amphibian second heart field: Xenopus islet-1 is required for cardiovascular development." Dev Biol **311**(2): 297-310.

Brand, T. (2003). "Heart development: molecular insights into cardiac specification and early morphogenesis." Dev Biol **258**(1): 1-19.

Brown, D. D., Martz, S. N., Binder, O., Goetz, S. C., Price, B. M. J., Smith, J. C. and Conlon, F. L. (2005). "Tbx5 and Tbx20 act synergistically to control vertebrate heart morphogenesis." Development **132**(3): 553-563.

Buckingham, M. (1992). "Making muscle in mammals." Trends in Genetics **8**(4): 144-149.

Bui, A. L., Horwich, T. B. and Fonarow, G. C. (2011). "Epidemiology and risk profile of heart failure." Nat Rev Cardiol **8**(1): 30-41.

Cai, M., Langer, E. M., Gill, J. G., Satpathy, A. T., Albring, J. C., Kc, W., Murphy, T. L. and Murphy, K. M. (2012). "Dual actions of Meis1 inhibit erythroid progenitor development and sustain general hematopoietic cell proliferation." Blood **120**(2): 335-346.

Chan, Sunny S.-K., Hagen, Hannah R., Swanson, Scott A., Stewart, R., Boll, Karly A., Aho, J., Thomson, James A. and Kyba, M. (2016). "Development of Bipotent Cardiac/Skeletal Myogenic Progenitors from MESP1+ Mesoderm." Stem Cell Reports **6**(1): 26-34.

Chan, Sunny S.-K., Shi, X., Toyama, A., Arpke, Robert W., Dandapat, A., Iacovino, M., Kang, J., Le, G., Hagen, Hannah R., Garry, Daniel J., et al. (2013). "Mesp1 Patterns Mesoderm into Cardiac, Hematopoietic, or Skeletal Myogenic Progenitors in a Context-Dependent Manner." Cell Stem Cell **12**(5): 587-601.

Chen, W. V. and Maniatis, T. (2013). "Clustered protocadherins." Development **140**(16): 3297-3302.

Chen, X. and Gumbiner, B. M. (2006). "Paraxial protocadherin mediates cell sorting and tissue morphogenesis by regulating C-cadherin adhesion activity." J Cell Biol **174**(2): 301-313.

Chiapparo, G., Lin, X., Lescroart, F., Chabab, S., Paulissen, C., Pitisci, L., Bondue, A. and Blanpain, C. (2016). "Mesp1 controls the speed, polarity, and directionality of cardiovascular progenitor migration." J Cell Biol **213**(4): 463-477.

Chong, J. J. H., Yang, X., Don, C. W., Minami, E., Liu, Y.-W., Weyers, J. J., Mahoney, W. M., Van Biber, B., Cook, S. M., Palpant, N. J., et al. (2014). "Human embryonic-stem-cell-derived cardiomyocytes regenerate non-human primate hearts." Nature **510**(7504): 273-277.

Christiaen, L., Davidson, B., Kawashima, T., Powell, W., Nolla, H., Vranizan, K. and Levine, M. (2008). "The Transcription/Migration Interface in Heart Precursors of Ciona intestinalis." Science **320**(5881): 1349-1352.

Christoforou, N., Chellappan, M., Adler, A. F., Kirkton, R. D., Wu, T., Addis, R. C., Bursac, N. and Leong, K. W. (2013). "Transcription Factors MYOCD, SRF, Mesp1 and SMARCD3 Enhance the Cardio-Inducing Effect of GATA4, TBX5, and MEF2C during Direct Cellular Reprogramming." PLoS One **8**(5): e63577.

Cleaver, O. B., Patterson, K. D. and Krieg, P. A. (1996). "Overexpression of the tinman-related genes XNkx-2.5 and XNkx-2.3 in Xenopus embryos results in myocardial hyperplasia." Development **122**(11): 3549-3556.

Cohen, E. D., Miller, M. F., Wang, Z., Moon, R. T. and Morrisey, E. E. (2012). "Wnt5a and Wnt11 are essential for second heart field progenitor development." Development **139**(11): 1931-1940.

Copenhaver, W. M. (1926). "Experiments on the development of the heart of Amblystoma punctatum." Journal of Experimental Zoology **43**(3): 321-371.

Costello, I., Pimeisl, I.-M., Drager, S., Bikoff, E. K., Robertson, E. J. and Arnold, S. J. (2011). "The T-box transcription factor Eomesodermin acts upstream of Mesp1 to specify cardiac mesoderm during mouse gastrulation." Nat Cell Biol **13**(9): 1084-1091.

Cox, C. M., D'Agostino, S. L., Miller, M. K., Heimark, R. L. and Krieg, P. A. (2006). "Apelin, the ligand for the endothelial G-protein-coupled receptor, APJ, is a potent angiogenic factor required for normal vascular development of the frog embryo." Dev Biol **296**(1): 177-189.

D'Aniello, C., Lonardo, E., Iaconis, S., Guardiola, O., Liguoro, A. M., Liguori, G. L., Autiero, M., Carmeliet, P. and Minchiotti, G. (2009). "G Protein-Coupled Receptor APJ and Its Ligand Apelin Act Downstream of Cripto to Specify Embryonic Stem

Cells Toward the Cardiac Lineage Through Extracellular Signal-Regulated Kinase/p70S6 Kinase Signaling Pathway." Circ Res **105**(3): 231-238.

David, R., Brenner, C., Stieber, J., Schwarz, F., Brunner, S., Vollmer, M., Mentele, E., Muller-Hocker, J., Kitajima, S., Lickert, H., et al. (2008). "MesP1 drives vertebrate cardiovascular differentiation through Dkk-1-mediated blockade of Wnt-signalling." Nat Cell Biol **10**(3): 338-345.

David, R., Jarsch, V. B., Schwarz, F., Nathan, P., Gegg, M., Lickert, H. and Franz, W. M. (2011). "Induction of MesP1 by Brachyury(T) generates the common multipotent cardiovascular stem cell." Cardiovasc Res **92**(1): 115-122.

Davidson, E. H., Rast, J. P., Oliveri, P., Ransick, A., Calestani, C., Yuh, C.-H., Minokawa, T., Amore, G., Hinman, V., Arenas-Mena, C., et al. (2002). "A Genomic Regulatory Network for Development." Science **295**(5560): 1669-1678.

de la Torre-Ubieta, L. and Bonni, A. (2011). "Transcriptional Regulation of Neuronal Polarity and Morphogenesis in the Mammalian Brain." Neuron **72**(1): 22-40.

Deimling, S. J. and Drysdale, T. A. (2011). "Fgf is required to regulate anterior-posterior patterning in the Xenopus lateral plate mesoderm." Mech Dev **128**(7-10): 327-341.

Devic, E., Paquereau, L., Vernier, P., Knibiehler, B. and Audigier, Y. (1996). "Expression of a new G protein-coupled receptor X-msr is associated with an endothelial lineage in Xenopus laevis." Mech Dev **59**(2): 129-140.

Diogo, R., Kelly, R. G., Christiaen, L., Levine, M., Ziermann, J. M., Molnar, J. L., Noden, D. M. and Tzahor, E. (2015). "A new heart for a new head in vertebrate cardiopharyngeal evolution." Nature **520**(7548): 466-473.

Drake, C. J. (2003). "Embryonic and adult vasculogenesis." Birth Defects Research Part C: Embryo Today: Reviews **69**(1): 73-82.

Elkan, E. R. (1938). "The Xenopus Pregnancy Test." British Medical Journal **2**(4067): 1253-1274.1252.

Engleka, K. A., Manderfield, L. J., Brust, R. D., Li, L., Cohen, A., Dymecki, S. M. and Epstein, J. A. (2012). "Islet1 Derivatives in the Heart Are of Both Neural Crest and Second Heart Field Origin." Circ Res **110**(7): 922-926.

Fahed, A. C., Gelb, B. D., Seidman, J. G. and Seidman, C. E. (2013). "Genetics of Congenital Heart Disease: The Glass Half Empty." Circ Res **112**(4): 707-720.

Finegold, J. A., Asaria, P. and Francis, D. P. (2013). "Mortality from ischaemic heart disease by country, region, and age: Statistics from World Health Organisation and United Nations." International Journal of Cardiology **168**(2): 934-945.

Fletcher, R. B. and Harland, R. M. (2008). "The role of FGF signaling in the establishment and maintenance of mesodermal gene expression in Xenopus." Developmental Dynamics **237**(5): 1243-1254.

Foley, A. C., Korol, O., Timmer, A. M. and Mercola, M. (2007). "Multiple functions of Cerberus cooperate to induce heart downstream of Nodal." Dev Biol **303**(1): 57-65.

Fu, J.-D., Stone, Nicole R., Liu, L., Spencer, C. I., Qian, L., Hayashi, Y., Delgado-Olguin, P., Ding, S., Bruneau, Benoit G. and Srivastava, D. (2013). "Direct Reprogramming of Human Fibroblasts toward a Cardiomyocyte-like State." Stem Cell Reports **1**(3): 235-247.

Garriock, R. J., D'Agostino, S. L., Pilcher, K. C. and Krieg, P. A. (2005). "Wnt11-R, a protein closely related to mammalian Wnt11, is required for heart morphogenesis in Xenopus." Dev Biol **279**(1): 179-192.

Gerhart, J. and Keller, R. (1986). "Region-Specific Cell Activities in Amphibian Gastrulation." Annual Review of Cell Biology **2**(1): 201-229.

Gessert, S. and Kuhl, M. (2009). "Comparative gene expression analysis and fate mapping studies suggest an early segregation of cardiogenic lineages in Xenopus laevis." Dev Biol **334**(2): 395-408.

Green, J. (1999). The Animal Cap Assay. Molecular Methods in Developmental Biology. M. Guille, Humana Press. **127:** 1-13.

Griffin, J. N., Sondalle, S. B., del Viso, F., Baserga, S. J. and Khokha, M. K. (2015). "The Ribosome Biogenesis Factor Nol11 Is Required for Optimal rDNA Transcription and Craniofacial Development in Xenopus." PLoS Genet **11**(3): e1005018.

Grifone, R. and Kelly, R. G. (2007). "Heartening news for head muscle development." Trends in Genetics **23**(8): 365-369.

Guner-Ataman, B., Paffett-Lugassy, N., Adams, M. S., Nevis, K. R., Jahangiri, L., Obregon, P., Kikuchi, K., Poss, K. D., Burns, C. E. and Burns, C. G. (2013). "Zebrafish second heart field development relies on progenitor specification in anterior lateral plate mesoderm and nkx2.5 function." Development **140**(6): 1353-1363.

Hardin, J. and Keller, R. (1988). "The behaviour and function of bottle cells during gastrulation of Xenopus laevis." Development **103**(1): 211-230.

Hardwick, L. J. A. and Philpott, A. (2015). "An oncologist's friend: How Xenopus contributes to cancer research." Dev Biol **408**(2): 180-187.

Harel, I., Nathan, E., Tirosh-Finkel, L., Zigdon, H., Guimarães-Camboa, N., Evans, S. M. and Tzahor, E. (2009). "Distinct Origins and Genetic Programs of Head Muscle Satellite Cells." Dev Cell **16**(6): 822-832.

Harland, R. M. and Grainger, R. M. (2011). "Xenopus research: metamorphosed by genetics and genomics." Trends in Genetics **27**(12): 507-515.

Hartung, S., Schwanke, K., Haase, A., David, R., Franz, W.-M., Martin, U. and Zweigerdt, R. (2012). "Directing Cardiomyogenic Differentiation of Human Pluripotent Stem Cells by Plasmid-Based Transient Overexpression of Cardiac Transcription Factors." Stem Cells and Development **22**(7): 1112-1125.

Harvey, R. P. (2002). "Patterning the vertebrate heart." Nat Rev Genet **3**(7): 544-556.

Hausen, P. a. R., M. (1991). The Early Development of Xenopus laevis: An Atlas of Histology. Berlin, Springer-Verlag.

Heasman, J. (2006). "Patterning the early Xenopus embryo." Development **133**(7): 1205-1217.

Heasman, J., Wylie, C. C., Hausen, P. and Smith, J. C. (1984). "Fates and states of determination of single vegetal pole blastomeres of X. laevis." Cell **37**(1): 185-194.

Hellsten, U., Harland, R. M., Gilchrist, M. J., Hendrix, D., Jurka, J., Kapitonov, V., Ovcharenko, I., Putnam, N. H., Shu, S., Taher, L., et al. (2010). "The Genome of the Western Clawed Frog Xenopus tropicalis." Science (New York, N.Y.) **328**(5978): 633-636.

Herion, N. J., Salbaum, J. M. and Kappen, C. (2014). "Traffic jam in the primitive streak: The role of defective mesoderm migration in birth defects." Birth Defects Research Part A: Clinical and Molecular Teratology **100**(8): 608-622.

Hitachi, K., Kondow, A., Danno, H., Nishimura, Y., Okabayashi, K. and Asashima, M. (2009). "Molecular analyses of Xenopus laevis Mesp-related genes." Integr Zool **4**(4): 387-394.

Hoffman, J. I. E. (1995). "Incidence of congenital heart disease: II. Prenatal incidence." Pediatr Cardiol **16**(4): 155-165.

Hoffman, J. I. E. and Kaplan, S. (2002). "The incidence of congenital heart disease." Journal of the American College of Cardiology **39**(12): 1890-1900.

Hukriede, N. A., Tsang, T. E., Habas, R., Khoo, P.-L., Steiner, K., Weeks, D. L., Tam, P. P. L. and Dawid, I. B. (2003). "Conserved Requirement of Lim1 Function for Cell Movements during Gastrulation." Dev Cell **4**(1): 83-94.

Inui, M., Fukui, A., Ito, Y. and Asashima, M. (2006). "Xapelin and Xmsr are required for cardiovascular development in Xenopus laevis." Dev Biol **298**(1): 188-200.

Islas, J. F., Liu, Y., Weng, K.-C., Robertson, M. J., Zhang, S., Prejusa, A., Harger, J., Tikhomirova, D., Chopra, M., Iyer, D., et al. (2012). "Transcription factors ETS2 and MESP1 transdifferentiate human dermal fibroblasts into cardiac progenitors." Proceedings of the National Academy of Sciences **109**(32): 13016-13021.

Jorgensen, P., Steen, J. A. J., Steen, H. and Kirschner, M. W. (2009). "The mechanism and pattern of yolk consumption provide insight into embryonic nutrition in Xenopus." Development (Cambridge, England) **136**(9): 1539-1548.

Jung, B., Kohler, A., Schambony, A. and Wedlich, D. (2011). "PAPC and the Wnt5a/Ror2 pathway control the invagination of the otic placode in Xenopus." BMC Dev Biol **11**: 36.

Kälin, R. E., Kretz, M. P., Meyer, A. M., Kispert, A., Heppner, F. L. and Brändli, A. W. (2007). "Paracrine and autocrine mechanisms of apelin signaling govern embryonic and tumor angiogenesis." Dev Biol **305**(2): 599-614.

Kaltenbrun, E., Tandon, P., Amin, N. M., Waldron, L., Showell, C. and Conlon, F. L. (2011). "Xenopus: An emerging model for studying congenital heart disease." Birth Defects Research Part A: Clinical and Molecular Teratology **91**(6): 495-510.

Kang, Y., Kim, J., Anderson, J. P., Wu, J., Gleim, S. R., Kundu, R. K., McLean, D. L., Kim, J.-d., Park, H., Jin, S.-w., et al. (2013). "Apelin-APJ Signaling Is a Critical Regulator of Endothelial MEF2 Activation in Cardiovascular Development." Circ Res **113**(1): 22-31.

Keller, R. (1991). Chapter 5 Early Embryonic Development of Xenopus laevis. Methods Cell Biol. K. K. Brian and H. B. Peng, Academic Press. **Volume 36:** 61-113.

Keller, R., Davidson, L., Edlund, A., Elul, T., Ezin, M., Shook, D. and Skoglund, P. (2000). "Mechanisms of convergence and extension by cell intercalation." Philosophical Transactions of the Royal Society B: Biological Sciences **355**(1399): 897-922.

Keller, R. and Hardin, J. (1987). "Cell Behaviour During Active Cell Rearrangement: Evidence and Speculations." J Cell Sci **1987**(Supplement 8): 369-393.

Keller, R. and Tibbetts, P. (1989). "Mediolateral cell intercalation in the dorsal, axial mesoderm of Xenopus laevis." Dev Biol **131**(2): 539-549.

Keller, R. E. (1975). "Vital dye mapping of the gastrula and neurula of Xenopus laevis: I. Prospective areas and morphogenetic movements of the superficial layer." Dev Biol **42**(2): 222-241.

Keller, R. E. (1976). "Vital dye mapping of the gastrula and neurula of Xenopus laevis: II. Prospective areas and morphogenetic movements of the deep layer." Dev Biol **51**(1): 118-137.

Kelly, R. G. (2012). Chapter two - The Second Heart Field. Current Topics in Developmental Biology. B. G. Bruneau, Academic Press. **Volume 100:** 33-65.

Kelly, R. G., Brown, N. A. and Buckingham, M. E. (2001). "The Arterial Pole of the Mouse Heart Forms from Fgf10-Expressing Cells in Pharyngeal Mesoderm." Dev Cell **1**(3): 435-440.

Kidoya, H. and Takakura, N. (2012). "Biology of the apelin-APJ axis in vascular formation." J Biochem **152**(2): 125-131.

Kidoya, H., Ueno, M., Yamada, Y., Mochizuki, N., Nakata, M., Yano, T., Fujii, R. and Takakura, N. (2008). "Spatial and temporal role of the apelin/APJ system in the caliber size regulation of blood vessels during angiogenesis." The EMBO Journal **27**(3): 522-534.

Kim, S. H., Jen, W. C., De Robertis, E. M. and Kintner, C. (2000). "The protocadherin PAPC establishes segmental boundaries during somitogenesis in xenopus embryos." Curr Biol **10**(14): 821-830.

Kim, S. H., Yamamoto, A., Bouwmeester, T., Agius, E. and Robertis, E. M. (1998). "The role of paraxial protocadherin in selective adhesion and cell movements of the mesoderm during Xenopus gastrulation." Development **125**(23): 4681-4690.

Kimelman, D. (2006). "Mesoderm induction: from caps to chips." Nat Rev Genet **7**(5): 360-372.

Kinoshita, M., Ariizumi, T., Yuasa, S., Miyoshi, S., Komazaki, S., Fukuda, K. and Asashima, M. (2010). "Creating frog heart as an organ: in vitro-induced heart functions as a circulatory organ in vivo." Int J Dev Biol **54**(5): 851-856.

Kirschner, M., Newport, J. and Gerhart, J. (1985). "The timing of early developmental events in Xenopus." Trends in Genetics **1**(0): 41-47.

Kitajima, S., Takagi, A., Inoue, T. and Saga, Y. (2000). "MesP1 and MesP2 are essential for the development of cardiac mesoderm." Development **127**(15): 3215-3226.

Klaus, A., Saga, Y., Taketo, M. M., Tzahor, E. and Birchmeier, W. (2007). "Distinct roles of Wnt/beta-catenin and Bmp signaling during early cardiogenesis." Proc Natl Acad Sci U S A **104**(47): 18531-18536.

Knower, H. M. (1907). "Effects of early removal of the heart and arrest of the circulation on the development of frog embryos." The Anatomical Record **1**(7): 161-165.

Konstantinidis, K., Whelan, R. S. and Kitsis, R. N. (2012). "Mechanisms of Cell Death in Heart Disease." Arteriosclerosis, Thrombosis, and Vascular Biology **32**(7): 1552-1562.

Koster, I., Jungwirth, M. S. and Steinbeisser, H. (2010). "xGit2 and xRhoGAP 11A regulate convergent extension and tissue separation in Xenopus gastrulation." Dev Biol **344**(1): 26-35.

Kraft, B., Berger, C. D., Wallkamm, V., Steinbeisser, H. and Wedlich, D. (2012). "Wnt-11 and Fz7 reduce cell adhesion in convergent extension by sequestration of PAPC and C-cadherin." J Cell Biol **198**(4): 695-709.

Kriegmair, M. C. M., Frenz, S., Dusl, M., Franz, W.-M., David, R. and Rupp, R. A. W. (2013). "Cardiac differentiation in Xenopus is initiated by mespa." Cardiovasc Res **97**(3): 454-463.

LaBonne, C. and Zorn, A. M. (2015). "Modeling human development and disease in Xenopus." Dev Biol **408**(2): 179.

Laflamme, M. A. and Murry, C. E. (2011). "Heart regeneration." Nature **473**(7347): 326-335.

Laforest, B. and Nemer, M. (2011). "GATA5 interacts with GATA4 and GATA6 in outflow tract development." Dev Biol **358**(2): 368-378.

Latinkic, B. V. (2003). "Induction of cardiomyocytes by GATA4 in Xenopus ectodermal explants." Development **130**(16): 3865-3876.

Laugwitz, K. L., Moretti, A., Caron, L., Nakano, A. and Chien, K. R. (2008). "Islet1 cardiovascular progenitors: a single source for heart lineages?" Development **135**(2): 193-205.

Lee, T. I., Rinaldi, N. J., Robert, F., Odom, D. T., Bar-Joseph, Z., Gerber, G. K., Hannett, N. M., Harbison, C. T., Thompson, C. M., Simon, I., et al. (2002). "Transcriptional Regulatory Networks in Saccharomyces cerevisiae." Science **298**(5594): 799-804.

Lee, Y. H. and Saint-Jeannet, J. P. (2011). "Cardiac neural crest is dispensable for outflow tract septation in Xenopus." Development **138**(10): 2025-2034.

Lescroart, F., Chabab, S., Lin, X., Rulands, S., Paulissen, C., Rodolosse, A., Auer, H., Achouri, Y., Dubois, C., Bondue, A., et al. (2014). "Early lineage restriction in temporally distinct populations of Mesp1 progenitors during mammalian heart development." Nat Cell Biol **16**(9): 829-840.

Lescroart, F., Kelly, R. G., Le Garrec, J.-F., Nicolas, J.-F., Meilhac, S. M. and Buckingham, M. (2010). "Clonal analysis reveals common lineage relationships between head muscles and second heart field derivatives in the mouse embryo." Development **137**(19): 3269-3279.

Levine, A. J., Munoz-Sanjuan, I., Bell, E., North, A. J. and Brivanlou, A. H. (2003). "Fluorescent labeling of endothelial cells allows in vivo, continuous characterization of the vascular development of Xenopus laevis." Dev Biol **254**(1): 50-67.

Lindsley, R. C., Gill, J. G., Murphy, T. L., Langer, E. M., Cai, M., Mashayekhi, M., Wang, W., Niwa, N., Nerbonne, J. M., Kyba, M., et al. (2008). "Mesp1 coordinately regulates cardiovascular fate restriction and epithelial-mesenchymal transition in differentiating ESCs." Cell Stem Cell **3**(1): 55-68.

Lozano, R., Naghavi, M., Foreman, K., Lim, S., Shibuya, K., Aboyans, V., Abraham, J., Adair, T., Aggarwal, R., Ahn, S. Y., et al. (2012). "Global and regional mortality from 235 causes of death for 20 age groups in 1990 and 2010: a systematic analysis for the Global Burden of Disease Study 2010." The Lancet **380**(9859): 2095-2128.

Luu, O., Damm, E. W., Parent, S. E., Barua, D., Smith, T. H. L., Wen, J. W. H., Lepage, S. E., Nagel, M., Ibrahim-Gawel, H., Huang, Y., et al. (2015). "PAPC mediates self/non–self-distinction during Snail1-dependent tissue separation." J Cell Biol **208**(6): 839-856.

Martin, B. L. and Kimelman, D. (2010). "Brachyury establishes the embryonic mesodermal progenitor niche." Genes Dev **24**(24): 2778-2783.

Medina, A., Swain, R. K., Kuerner, K. M. and Steinbeisser, H. (2004). "Xenopus paraxial protocadherin has signaling functions and is involved in tissue separation." The EMBO Journal **23**(16): 3249-3258.

Menasché, P., Vanneaux, V., Hagège, A., Bel, A., Cholley, B., Cacciapuoti, I., Parouchev, A., Benhamouda, N., Tachdjian, G., Tosca, L., et al. (2015). "Human embryonic stem cell-derived cardiac progenitors for severe heart failure treatment: first clinical case report." European Heart Journal **36**(30): 2011-2017.

Méreau, A., Le Sommer, C., Lerivray, H., Lesimple, M. and Hardy, S. (2007). "Xenopus as a model to study alternative splicing in vivo." Biology of the Cell **99**(1): 55-65.

Mills, K. R., Kruep, D. and Saha, M. S. (1999). "Elucidating the Origins of the Vascular System: A Fate Map of the Vascular Endothelial and Red Blood Cell Lineages inXenopus laevis." Dev Biol **209**(2): 352-368.

Mohun, T. (2003). "The Origins of Cardiac Tissue in the Amphibian, Xenopus laevis." Trends Cardiovasc Med **13**(6): 244-248.

Mohun, T. J., Leong, L. M., Weninger, W. J. and Sparrow, D. B. (2000). "The Morphology of Heart Development in Xenopus laevis." Dev Biol **218**(1): 74-88.

Moreno, T. A., Jappelli, R., Izpisua Belmonte, J. C. and Kintner, C. (2008). "Retinoic acid regulation of the Mesp-Ripply feedback loop during vertebrate segmental patterning." Dev Biol **315**(2): 317-330.

Murre, C., McCaw, P. S., Vaessin, H., Caudy, M., Jan, L. Y., Jan, Y. N., Cabrera, C. V., Buskin, J. N., Hauschka, S. D., Lassar, A. B., et al. (1989). "Interactions between heterologous helix-loop-helix proteins generate complexes that bind specifically to a common DNA sequence." Cell **58**(3): 537-544.

Murry, C. E., Reinecke, H. and Pabon, L. M. (2006). "Regeneration Gaps: Observations on Stem Cells and Cardiac Repair." Journal of the American College of Cardiology **47**(9): 1777-1785.

Musunuru, K., Domian, I. J. and Chien, K. R. (2010). "Stem cell models of cardiac development and disease." Annu Rev Cell Dev Biol **26**: 667-687.

Nathan, E., Monovich, A., Tirosh-Finkel, L., Harrelson, Z., Rousso, T., Rinon, A., Harel, I., Evans, S. M. and Tzahor, E. (2008). "The contribution of Islet1-expressing

splanchnic mesoderm cells to distinct branchiomeric muscles reveals significant heterogeneity in head muscle development." Development **135**(4): 647-657.

Newport, J. and Kirschner, M. (1982). "A major developmental transition in early xenopus embryos: II. control of the onset of transcription." Cell **30**(3): 687-696.

Nieuwkoop, P. D. and Faber, J. (1967). "Normal table of Xenopus laevis (Daudin) : a systematical and chronological survey of the development from the fertilized egg till the end of metamorphosis." North-Holland Pub. Co.

Noseda, M., Peterkin, T., Simoes, F. C., Patient, R. and Schneider, M. D. (2011). "Cardiopoietic factors: extracellular signals for cardiac lineage commitment." Circ Res **108**(1): 129-152.

O'Dowd, B. F., Heiber, M., Chan, A., Heng, H. H. Q., Tsui, L.-C., Kennedy, J. L., Shi, X., Petronis, A., George, S. R. and Nguyen, T. (1993). "A human gene that shows identity with the gene encoding the angiotensin receptor is located on chromosome 11." Gene **136**(1–2): 355-360.

Olson, E. N. (2006). "Gene Regulatory Networks in the Evolution and Development of the Heart." Science **313**(5795): 1922-1927.

Park, B.-Y. and Saint-Jeannet, J.-P. (2010). "Expression analysis of Runx3 and other Runx family members during Xenopus development." Gene Expression Patterns **10**(4–5): 159-166.

Penn, B. H., Bergstrom, D. A., Dilworth, F. J., Bengal, E. and Tapscott, S. J. (2004). "A MyoD-generated feed-forward circuit temporally patterns gene expression during skeletal muscle differentiation." Genes Dev **18**(19): 2348-2353.

Peterkin, T., Gibson, A., Loose, M. and Patient, R. (2005). "The roles of GATA-4, -5 and -6 in vertebrate heart development." Semin Cell Dev Biol **16**(1): 83-94.

Prall, O. W. J., Menon, M. K., Solloway, M. J., Watanabe, Y., Zaffran, S., Bajolle, F., Biben, C., McBride, J. J., Robertson, B. R., Chaulet, H., et al. (2007). "An Nkx2-5/Bmp2/Smad1 Negative Feedback Loop Controls Heart Progenitor Specification and Proliferation." Cell **128**(5): 947-959.

Ptaszek, L. M., Mansour, M., Ruskin, J. N. and Chien, K. R. (2012). "Towards regenerative therapy for cardiac disease." The Lancet **379**(9819): 933-942.

Risau, W. and Flamme, I. (1995). "Vasculogenesis." Annu Rev Cell Dev Biol **11**(1): 73-91.

Roberts, A. and Smyth, D. (1974). "The development of a dual touch sensory system in embryos of the amphibianXenopus laevis." Journal of comparative physiology **88**(1): 31-42.

Rupp, R. A., Snider, L. and Weintraub, H. (1994). "Xenopus embryos regulate the nuclear localization of XMyoD." Genes Dev **8**(11): 1311-1323.

Saga, Y. (1998). "Genetic rescue of segmentation defect in MesP2-deficient mice by MesP1 gene replacement." Mech Dev **75**(1-2): 53-66.

Saga, Y., Hata, N., Kobayashi, S., Magnuson, T., Seldin, M. F. and Taketo, M. M. (1996). "MesP1: a novel basic helix-loop-helix protein expressed in the nascent mesodermal cells during mouse gastrulation." Development **122**(9): 2769-2778.

Saga, Y., Kitajima, S. and Miyagawa-Tomita, S. (2000). "Mesp1 expression is the earliest sign of cardiovascular development." Trends Cardiovasc Med **10**(8): 345-352.

Saga, Y., Miyagawa-Tomita, S., Takagi, A., Kitajima, S., Miyazaki, J. and Inoue, T. (1999). "MesP1 is expressed in the heart precursor cells and required for the formation of a single heart tube." Development **126**(15): 3437-3447.

Sahara, M., Santoro, F. and Chien, K. R. (2015). "Programming and reprogramming a human heart cell." The EMBO Journal **34**(6): 710-738.

Samuel, L. J. and Latinkic, B. V. (2009). "Early activation of FGF and nodal pathways mediates cardiac specification independently of Wnt/beta-catenin signaling." PLoS One **4**(10): e7650.

Sater, A. K. and Jacobson, A. G. (1989). "The specification of heart mesoderm occurs during gastrulation in Xenopus laevis." Development **105**(4): 821-830.

Sater, A. K. and Jacobson, A. G. (1990). "The role of the dorsal lip in the induction of heart mesoderm in Xenopus laevis." Development **108**(3): 461-470.

Sawada, A., Fritz, A., Jiang, Y. J., Yamamoto, A., Yamasu, K., Kuroiwa, A., Saga, Y. and Takeda, H. (2000). "Zebrafish Mesp family genes, mesp-a and mesp-b are segmentally expressed in the presomitic mesoderm, and Mesp-b confers the anterior identity to the developing somites." Development **127**(8): 1691-1702.

Scarpa, E. and Mayor, R. (2016). "Collective cell migration in development." J Cell Biol **212**(2): 143-155.

Schneider, V. A. and Mercola, M. (2001). "Wnt antagonism initiates cardiogenesis in Xenopus laevis." Genes Dev **15**(3): 304-315.

Schultheiss, T. M. and Lassar, A. B. (1999). Vertebrate Heart Induction. Heart Development. San Diego, Academic Press**:** 51-62.

Sosa-Pineda, B., Wigle, J. T. and Oliver, G. (2000). "Hepatocyte migration during liver development requires Prox1." Nat Genet **25**(3): 254-255.

Sparrow, D. B., Cai, C., Kotecha, S., Latinkic, B., Cooper, B., Towers, N., Evans, S. M. and Mohun, T. J. (2000). "Regulation of the tinman Homologues in Xenopus Embryos." Dev Biol **227**(1): 65-79.

Spemann, H. and Mangold, H. (1924). "Über Induktion von Embryonalanlagen durch Implantation artfremder Organisatoren." Archiv für Mikroskopische Anatomie und Entwicklungsmechanik **100**: 599-638.

Stallmeyer, B., Fenge, H., Nowak-Göttl, U. and Schulze-Bahr, E. (2010). "Mutational spectrum in the cardiac transcription factor gene NKX2.5 (CSX) associated with congenital heart disease." Clinical Genetics **78**(6): 533-540.

Stehlik, J. E., L.B; Kucheryavaya, AY; et al. (2011). "The Registry of the International Society for Heart and Lung Transplantation: twenty-seventh official adult heart transplant report." J Heart Lung Transplant **30**: 1078-1094.

Steinbach, O. C., Ulshöfer, A., Authaler, A. and Rupp, R. A. W. (1998). "Temporal Restriction of MyoD Induction and Autocatalysis duringXenopusMesoderm Formation." Dev Biol **202**(2): 280-292.

Stolfi, A., Gainous, T. B., Young, J. J., Mori, A., Levine, M. and Christiaen, L. (2010). "Early Chordate Origins of the Vertebrate Second Heart Field." Science **329**(5991): 565-568.

Terasaki, H., Murakami, R., Yasuhiko, Y., Shin, I. T., Kohara, Y., Saga, Y. and Takeda, H. (2006). "Transgenic analysis of the medaka mesp-b enhancer in somitogenesis." Dev Growth Differ **48**(3): 153-168.

Tucker, B., Hepperle, C., Kortschak, D., Rainbird, B., Wells, S., Oates, A. C. and Lardelli, M. (2007). "Zebrafish Angiotensin II Receptor-like 1a (agtrl1a) is expressed in migrating hypoblast, vasculature, and in multiple embryonic epithelia." Gene Expression Patterns **7**(3): 258-265.

Tzahor, E. (2009). "Heart and craniofacial muscle development: A new developmental theme of distinct myogenic fields." Dev Biol **327**(2): 273-279.

Unterseher, F., Hefele, J. A., Giehl, K., De Robertis, E. M., Wedlich, D. and Schambony, A. (2004). "Paraxial protocadherin coordinates cell polarity during convergent extension via Rho A and JNK." The EMBO Journal **23**(16): 3259-3269.

van den Ameele, J., Tiberi, L., Bondue, A., Paulissen, C., Herpoel, A., Iacovino, M., Kyba, M., Blanpain, C. and Vanderhaeghen, P. (2012). "Eomesodermin induces Mesp1 expression and cardiac differentiation from embryonic stem cells in the absence of Activin." EMBO Rep **13**(4): 355-362.

van der Bom, T., Zomer, A. C., Zwinderman, A. H., Meijboom, F. J., Bouma, B. J. and Mulder, B. J. M. (2011). "The changing epidemiology of congenital heart disease." Nat Rev Cardiol **8**(1): 50-60.

van der Linde, D., Konings, E. E. M., Slager, M. A., Witsenburg, M., Helbing, W. A., Takkenberg, J. J. M. and Roos-Hesselink, J. W. (2011). "Birth Prevalence of Congenital Heart Disease Worldwide: A Systematic Review and Meta-Analysis." Journal of the American College of Cardiology **58**(21): 2241-2247.

Waldo, K. L., Kumiski, D. H., Wallis, K. T., Stadt, H. A., Hutson, M. R., Platt, D. H. and Kirby, M. L. (2001). "Conotruncal myocardium arises from a secondary heart field." Development **128**(16): 3179-3188.

Wallingford, J. B., Liu, K. J. and Zheng, Y. (2010). "Xenopus." Current Biology **20**(6): R263-R264.

Walmsley, M. (2002). "Adult and embryonic blood and endothelium derive from distinct precursor populations which are differentially programmed by BMP in Xenopus." Development **129**(24): 5683-5695.

Wang, J., Li, S., Chen, Y. and Ding, X. (2007). "Wnt/beta-catenin signaling controls Mespo expression to regulate segmentation during Xenopus somitogenesis." Dev Biol **304**(2): 836-847.

Wang, Y., Janicki, P., Köster, I., Berger, C. D., Wenzl, C., Großhans, J. and Steinbeisser, H. (2008). "Xenopus Paraxial Protocadherin regulates morphogenesis by antagonizing Sprouty." Genes Dev **22**(7): 878-883.

Wang, Y. and Steinbeisser, H. (2009). "Molecular basis of morphogenesis during vertebrate gastrulation." Cell Mol Life Sci **66**(14): 2263-2273.

Warkman, A. S. and Krieg, P. A. (2007). "Xenopus as a model system for vertebrate heart development." Semin Cell Dev Biol **18**(1): 46-53.

Watanabe, Y., Zaffran, S., Kuroiwa, A., Higuchi, H., Ogura, T., Harvey, R. P., Kelly, R. G. and Buckingham, M. (2012). "Fibroblast growth factor 10 gene regulation in the second heart field by Tbx1, Nkx2-5, and Islet1 reveals a genetic switch for down-regulation in the myocardium." Proceedings of the National Academy of Sciences **109**(45): 18273-18280.

Weintraub, H., Davis, R., Tapscott, S., Thayer, M., Krause, M., Benezra, R., Blackwell, T., Turner, D., Rupp, R., Hollenberg, S., et al. (1991). "The myoD gene family: nodal point during specification of the muscle cell lineage." Science **251**(4995): 761-766.

Werner, P., Latney, B., Deardorff, M. A. and Goldmuntz, E. (2016). "MESP1 Mutations in Patients with Congenital Heart Defects." Human Mutation **37**(3): 308-314.

Wheeler, G. N. and Brändli, A. W. (2009). "Simple vertebrate models for chemical genetics and drug discovery screens: Lessons from zebrafish and Xenopus." Developmental Dynamics **238**(6): 1287-1308.

WHO (2012) Fact sheet: The top 10 causes of death [Internet].

Wilson, P. A., Oster, G. and Keller, R. (1989). "Cell rearrangement and segmentation in Xenopus: direct observation of cultured explants." Development **105**(1): 155-166.

Wilson, V., Manson, L., Skarnes, W. C. and Beddington, R. S. (1995). "The T gene is necessary for normal mesodermal morphogenetic cell movements during gastrulation." Development **121**(3): 877-886.

Wolpert, L. T., Cheryll (2011). Principles of development. Oxford, Oxford University Press.

Wu, S. M., Chien, K. R. and Mummery, C. (2008). "Origins and fates of cardiovascular progenitor cells." Cell **132**(4): 537-543.

Xavier-Neto, J., Trueba, S. S., Stolfi, A., Souza, H. M., Sobreira, T. J. P., Schubert, M. and Castillo, H. A. (2012). "An Unauthorized Biography of the Second Heart Field and a Pioneer/Scaffold Model for Cardiac Development." Heart Development **100**: 67-105.

Yu, J. S., Koujak, S., Nagase, S., Li, C. M., Su, T., Wang, X., Keniry, M., Memeo, L., Rojtman, A., Mansukhani, M., et al. (2008). "PCDH8, the human homolog of PAPC, is a candidate tumor suppressor of breast cancer." Oncogene **27**(34): 4657-4665.

Zeng, X. X., Wilm, T. P., Sepich, D. S. and Solnica-Krezel, L. (2007). "Apelin and its receptor control heart field formation during zebrafish gastrulation." Dev Cell **12**(3): 391-402.

Zhang, L., Nomura-Kitabayashi, A., Sultana, N., Cai, W., Cai, X., Moon, A. M. and Cai, C.-L. (2014). "Mesodermal Nkx2.5 is necessary and sufficient for early second heart field development." Dev Biol **390**(1): 68-79.

Zhao, R., Watt, A. J., Battle, M. A., Li, J., Bondow, B. J. and Duncan, S. A. (2008). "Loss of both GATA4 and GATA6 blocks cardiac myocyte differentiation and results in acardia in mice." Dev Biol **317**(2): 614-619.